BUREAU OF MINERAL RESOURCES,
GEOLOGY AND GEOPHYSICS

Report 192

*BMR Microform MF 11*

# Some earthquake focal mechanisms in the New Guinea / Solomon Islands region, 1969–1971

by I.D. Ripper

DEPARTMENT OF NATIONAL RESOURCES 1977

DEPARTMENT OF NATIONAL RESOURCES

Minister: The Rt Hon. J.D. Anthony, M.P.

Secretary: J. Scully

BUREAU OF MINERAL RESOURCES, GEOLOGY AND GEOPHYSICS

Director: L.C. Noakes

Assistant Director, Geophysical Branch: N.G. Chamberlain

Published for the Bureau of Mineral Resources, Geology and Geophysics by the Australian Government Publishing Service

## CONTENTS



## TABLES



## FIGURES



## PLATES

## SUMMARY

Focal mechanism stereographic projections were plotted for 34 earthquakes that occurred in the New Guinea/Solomon Islands region between 1969 and 1971. Solutions have been obtained for 31 of the earthquakes, of which 27 are reasonably good; of these, six are strike-slip and 21 are dip-slip (13 overthrust, seven normal, and one having one horizontal and one vertical nodal plane).

The data used were P-wave first arrivals, recorded mainly on the World Wide Standard Seismograph Network.

The complexity of the essentially compressional collision zone between the Pacific Plate and the Australian Plate is indicated by several earthquakes for which dip-slip normal solutions were obtained: in the South Bismarck Volcanic Arc; on the Solomon Sea side of the New Britain Trench; in the D'Entrecasteaux Islands region of southeast Papua; on Santa Ysabel Island; and at depths of 115 and 118 km below the Ramu Markham Valley.

# INTRODUCTION

Ripper (1975) plotted focal mechanism stereographic projections for 59 earthquakes that occurred in the New Guinea/Solomon Islands region between 1963 and 1968, and obtained graphical solutions for 48 of them, of which 33 are good. In this Report, 34 earthquakes that occurred in the same region between 1969 and 1971 are examined; 27 good focal mechanism solutions have been obtained, and these are plotted in Plates 2 and 3. Plate 1 is a locality map of the region.

Although the technique for determining focal mechanism solutions has been described by Ripper (1975), it is repeated below to make this Report complete.

Copies of 35-mm films of World Wide Standard Seismograph Network (WWSSN) seismograms were acquired from the World Data Centre, and these were supplemented by requests for seismograms from non-standard stations.

A focal mechanism solution is obtained from the seismograph station data as follows:

1. The azimuth and epicentral distance of each station from the epicentre are computed.

2. The angle of incidence - that is, the angle between the vertical and the seismic ray as it leaves the earthquake focus - is determined using the graphs of Bessonova et al. (1960) or the tables of either Hodgson & Storey (1953) or Nuttli (1969), which relate angle of incidence to epicentral distance. The direction of a P ray as it leaves the focus is thus defined by its azimuth and angle of incidence. If the rays are assumed to travel in straight lines until they pass through a hypothetical sphere (called the focal sphere) centred on the focus, the ray directions can be represented by positions on the sphere. The sphere is, in turn, represented by a Wulff stereographic projection on which points are defined by their azimuth and angle from the vertical.

3. Seismograph station positions are thus represented on the focal sphere by the points at which the seismic rays to the stations pass through the sphere. The standard station codes (Appendix) are used to identify the stations. Different symbols indicate the P-wave polarities, either compression or dilatation, recorded at each seismograph station.

4. Zones of P-wave compression and dilatation on the focal sphere are then separated by two orthogonal planes, which pass through the focus and are represented on the stereographic projection by two arcs. Orthogonality is enforced by ensuring that each arc passes through the pole of the other. The quadrants are alternately compression and dilatation, and the planes are called nodal planes.

5. Each nodal plane is defined by the azimuth of its dip direction and the angle of dip, or by the azimuth and plunge of its pole.

6. The lines bisecting the angle between the poles of the orthogonal nodal planes, drawn in the third orthogonal plane, are called the compressional (P) and tensional (T) stress of the focal mechanism solution, and fall in the P-wave dilatational and compressional quadrants respectively. Each stress axis is defined by the azimuth of its plunge direction and the plunge measured from the horizontal.

The division of the P-wave polarity field into four quadrants by orthogonal nodal planes is widely accepted. Ritsema (1967) conducted a survey of 63 non-orthogonal earthquake solutions in the literature, and obtained an orthogonal solution for every earthquake except one. He suggested that the effect of near-focal crustal inhomogeneities caused the exception. Sykes (1968) stated that he did not know of any earthquake for which the orthogonal P-wave solution was not a reasonable approximation of the observations.

The terminology, 'compressional' and 'tensional' stress axes of the focal mechanism solution, allows these axes to be distinguished from the maximum and minimum principal stresses of the tectonic stress field. McKenzie (1969) notes that if the medium in which the earthquake occurs is already faulted the tectonic stress axes need not coincide with the solution axes, but may fall anywhere within the respective P-wave polarity quadrant, and may differ by up to $90^{\circ}$.

One of the main difficulties in obtaining good focal mechanism solutions is the uneven seismograph station coverage of the focal sphere. For a normal-depth earthquake, the epicentral distance range of $0-22^{\circ}$ corresponds to 85 percent of the focal sphere, and $0-90^{\circ}$, 97 percent; distant seismograph stations provide P-wave information for only 3 percent of the focal sphere. Unless there are many stations within about $20^{\circ}$ of the epicentre, the coverage of

the focal sphere will be limited, and, although an orthogonal nodal plane solution may be obtained, other types of solution may be possible.

The Wulff projections of the focal mechanism solutions are shown in Figures 2 to 35. The hypocentres of the earthquakes investigated in this Report are listed in Table 1; the station polarities in Table 2; and the solutions in Table 3. Failure to obtain solutions applied mainly to earthquakes with weak P-wave arrivals and consequently with few station polarities, inconsistent results, and poor coverage of the focal sphere.

A measure of the uncertainty of each solution is provided by the solid angle of uncertainty of the axis of intersection of the orthogonal nodal planes (the B axis). This solid angle is obtained by tracing all possible positions of the ends of the B axis on the focal sphere. The areas thus traced out are shown on the relevant Figures, and the dimensions of the solid angle are given in Table 3 for all earthquakes except those for which an orthogonal solution was not obtained.

A non-orthogonal solution normally does not imply that an orthogonal solution is impossible. Non-orthogonal solutions are generally caused by one or more anomalous readings close to a nodal plane, and these can usually be accounted for by uncertainty in crustal or upper mantle structure at the earthquake focus or along the P-wave path. Hence a non-orthogonal solution usually implies a tight solution.

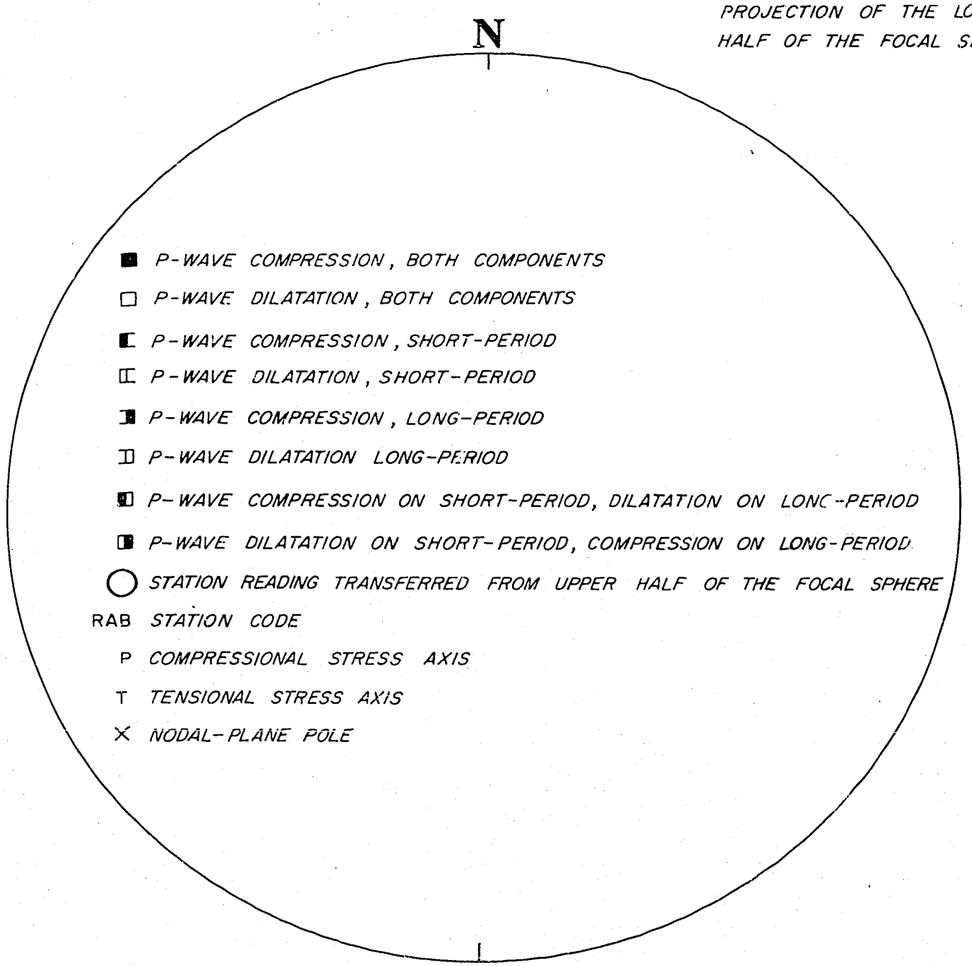


Fig. I. SYMBOLS USED IN FIGURES 2-35

PNG/B9-217A

## THE SOLUTIONS

The solutions are presented in chronological order, one per page, with the Wulff projection of each solution opposite each description (Figs 2 - 35). Figure 1, opposite this page, explains the symbols, except for the B-axis uncertainty, which has been discussed under 'Introduction'.

The solutions are numbered from 49 to 82; they follow on from the 48 solutions obtained for the 1963 - 1968 period (Ripper, 1975).

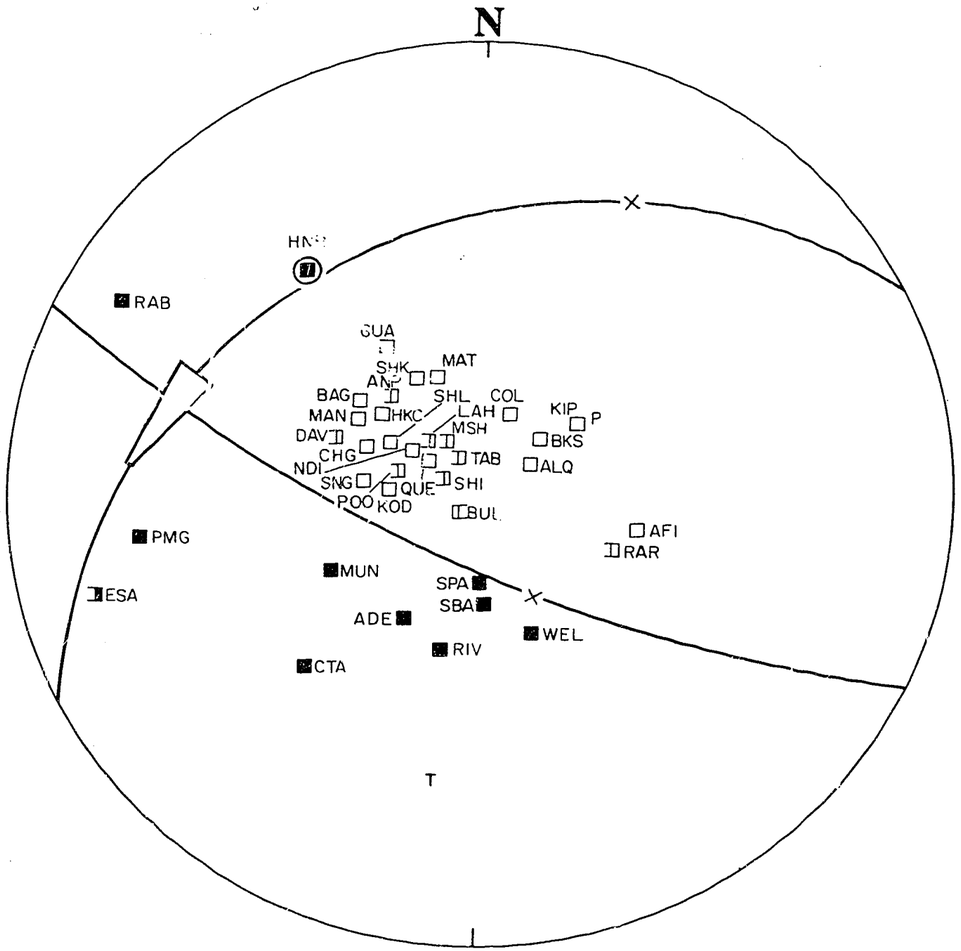


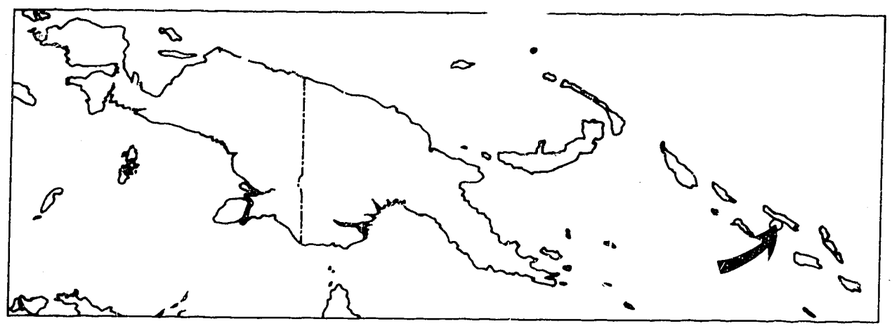

Fig. 2

PNG/B9-231-1A

Figure 2

| | | | | |
|---|---|---|---|---|
| Number | : | 49 | | |
| Location | : | 8.0°S, 158.9°E; west coast of Santa Ysabel Island | | |
| Origin Time | : | 5 January 1969 at 13 26 39.9 UT | | |
| Depth | : | 47 km | | |
| Magnitude (M) | : | 7.1 | | |
| Type | : | Dip-slip normal | | |
| Nodal Planes | : | Azimuth of Dip | Dip | |
| | : | 333 | 28 | |
| | : | 206 | 72 | |
| Nodal-Plane Poles | : | Azimuth | Plunge | |
| | : | 153 | 62 | |
| | : | 026 | 18 | |
| P Axis | : | 055 | 58 | |
| T Axis | : | 189 | 23 | |
| | | Azimuth | Plunge | Uncertainty |
| B Axis | : | 289 | 20 | 21 x 6 |

The solution is reasonably well defined as dip-slip normal. There are no anomalous station readings.

The tectonic significance of the solution is not clear. The earthquake originated from an isolated pocket of seismic activity that is located beneath the Santa Ysabel Island/New Georgia Sound area, on the northeast side of the Solomon Island double chain. The main seismic belt passes along the southwest line of islands. The solution of another earthquake of the same cluster (2 June 1968, No. 37, Ripper, 1975) is strike-slip. Both earthquakes may be associated with the apparent tensional opening in the Solomon Sea southwest of New Georgia, between the Australian Plate and the Pacific Plate (Johnson & Molnar, 1972).

Plotted in Plate 3.

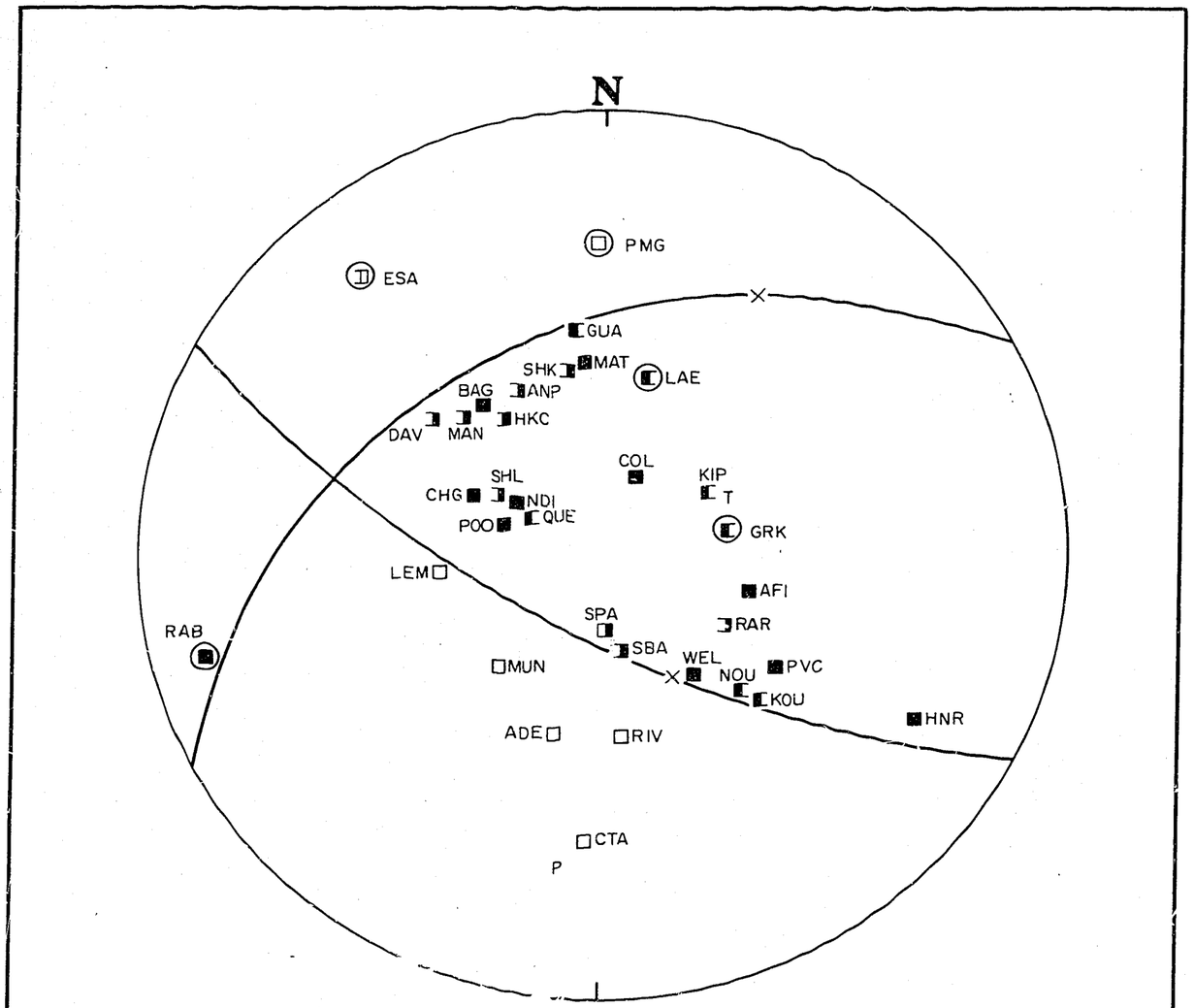


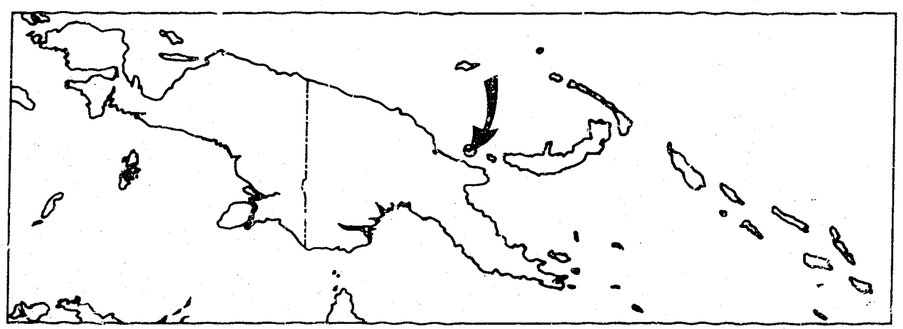

Fig.3

PNG/B9-231-2A

Figure 3

| | | | | |
|---|---|---|---|---|
| Number | : | 50 | | |
| Location | : | 5.6°S, 147.2°E; 10 km south of Long Island volcano | | |
| Origin Time | : | 10 March 1969 at 06 54 17.6 UT | | |
| Depth | : | 206 km | | |
| Magnitude (M) | : | 6.4 | | |
| Type | : | Dip-slip overthrust | | |
| Nodal Planes | : | Azimuth of Dip | Dip | |
| | : | 209 | 68 | |
| | : | 332 | 36 | |
| Nodal-Plane Poles | : | Azimuth | Plunge | |
| | : | 029 | 22 | |
| | : | 152 | 54 | |
| P Axis | : | 187 | 19 | |
| T Axis | : | 066 | 57 | |
| | | Azimuth | Plunge | Uncertainty |
| B Axis | : | 287 | 26 | 1 x 1 |

The dip-slip overthrust solution is similar to those of two other earthquakes (Nos. 4 and 26, Ripper, 1975) in the same earthquake cluster beneath Long Island volcano. One strike-slip solution has also been obtained (No. 38, Ripper, 1975).

Plotted in Plate 3.

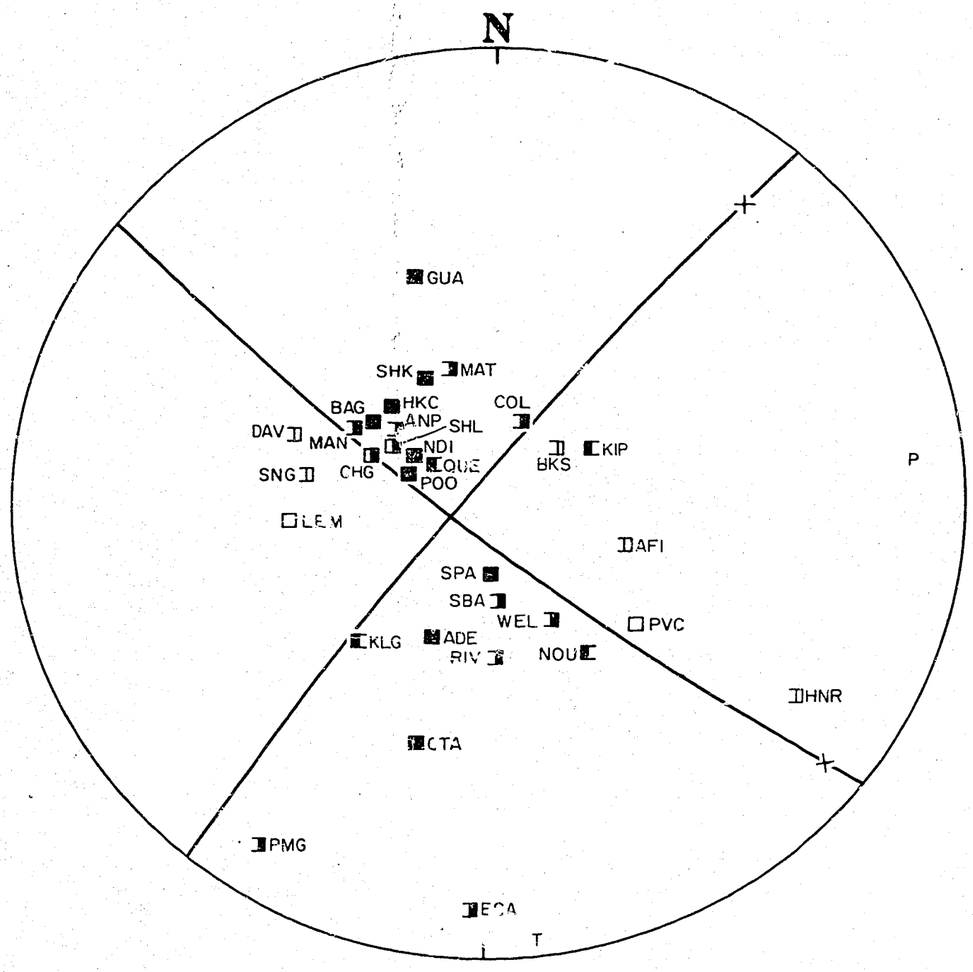


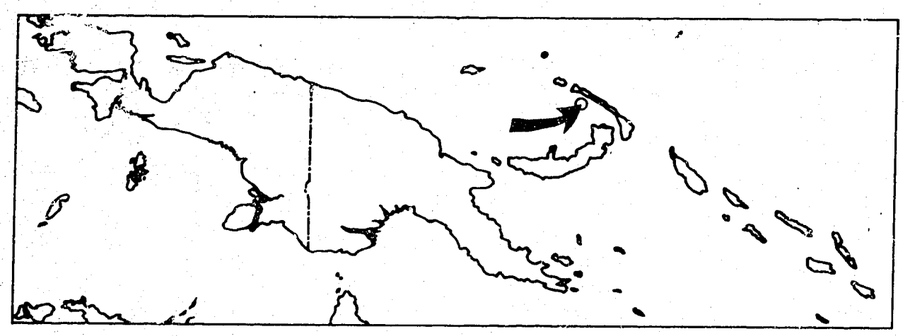

Fig.4

PNG/B9-231-3A

Figure 4

| | | | |
|---|---|---|---|
| Number | : | 51 | |
| Location | : | 3.5°S, 151.0°E; Bismarck Sea seismic lineation 50 km south of Kavieng, New Ireland | |
| Origin Time | : | 16 April 1969 at 01 22 47.5 UT | |
| Depth | : | 39 km | |
| Magnitude (M) | : | 6.4 | |
| Type | : | Strike-slip | |
| Nodal Planes | : | Azimuth of Dip | Dip |
| | : | 219 | 81 |
| | : | 308 | 85 |
| Nodal-Plane Poles | : | Azimuth | Plunge |
| | : | 039 | 09 |
| | : | 128 | 05 |
| P Axis | : | 083 | 06 |
| T Axis | : | 173 | 01 |
| | | Azimuth | Plunge Uncertainty |
| B Axis | : | 245 | 80 8 x 2 |

The solution is strike-slip. There are two stations (CHG and SHL) with short-period and long-period P-wave arrivals of opposite polarity, but these are close to a nodal plane. Station KIP recorded an anomalous P-wave compression within a dilatational quadrant, but the micro-seismic level was high and may have obscured an initial dilatation.

The epicentre is at the eastern end of the Bismarck Sea seismic lineation, south of New Ireland. If the nodal plane parallel to New Ireland is the fault plane, the motion is sinistral.

Plotted in Plate 2.

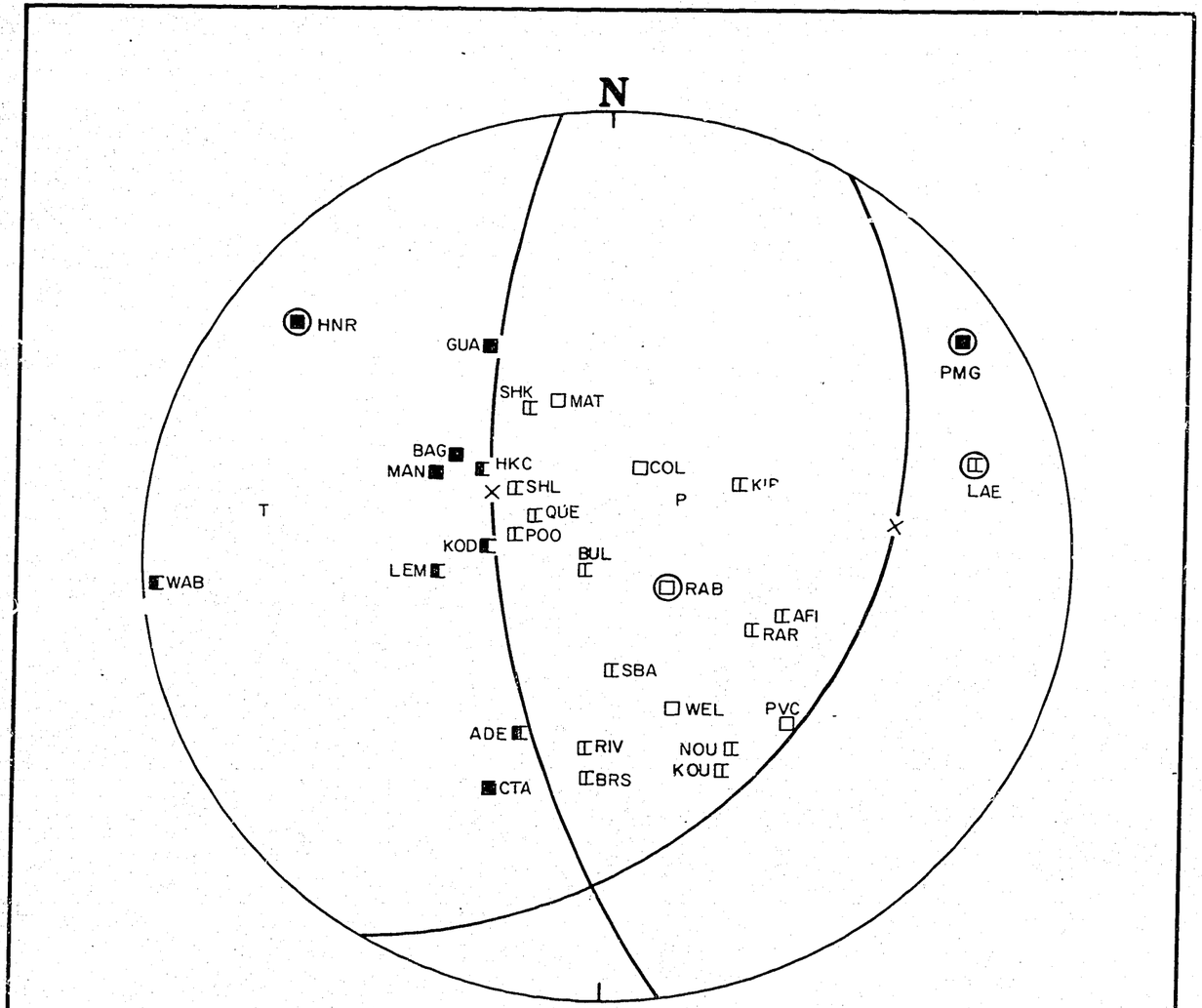


Fig.5

PNG/89-231-4A

Figure 5

| | | | |
|---|---|---|---|
| Number | : | 52 | |
| Location | : | 4.9°S, 154.2°E; 20 km northwest of Buka Island | |
| Origin Time | : | 31 May 1969 at 23 56 21.6 UT | |
| Depth | : | 403 km | |
| Magnitude (M) | : | 6.1 | |
| Type | : | Dip-slip normal, non-orthogonal | |
| Nodal Planes | : | Azimuth of Dip | Dip |
| | : | 263 | 63 |
| | : | 121 | 32 |
| Nodal-Plane Poles | : | Azimuth | Plunge |
| | : | 083 | 27 |
| | : | 301 | 58 |
| P Axis | : | 051 | 67 |
| T Axis | : | 277 | 17 |
| | | Azimuth | Plunge Uncertainty |
| B Axis | : | 182 | 17 - |

The solution is non-orthogonal as one station (LAE) is close to but on the wrong side of a nodal plane. The position of LAE on the focal sphere is sufficiently uncertain to explain the anomaly.

The compressional axis is inclined at an acute angle (23°) to the vertical dip of the seismic zone at the hypocentre.

Plotted in Plate 3.

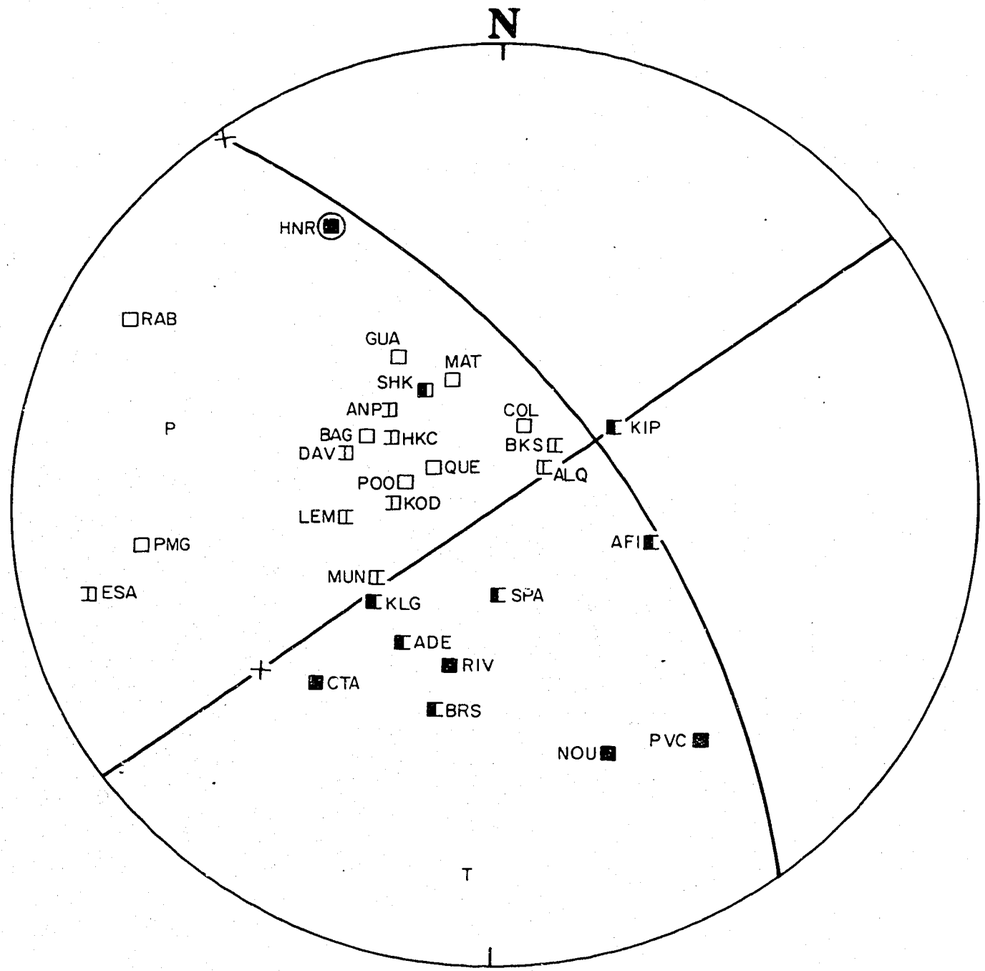


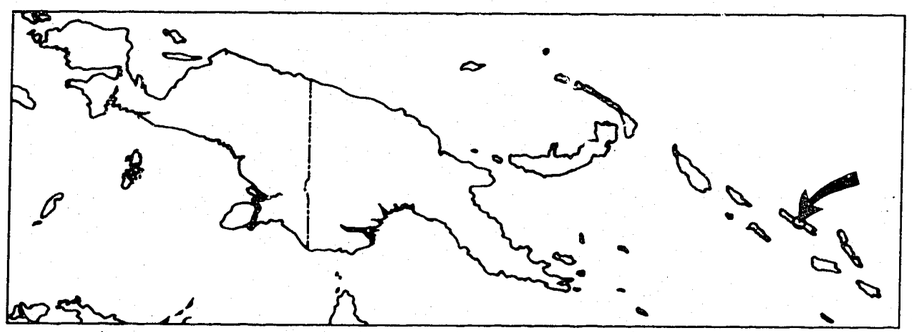

Fig. 6

PNG/B9-231-5A

Figure 6

| | | |
|---|---|---|
| Number | : | 53 |
| Location | : | 7.9°S, 159.0°E; Santa Ysabel Island |
| Origin Time | : | 14 June 1969 at 03 22 56.8 UT |
| Depth | : | 62 km |
| Magnitude (M) | : | 6.6 |
| Type | : | Strike-slip or dip-slip, non-orthogonal |
| Nodal Planes | : | Azimuth of Dip  Dip |
| | : | 144  89 |
| | : | Too uncertain |
| Nodal-Plane Poles | : | Azimuth  Plunge |
| | : | 324  01 |
| | : | Too uncertain |
| P Axis | : | |
| T Axis | : | |
| | | Azimuth  Plunge  Uncertainty |
| B Axis | : | |

The solution is poor as there are insufficient stations. There are no readings in the eastern quadrant. HNR is anomalous, and renders the solution non-orthogonal. However, the position of HNR on the focal sphere is uncertain. If HNR is moved to the edge of the projection (Fig. 6), the attitude of the nodal plane which is shown dipping steeply to the northeast can change to roughly horizontal.

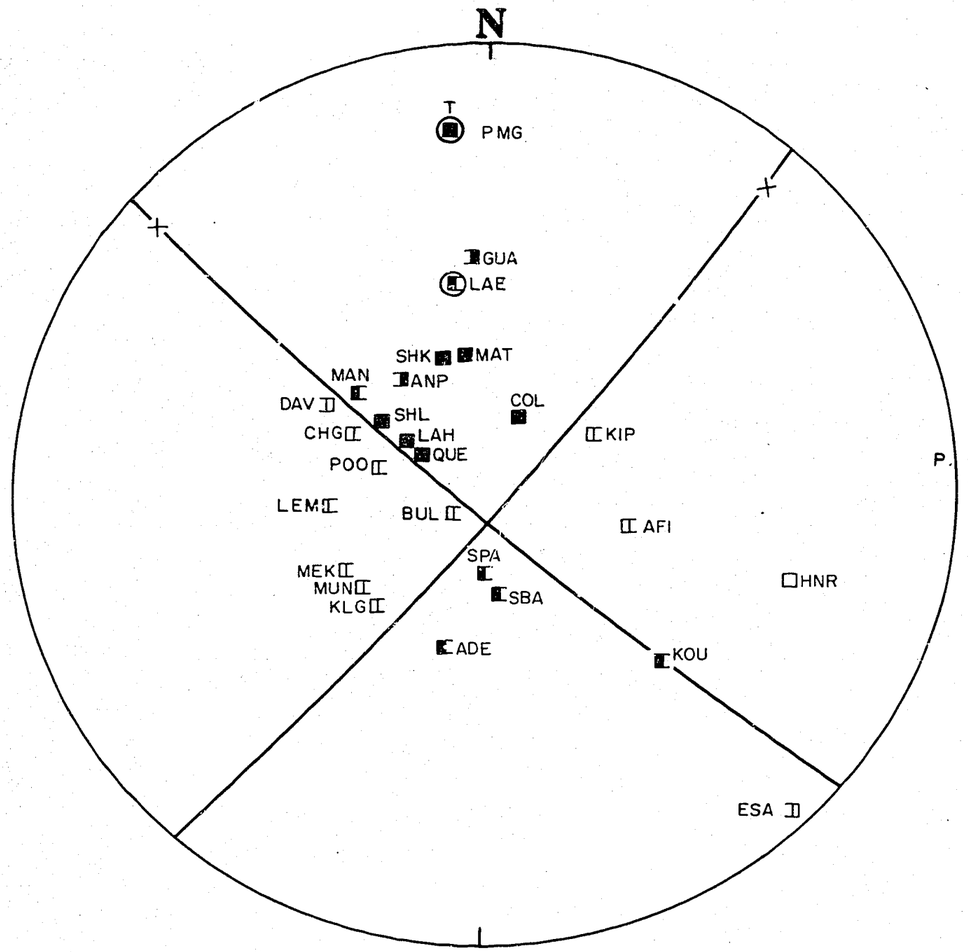


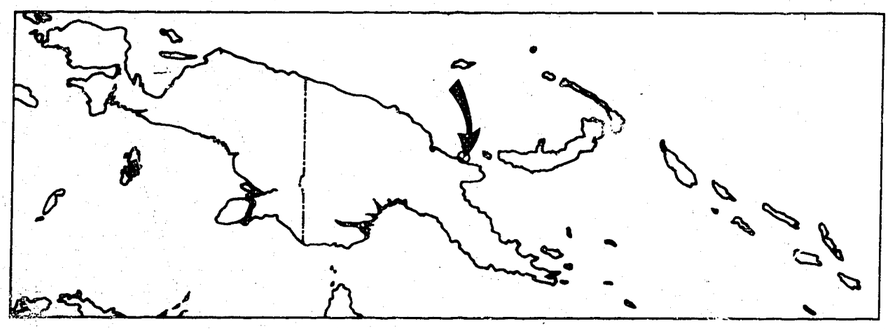

Fig. 7

PNG/BS-231-6A

Figure 7

| | | | |
|---|---|---|---|
| Number | : | 54 | |
| Location | : | 5.8°S, 146.8°E; north New Guinea coast opposite Long Island | |
| Origin Time | : | 24 June 1969 at 03 29 17.3 UT | |
| Depth | : | 113 km | |
| Magnitude (M) | : | 6.0 | |
| Type | : | Strike-slip, non-orthogonal | |
| Nodal Planes | : | Azimuth of Dip | Dip |
| | : | 130 | 85 |
| | : | 221 | 84 |
| Nodal-Plane Poles | : | Azimuth | Plunge |
| | : | 310 | 05 |
| | : | 041 | 06 |
| P Axis | : | 085 | 01 |
| T Axis | : | 354 | 08 |
| | | Azimuth | Plunge Uncertainty |
| B Axis | : | 183 | 82 - |

The solution is tight in that ESA is close to but on the wrong side of a nodal plane and renders the solution non-orthogonal. There are station readings in all four quadrants.

The earthquake hypocentre is on the border between the South Bismarck Plate and the Australian Plate, in a seismic zone which dips northward on an apparent westward extension of the New Britain Benioff zone. However, the strike-slip solution suggests that sinistral strike-slip motion is involved in the interaction of the two plates along the northern New Guinea margin.

Plotted in Plate 2.

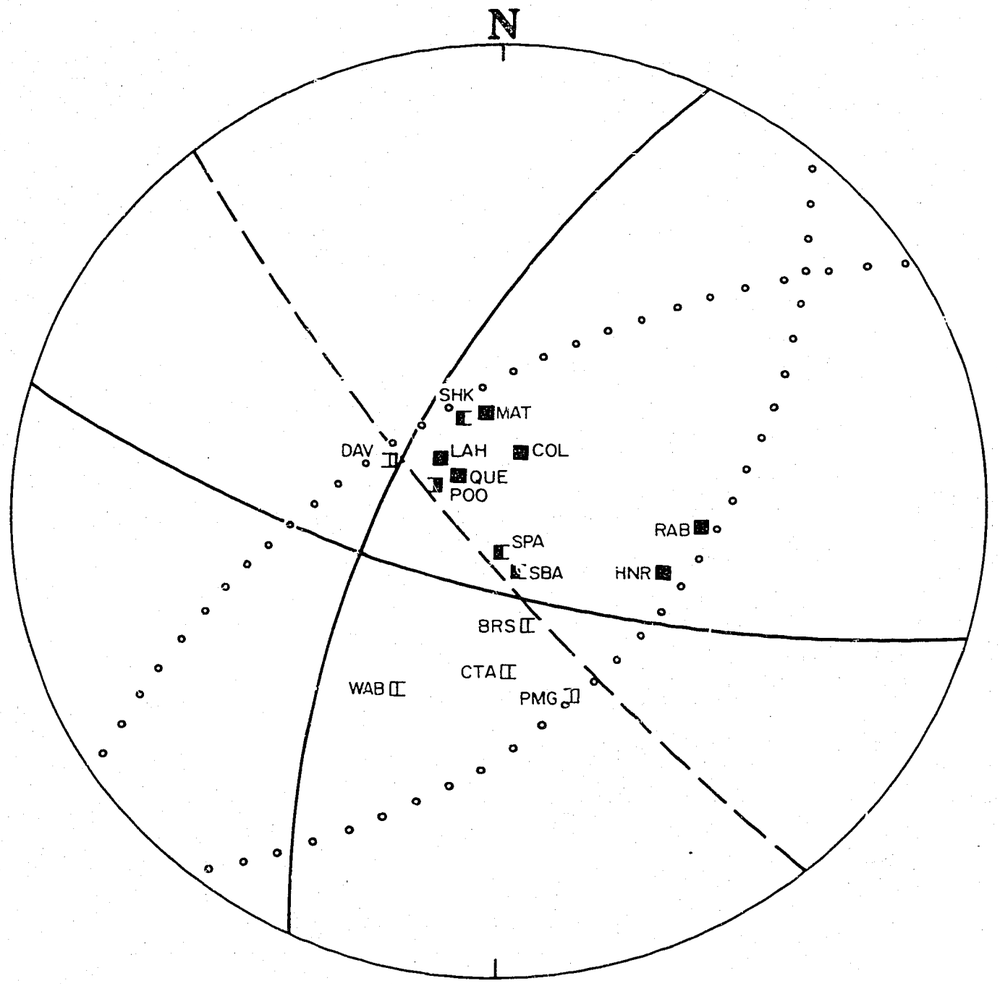


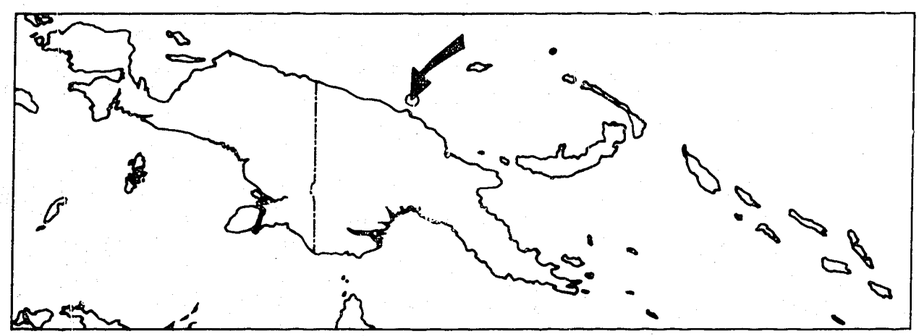

Fig. 8

PNG/89-231-7A

Figure 8

| | | |
|---|---|---|
| Number | : | 55 |
| Location | : | 3.4°S, 144.8°E; Bismarck Sea seismic lineation, Schouten Islands |
| Origin Time | : | 29 July 1969 at 01 55 20.4 UT |
| Depth | : | 6 km |
| Magnitude (M) | : | 5.9 |
| Type | : | |
| Nodal Planes | : | Azimuth of Dip Dip |
| | : | |
| | : | Too uncertain |
| Nodal-Plane Poles | : | Azimuth Plunge |
| | : | |
| | : | |
| P Axis | : | |
| T Axis | : | |

| | Azimuth | Plunge | Uncertainty |
|---|---|---|---|
| B Axis | : | | |

The solution is poor: most P-wave arrivals are emergent. Several nodal plane configurations are possible. The solid lines (Fig. 8) show one solution, in which, if the east-west-trending nodal plane is the fault plane, the motion is dextral on the Bismarck Sea seismic lineation.

The dashed line shows one nodal plane of another solution, and the two dotted lines the limiting orientations of the other nodal plane. Both sinistral motion of the Bismarck Sea seismic lineation, and a north-south overthrust, are possible interpretations.

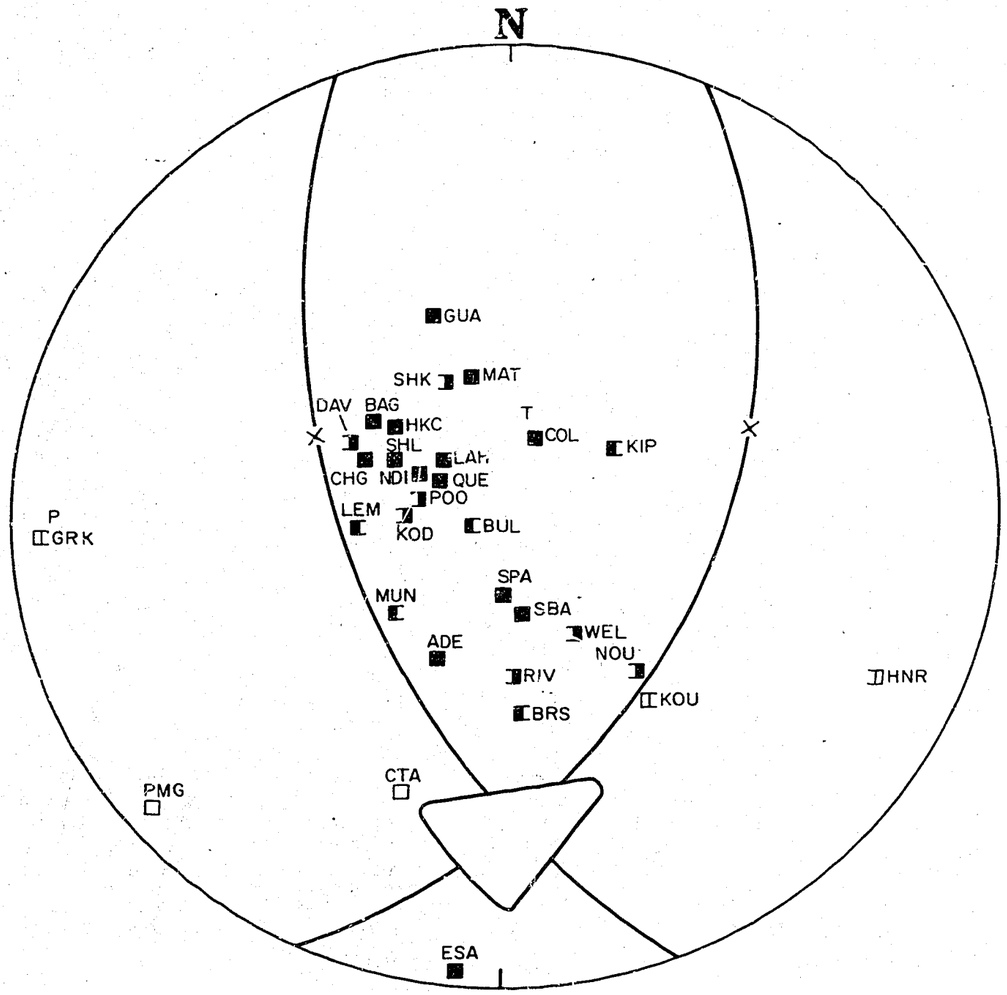


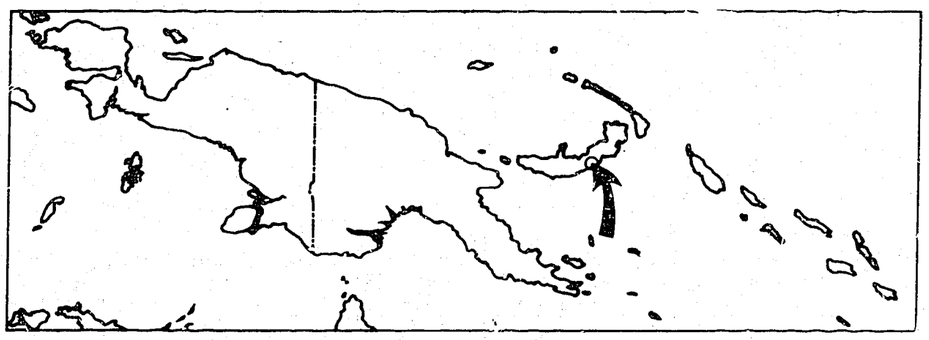

Fig. 9

PNG/B9-231-8A

Figure 9

| | | | |
|---|---|---|---|
| Number | : | 56 | |
| Location | : | 5.8°S, 151.2°E; south New Britain | |
| Origin Time | : | 26 August 1969 at 16 58 02.3 UT | |
| Depth | : | 59 km | |
| Magnitude (M) | : | 6.3 | |
| Type | : | Dip-slip overthrust | |
| Nodal Planes | : | Azimuth of Dip | Dip |
| | : | 250 | 54 |
| | : | 114 | 45 |
| Nodal-Plane Poles | : | Azimuth | Plunge |
| | : | 070 | 36 |
| | : | 294 | 45 |
| P Axis | : | 270 | 05 |
| T Axis | : | 011 | 66 |
| | | Azimuth | Plunge |
| B Axis | : | 178 | 24 |

Uncertainty: 28 x 18

The north-south strike of the overthrust is constrained by the ESA P-wave compression at the southern edge of the projection.

In terms of plate tectonics, the solution represents subduction of the Solomon Sea Plate in a westerly direction beneath New Britain.

Plotted in Plate 3.

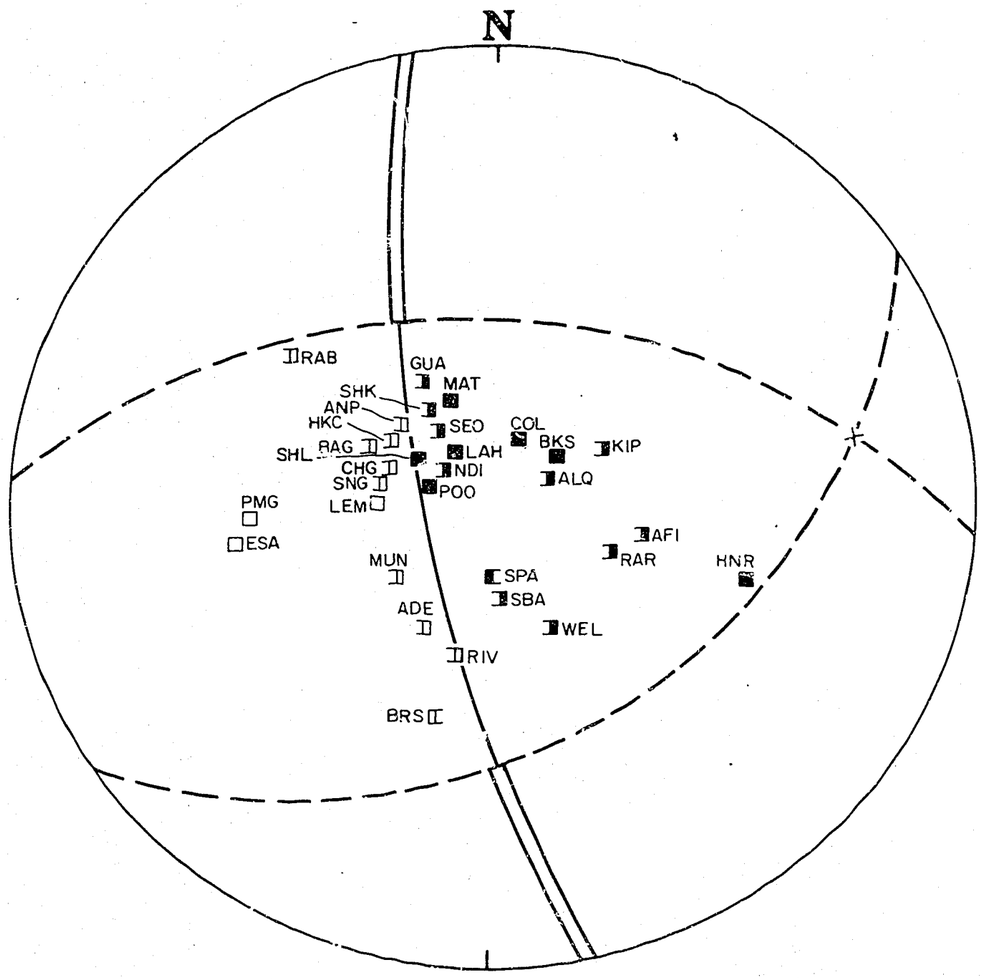


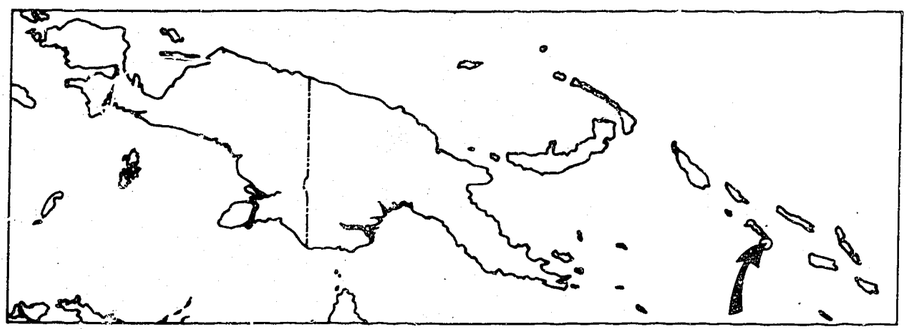

Fig. 10

PNG/B9-231-9A

Figure 10

| | | |
|---|---|---|
| Number | : | 57 |
| Location | : | 8.8°S, 157.8°E; southeast New Georgia Islands |
| Origin Time | : | 6 September 1969 at 14 49 55.9 UT |
| Depth | : | 15 km |
| Magnitude (M) | : | 6.2 |
| Type | : | Dip-slip overthrust |

| | | | |
|---|---|---|---|
| Nodal Planes | : | Azimuth of Dip | Dip |
| | : | 260 | 75 |
| | : | Too uncertain | |
| Nodal-Plane Poles | : | Azimuth | Plunge |
| | : | 080 | 15 |
| | : | Too uncertain | |

| | | | | |
|---|---|---|---|---|
| P Axis | : | | | |
| T Axis | : | | | |
| | | Azimuth | Plunge | Uncertainty |
| B Axis | : | | | |

One nodal plane is well defined, but there is virtually no constraint over the orientation of the other nodal plane, whose azimuth of dip can vary from southeast through east to north. The limiting orientations of the second nodal plane are shown as dashed lines in Figure 10.

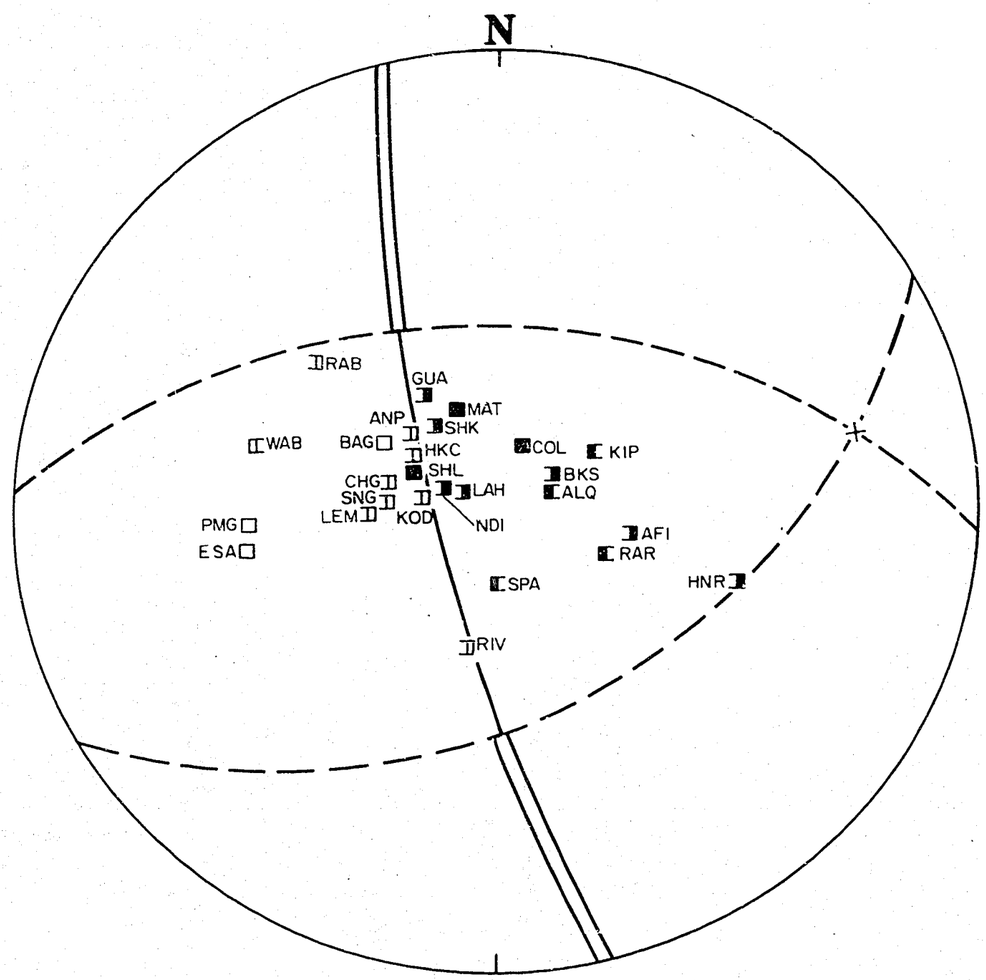


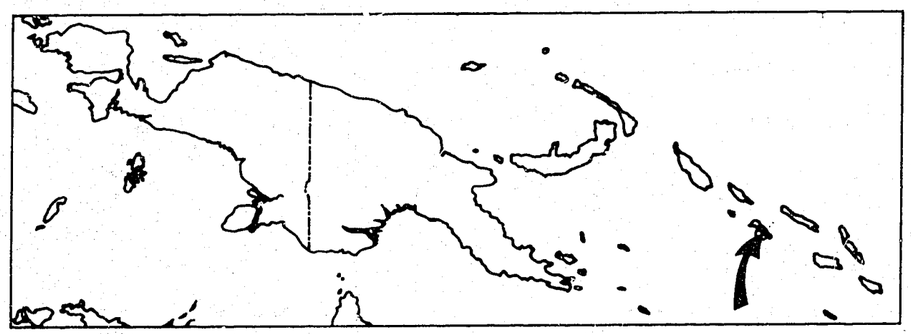

Fig. 11

PNG/89-231-10A

Figure 11

| | | |
|---|---|---|
| Number | : | 58 |
| Location | : | 8.9°S, 157.9°E; southeast New Georgia Islands |
| Origin Time | : | 6 September 1969 at 17 08 03.2 UT |
| Depth | : | 10 km |
| Magnitude (M) | : | 6.4 |
| Type | : | Dip-slip overthrust |
| Nodal Planes | : | Azimuth of Dip  Dip |
| | : | 257  75 |
| | : | Too uncertain |
| Nodal-Plane Poles | : | Azimuth  Plunge |
| | : | 077  15 |
| | : | Too uncertain |
| P Axis | : | |
| T Axis | : | |

| | Azimuth | Plunge | Uncertainty |
|---|---|---|---|
| B Axis | : | | |

One nodal plane is well defined, but there is virtually no constraint over the orientation of the other nodal plane, whose azimuth of dip can vary from southeast through east to north. The limiting orientations of the second nodal plane are shown as dashed lines in Figure 11.

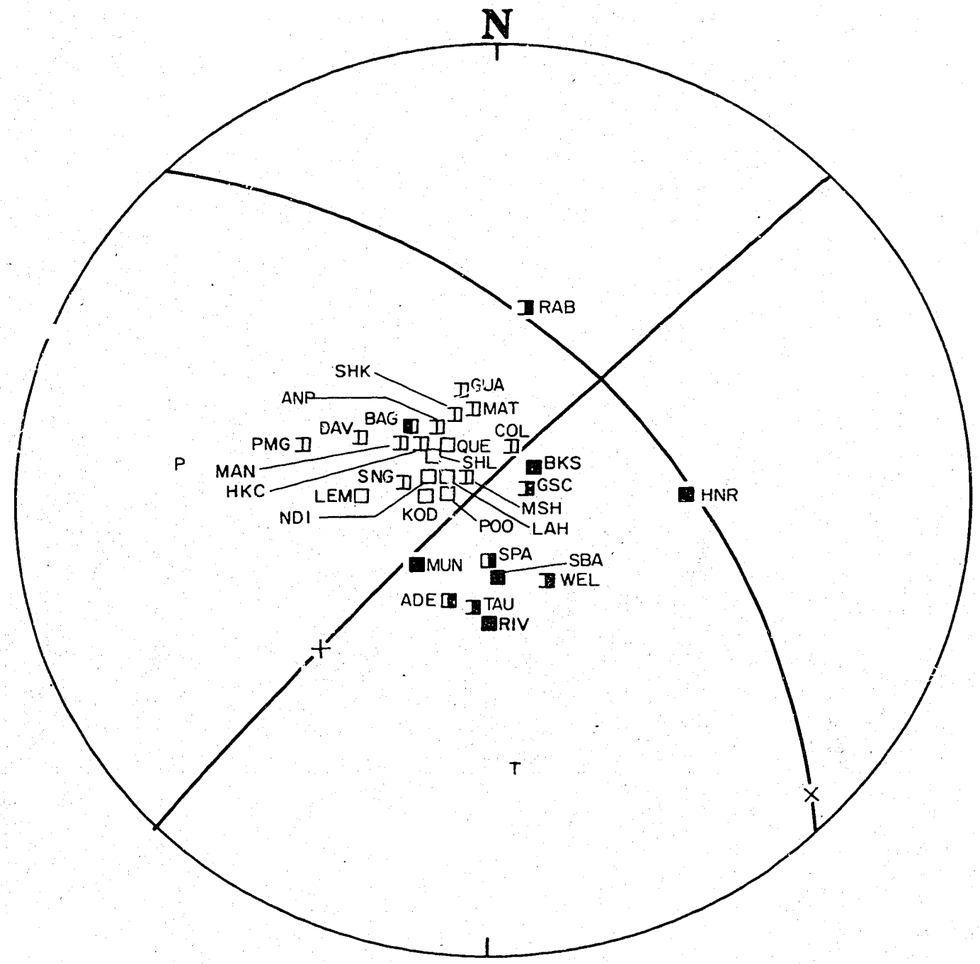


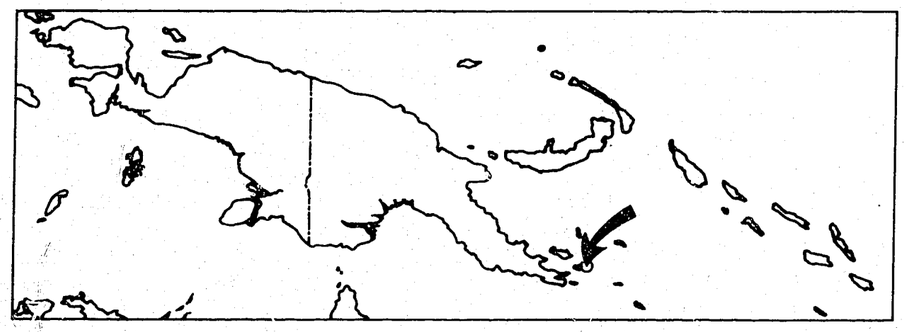

Fig. 12

PNG/B9-231-11A

Figure 12

| | | | | |
|---|---|---|---|---|
| Number | : | 59 | | |
| Location | : | 9.6°S, 151.5°E; D'Entrecasteaux Islands 60 km east of Fergusson Island | | |
| Origin Time | : | 6 January 1970 at 05 35 51.8 UT | | |
| Depth | : | 8 km | | |
| Magnitude (M) | : | 6.2 | | |
| Type | : | Strike-slip | | |
| Nodal Planes | : | Azimuth of Dip | Dip | |
| | : | 048 | 53 | |
| | : | 315 | 86 | |
| Nodal-Plane Poles | : | Azimuth | Plunge | |
| | : | 228 | 37 | |
| | : | 135 | 04 | |
| P Axis | : | 278 | 22 | |
| T Axis | : | 174 | 28 | |
| | | Azimuth | Plunge | Uncertainty |
| B Axis | : | 039 | 53 | 1 x 1 |

One nodal plane of the solution is clearly defined. The other is restrained by only two stations, RAB and HNR, whose positions on the focal sphere depend on the P-wave velocity at the earthquake focus. The tables of Bessonova et al. (1960), which assume a surface P-wave velocity of 5.6 km/sec, were used; they indicated a nodal-plane dip of 53° and a strike-slip solution. If a higher P-wave velocity is assumed the nodal-plane dip decreases, and the solution changes to predominantly dip-slip.

Short-period P-wave arrivals were generally emergent, and probably account for the anomalous short-period polarities recorded at stations SPA, ADE, and BAG (Fig. 12).

Curtis (1973), who used only short-period seismograms, obtained a strike-slip solution of opposite polarity for the earthquake.

Plotted in Plate 2.

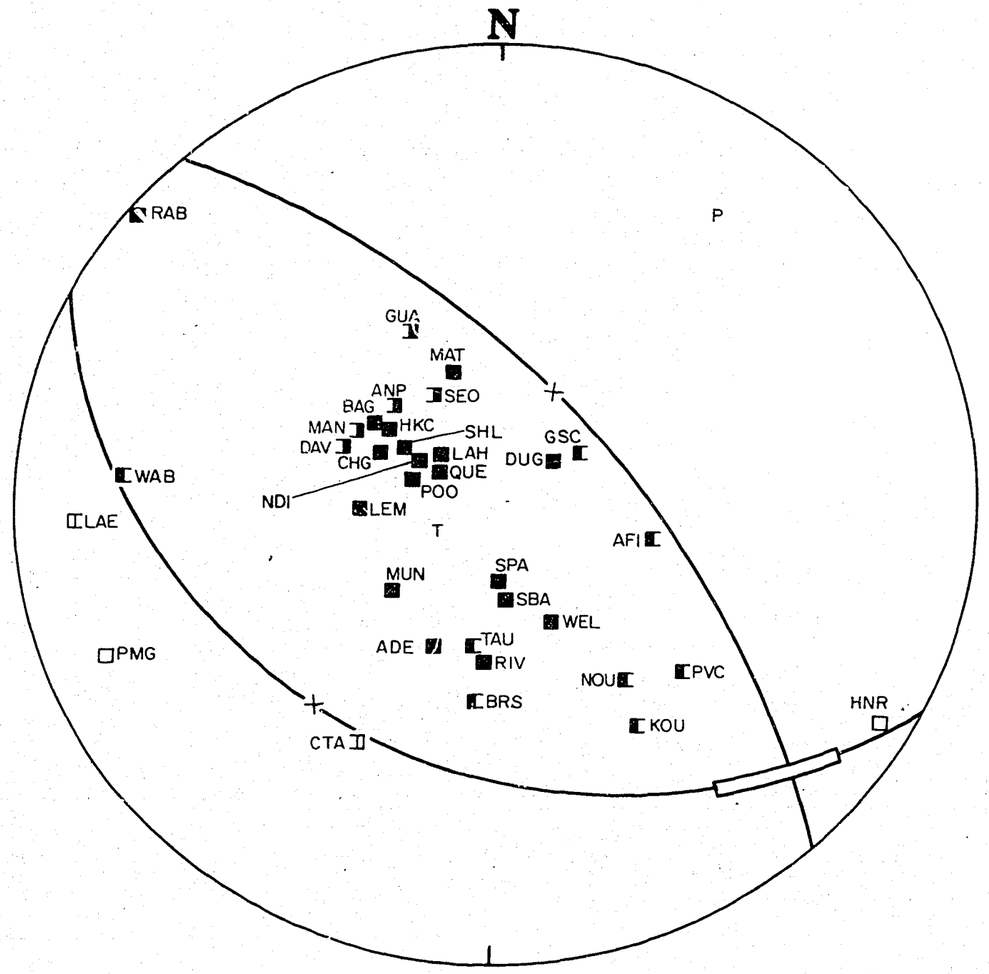


Fig.13

PNG/B9-231-12A

Figure 13

| | | | |
|---|---|---|---|
| Number | : | 60 | |
| Location | : | 6.3°S, 154.6°E; 30 km west of Bougainville | |
| Origin Time | : | 28 March 1970 at 07 45 59.9 UT | |
| Depth | : | 64 km | |
| Magnitude (M) | : | 5.9 | |
| Type | : | Dip-slip overthrust | |
| Nodal Planes | : | Azimuth of Dip | Dip |
| | : | 207 | 30 |
| | : | 049 | 62 |
| Nodal-Plane Poles | : | Azimuth | Plunge |
| | : | 037 | 60 |
| | : | 229 | 28 |
| P Axis | : | 036 | 15 |
| T Axis | : | 238 | 74 |
| | | Azimuth | Plunge Uncertainty |
| B Axis | : | 134 | 09 18 x 2 |

Although there is only one station in the northeast dilatational quadrant, the solution is reasonably good, as one nodal plane is well defined and the other is constrained by the orthogonality criterion.

The overthrust solution is consistent with the concept of subduction of the Solomon Sea Plate at Bougainville.

Plotted in Plate 3.

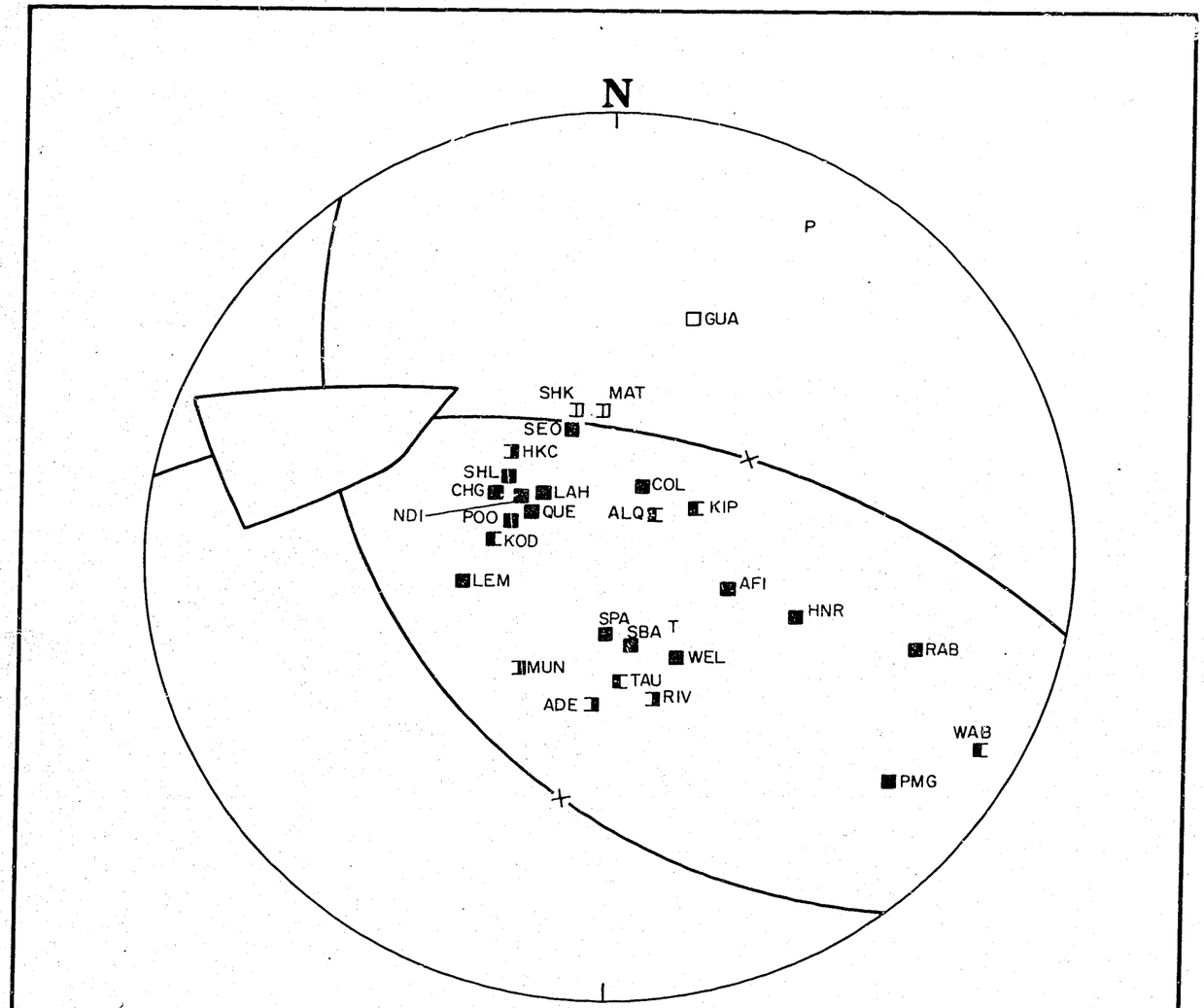


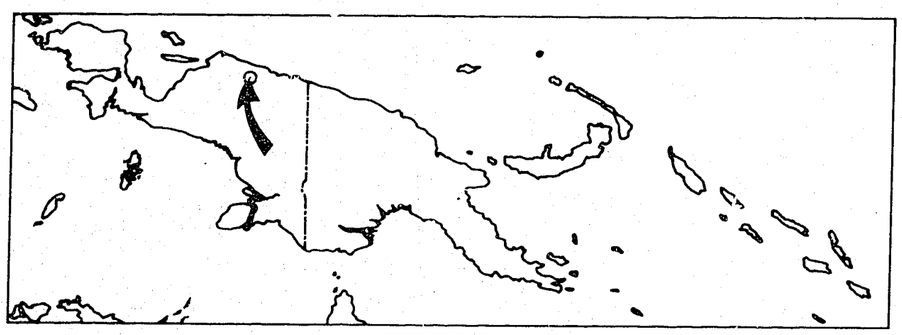

Fig. 14

PNG/B9-231-13A

Figure 14

| | | | |
|---|---|---|---|
| Number | : | 61 | |
| Location | : | 2.9°S, 139.1°E; Irian Jaya, 300 km east of Geelvink Bay | |
| Origin Time | : | 12 June 1970 at 08 06 16.6 UT | |
| Depth | : | 32 km | |
| Magnitude (M) | : | 6.3 | |
| Type | : | Dip-slip overthrust | |
| Nodal Planes | : | Azimuth of Dip | Dip |
| | : | 233 | 40 |
| | : | 009 | 59 |
| Nodal-Plane Poles | : | Azimuth | Plunge |
| | : | 053 | 50 |
| | : | 189 | 31 |
| P Axis | : | 029 | 09 |
| T Axis | : | 141 | 65 |
| | | Azimuth | Plunge Uncertainty |
| B Axis | : | 295 | 22 40 x 20 |

The solution is clearly overthrust even though there are no stations in the southwest dilatational quadrant.

The compressional axis orientation is 029°, which is significantly different from Le Pichon's (1968, 1970) plate collision azimuth of 075°.

Plotted in Plate 3.

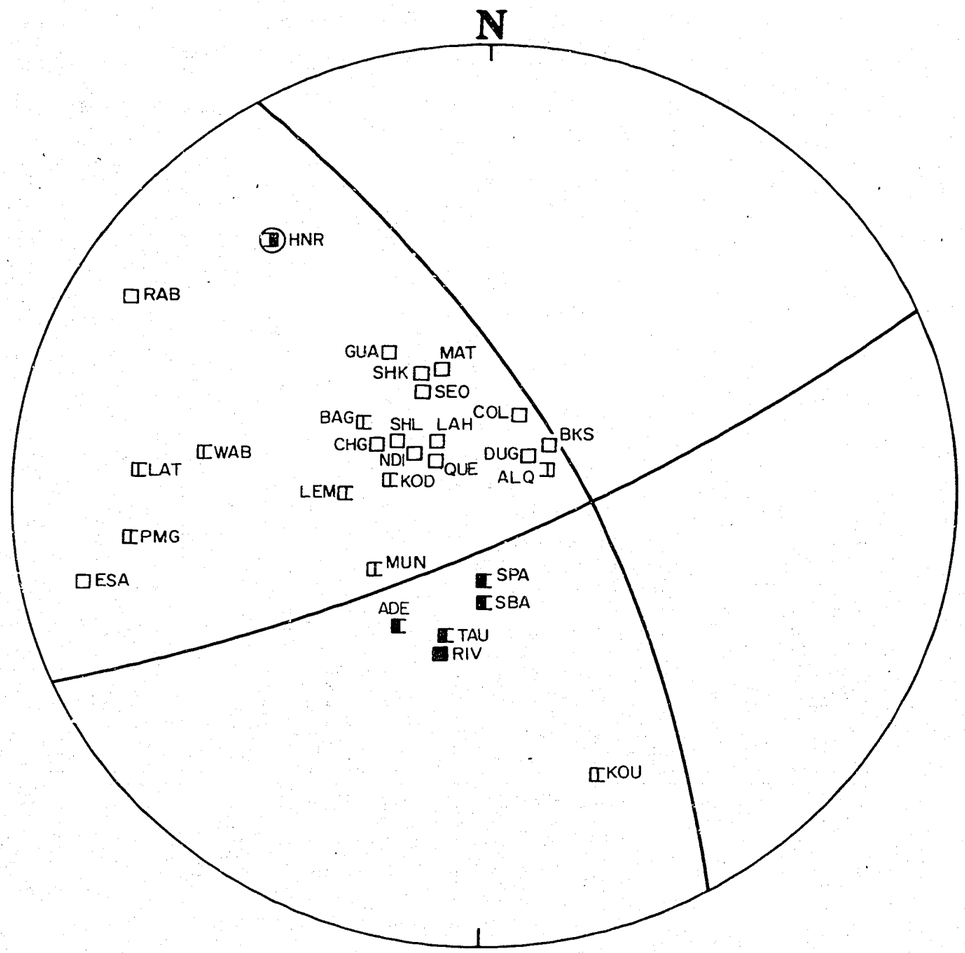


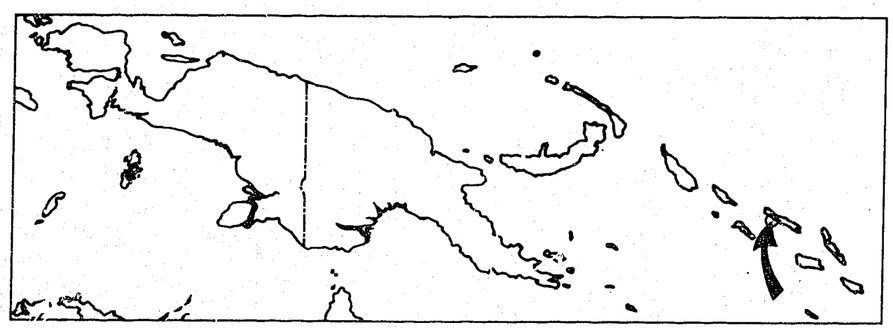

Fig. 15

PNG/B9-231-14A

Figure 15

| | | |
|---|---|---|
| Number | : | 62 |
| Location | : | 7.9°S, 158.7°E; Santa Ysabel Island |
| Origin Time | : | 3 August 1970 at 07 01 11.9 UT |
| Depth | : | 67 km |
| Magnitude (M) | : | 6.6 |
| Type | : | Strike-slip or dip-slip; non-orthogonal |
| Nodal Planes | : | Azimuth of Dip Dip |
| | : | |
| | : | Too uncertain |
| Nodal-Plane Poles | : | Azimuth Plunge |
| | : | |
| | : | Too uncertain |
| P Axis | : | |
| T Axis | : | |

| | Azimuth | Plunge | Uncertainty |
|---|---|---|---|
| B Axis | : | | |

The solution is extremely poor: there are no stations in the northeast and southeast quadrants; and two stations, HNR and KOU, are anomalous, and introduce a large degree of uncertainty into the solution.

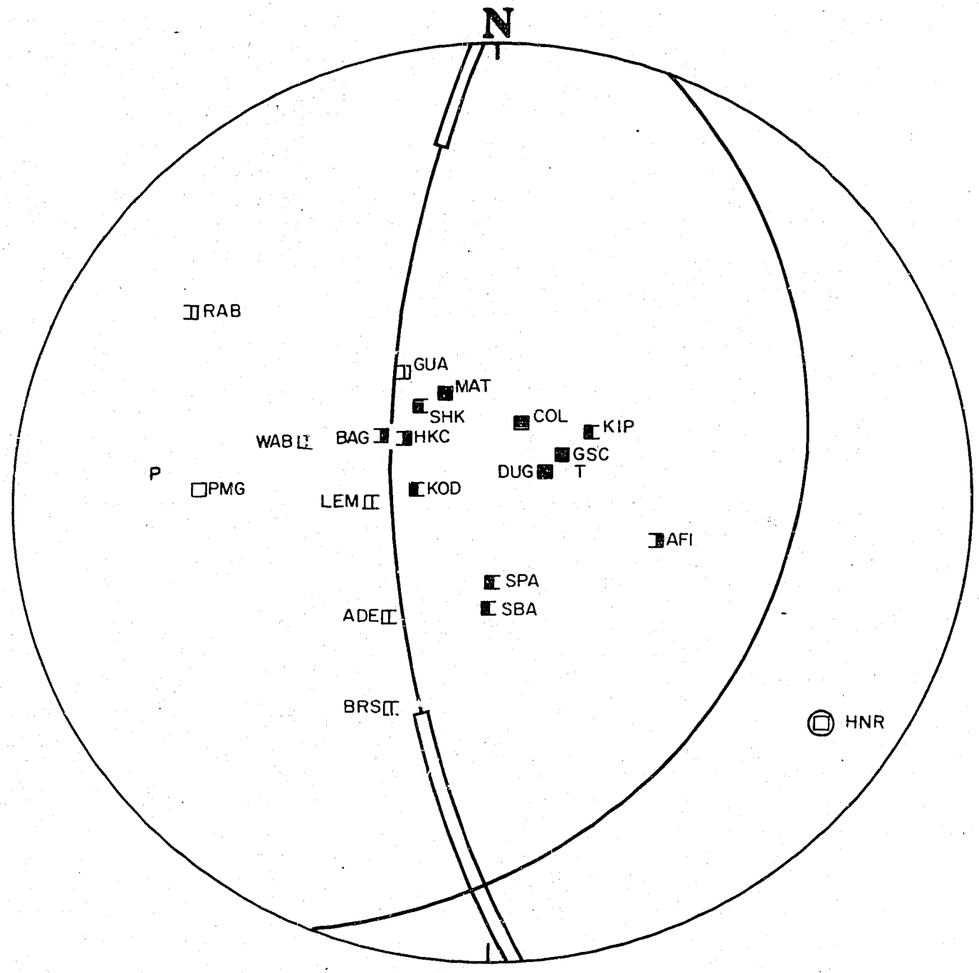


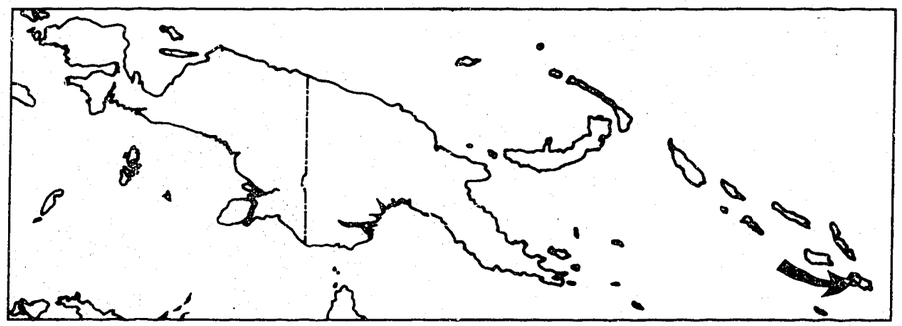

Fig.16

PNG/B9-231-15A

Figure 16

| | | | | |
|---|---|---|---|---|
| Number | : | 63 | | |
| Location | : | 10.5°S, 161.5°E; San Cristobal Island | | |
| Origin Time | : | 19 August 1970 at 02 11 09.4 UT | | |
| Depth | : | 33 km | | |
| Magnitude (M) | : | 6.1 | | |
| Type | : | Dip-slip overthrust | | |
| Nodal Planes | : | Azimuth of Dip | Dip | |
| | : | 112 | 26 | |
| | : | 267 | 66 | |
| Nodal-Plane Poles | : | Azimuth | Plunge | |
| | : | 292 | 64 | |
| | : | 087 | 24 | |
| P Axis | : | 276 | 21 | |
| T Axis | : | 068 | 67 | |
| | | Azimuth | Plunge | Uncertainty |
| B Axis | : | 182 | 10 | 58 x 1 |

The solution is poor: the P-wave first arrivals are generally weak; and, because of poor station distribution, there is virtually no control on the orientation of one nodal plane.

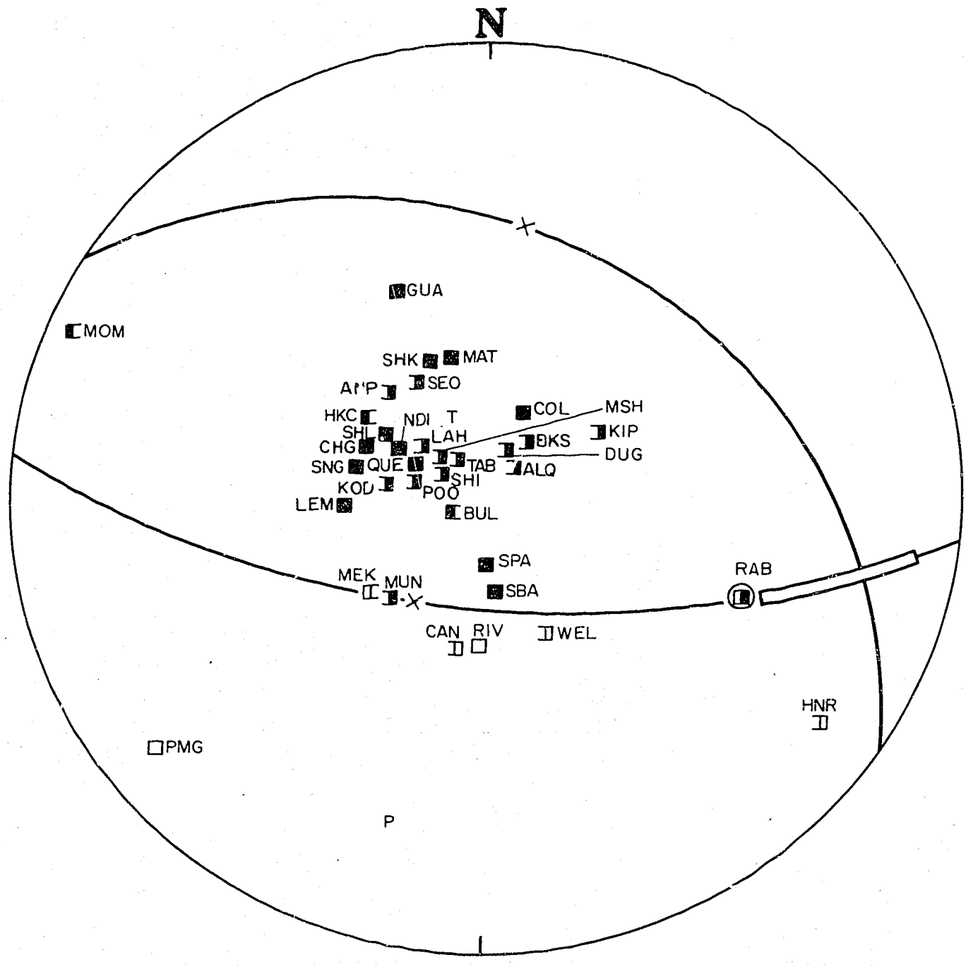


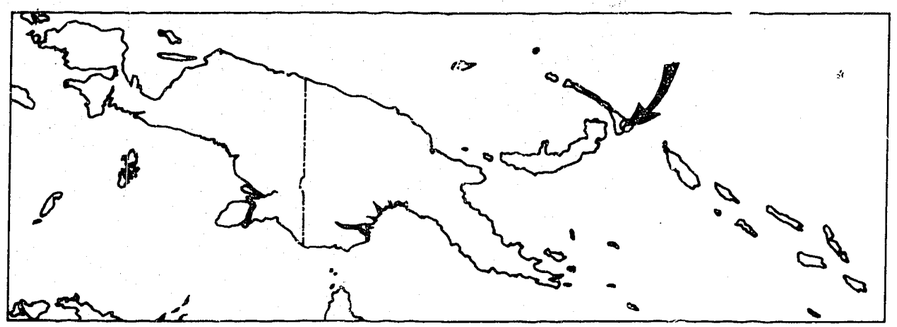

Fig.17

PNG/B9-231-16A

Figure 17

| | | | |
|---|---|---|---|
| Number | : | 64 | |
| Location | : | 4.6°S, 153.1°E; southeast New Ireland | |
| Origin Time | : | 28 August 1970 at 01 02 48.9 UT | |
| Depth | : | 88 km | |
| Magnitude (M) | : | 6.6 | |
| Type | : | Dip-slip overthrust | |
| Nodal Planes | : | Azimuth of Dip | Dip |
| | : | 035 | 30 |
| | : | 187 | 63 |
| Nodal-Plane Poles | : | Azimuth | Plunge |
| | : | 215 | 60 |
| | : | 007 | 27 |
| P Axis | : | 196 | 17 |
| T Axis | : | 337 | 69 |
| | | Azimuth | Plunge Uncertainty |
| B Axis | : | 103 | 12 26 x 1 |

One nodal plane is reasonably well defined. It is drawn to pass through RAB, which recorded a short-period dilatation and a long-period compression. There is little control over the other nodal plane.

The hypocentre is at the triple junction of the South Bismarck, Solomon Sea, and Pacific Plates. The overthrust solution is consistent with subduction of the Solomon Sea Plate. The northeast azimuth of fault plane dip suggests that the earthquake occurred on the border between the Solomon Sea and Pacific Plates.

Plotted in Plate 3.

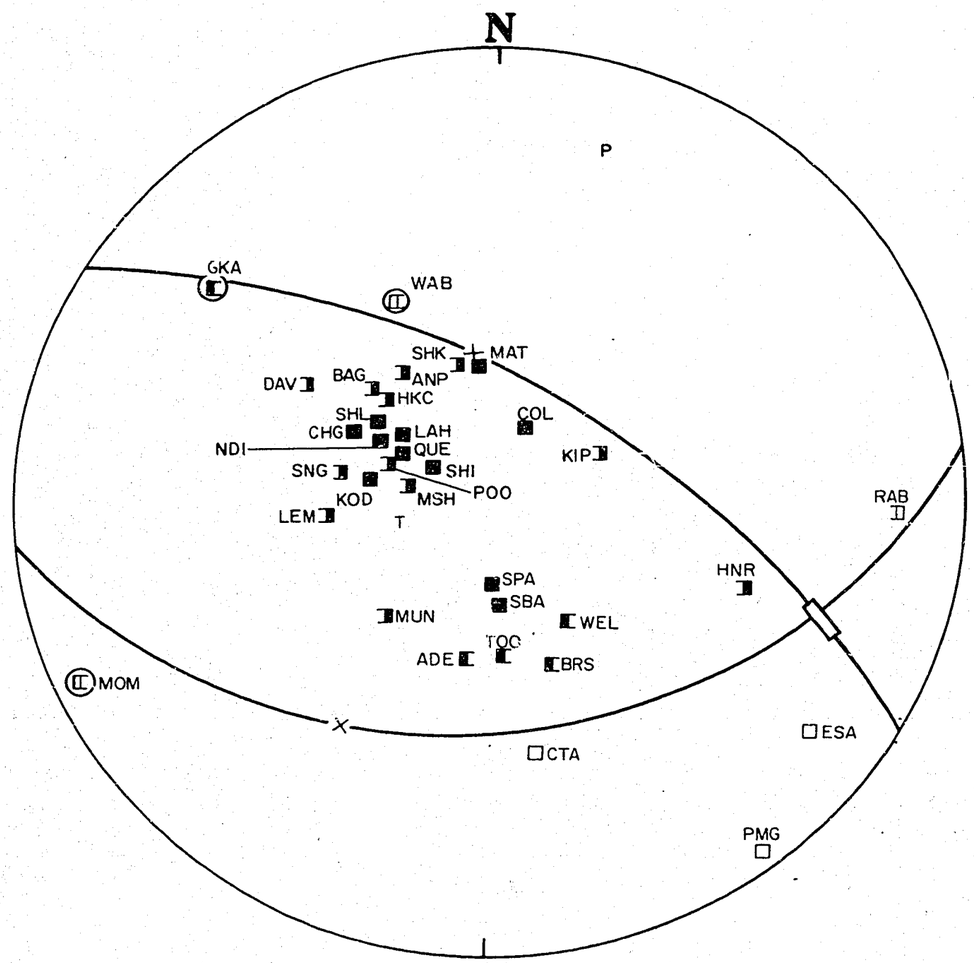


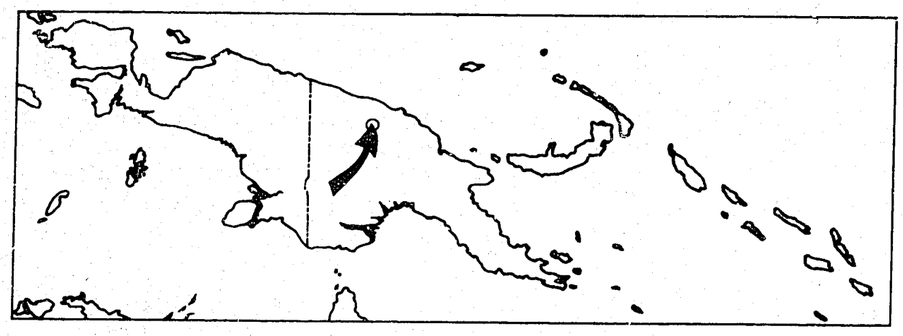

Fig.18

PNG/89-231-17A

Figure 18

| | | | | |
|---|---|---|---|---|
| Number | : | 65 | | |
| Location | : | 4.1°S, 143.0°E; Sepik River plains 90 km southwest of Wewak | | |
| Origin Time | : | 13 October 1970 at 18 53 30.0 UT | | |
| Depth | : | 120 km | | |
| Magnitude (M) | : | 6.3 | | |
| Type | : | Dip-slip overthrust | | |
| Nodal Planes | : | Azimuth of Dip | Dip | |
| | : | 031 | 60 | |
| | : | 173 | 36 | |
| Nodal-Plane Poles | : | Azimuth | Plunge | |
| | : | 211 | 30 | |
| | : | 353 | 54 | |
| P Axis | : | 016 | 12 | |
| T Axis | : | 254 | 68 | |
| | | Azimuth | Plunge | Uncertainty |
| B Axis | : | 110 | 18 | 12 x 1 |

The overthrust solution is reasonably well defined. The compressional axis is oriented north-northeast and the tensional axis is near-vertical.

The tectonic significance of the earthquake is obscure. It occurred at a depth of 120 km, which is below the lithosphere, in a zone of hypocentres beneath the Sepik River. At an azimuth of 016°, the compressional axis orientation is different from Le Pichon's (1968, 1970) 075° plate collision azimuth.

Plotted in Plate 3.

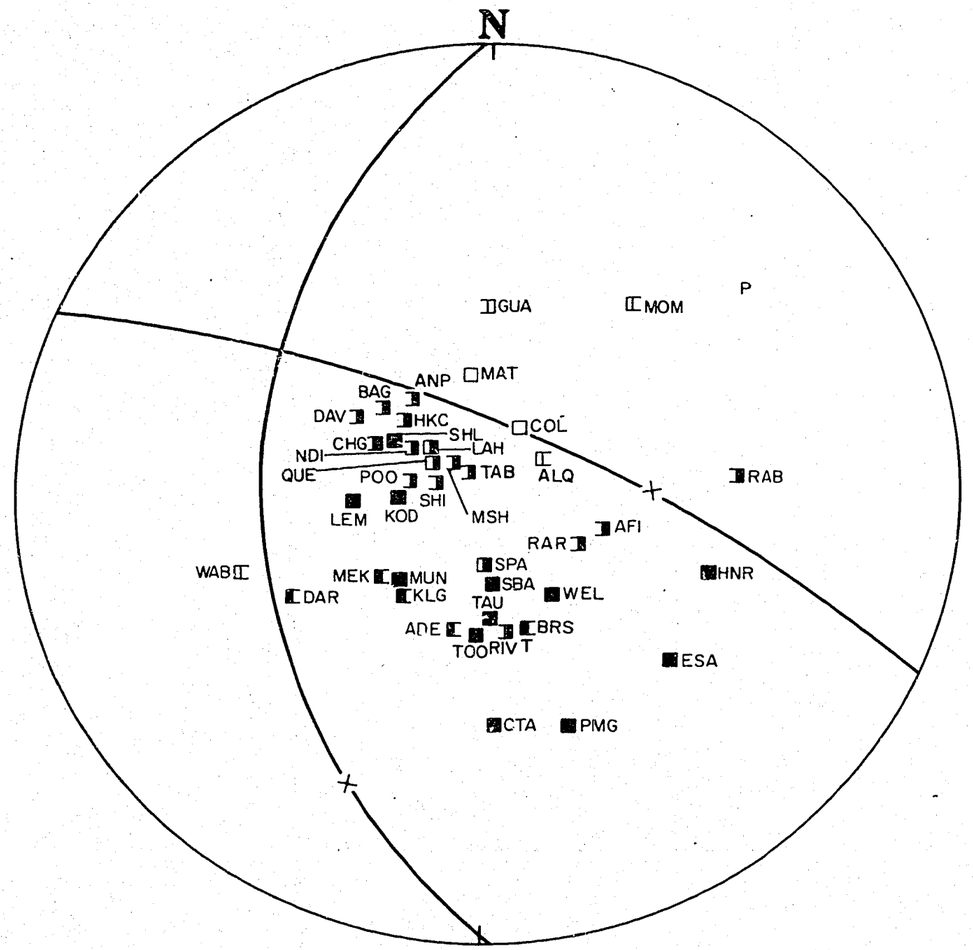


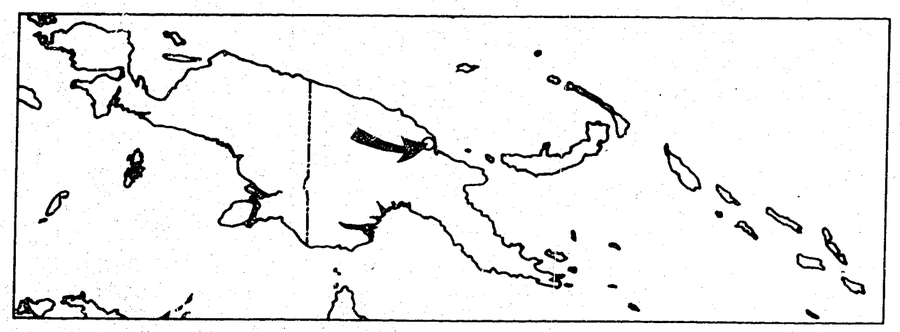

Fig. 19

PNG/89-231-18A

Figure 19

| | | | | |
|---|---|---|---|---|
| Number | : | 66 | | |
| Location | : | 4.9°S, 145.5°E; 25 km northwest of Madang, beneath the Adelbert Range | | |
| Origin Time | : | 31 October 1970 at 17 53 09.3 UT | | |
| Depth | : | 42 km | | |
| Magnitude (M) | : | 7.0 | | |
| Type | : | Dip-slip overthrust, non-orthogonal | | |
| Nodal Planes | : | Azimuth of Dip | Dip | |
| | : | 024 | 72 | |
| | : | 269 | 38 | |
| Nodal-Plane Poles | : | Azimuth | Plunge | |
| | : | 204 | 18 | |
| | : | 089 | 52 | |
| P Axis | : | 048 | 19 | |
| T Axis | : | 164 | 51 | |
| | | Azimuth | Plunge | Uncertainty |
| B Axis | : | 306 | 33 | - |

The solution is non-orthogonal because the RAB P-wave arrival, a compression, is in a dilatational quadrant. A better, but still non-orthogonal fit is obtained by assuming a crustal focus, either at a depth shallower than 42 km or at a depth of 42 km within a crust thicker than 42 km beneath the 1600-m-high Adelbert Range. This solution is shown in Figure 19. High local Modified Mercalli intensities of 8, and possibly 9 (Everingham, 1975a), suggest that the focal depth may have been less than 42 km.

Several anomalous short-period dilatations were recorded within the central compressional quadrant. A possible reason for the anomalous RAB arrival is that the P-wave path was refracted along the South Bismarck Volcanic Arc.

The aftershock pattern of the earthquake is elongated on an east-northeast azimuth and suggests strike-slip motion on a vertical plane (Everingham, 1975a). The overthrust solution is at variance with the strike-slip hypothesis.

Plotted in Plate 3.

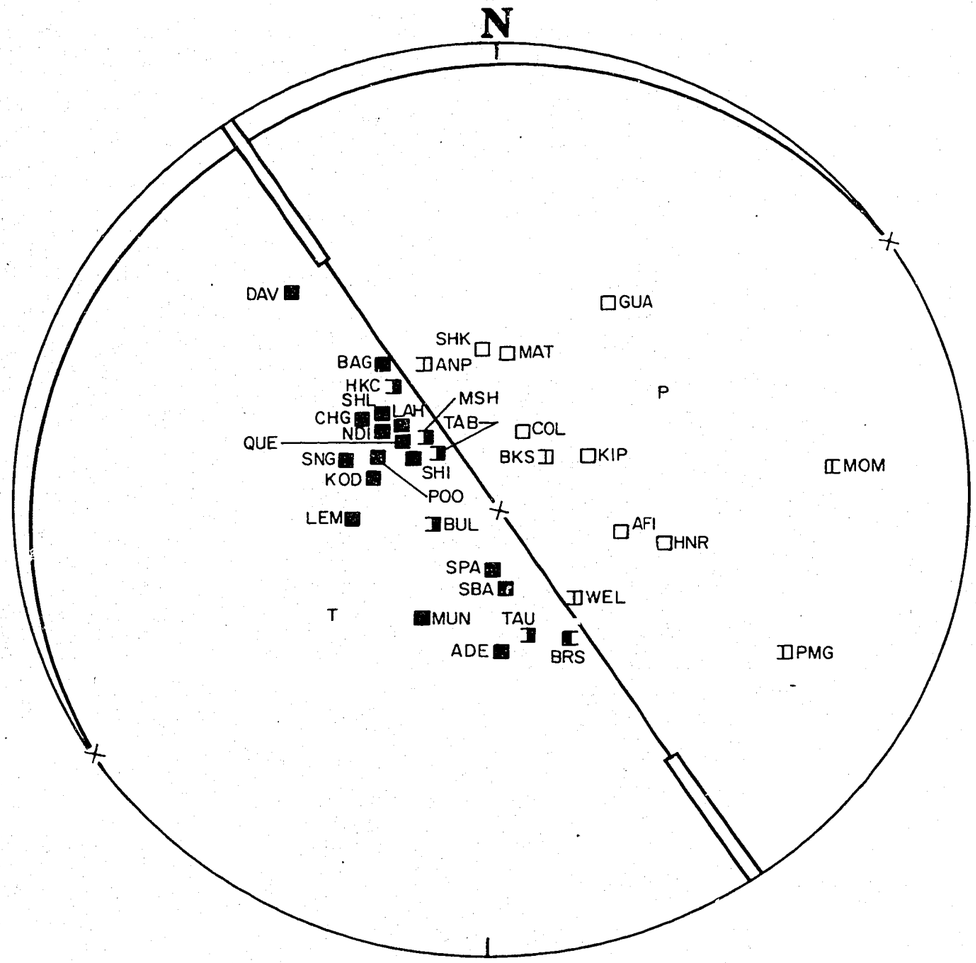


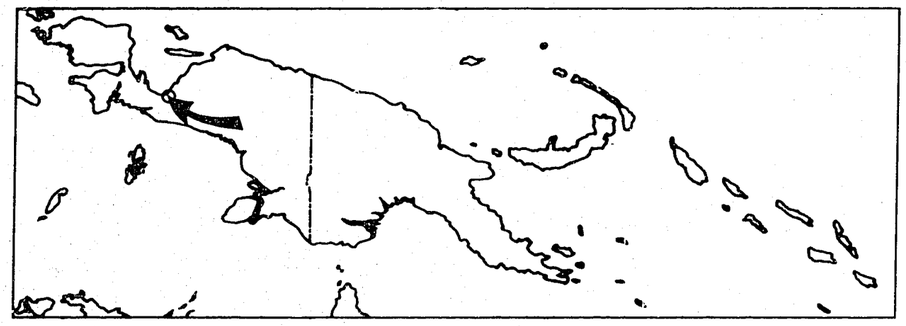

Fig. 20

PNG/89-231-19A

Figure 20

| | | | |
|---|---|---|---|
| Number | : | 67 | |
| Location | : | $3.4^{o}$S, $135.6^{o}$E; Irian Jaya, south coast of Geelvink Bay | |
| Origin Time | : | 8 November 1970 at 22 35 46.7 UT | |
| Depth | : | 33 km | |
| Magnitude (M) | : | 7.0 | |
| Type | : | Motion on a vertical plane, or horizontal motion on a slightly inclined plane | |
| Nodal Planes | : | Azimuth of Dip | Dip |
| | : | 056 | 90 |
| | : | 326 | 03 |
| Nodal-Plane Poles | : | Azimuth | Plunge |
| | : | 056 | 00 |
| | : | 146 | 87 |
| P Axis | : | 059 | 45 |
| T Axis | : | 233 | 45 |
| | | Azimuth | Plunge | Uncertainty |
| B Axis | : | 326 | 03 | 46 x 1 |

One plane is vertical and well defined, while one other, which is almost horizontal, has an uncertain orientation that is due to the absence of local and regional seismic stations.

The solution may represent movement on either a vertical or roughly horizontal fault plane.

Plotted in Plate 3.

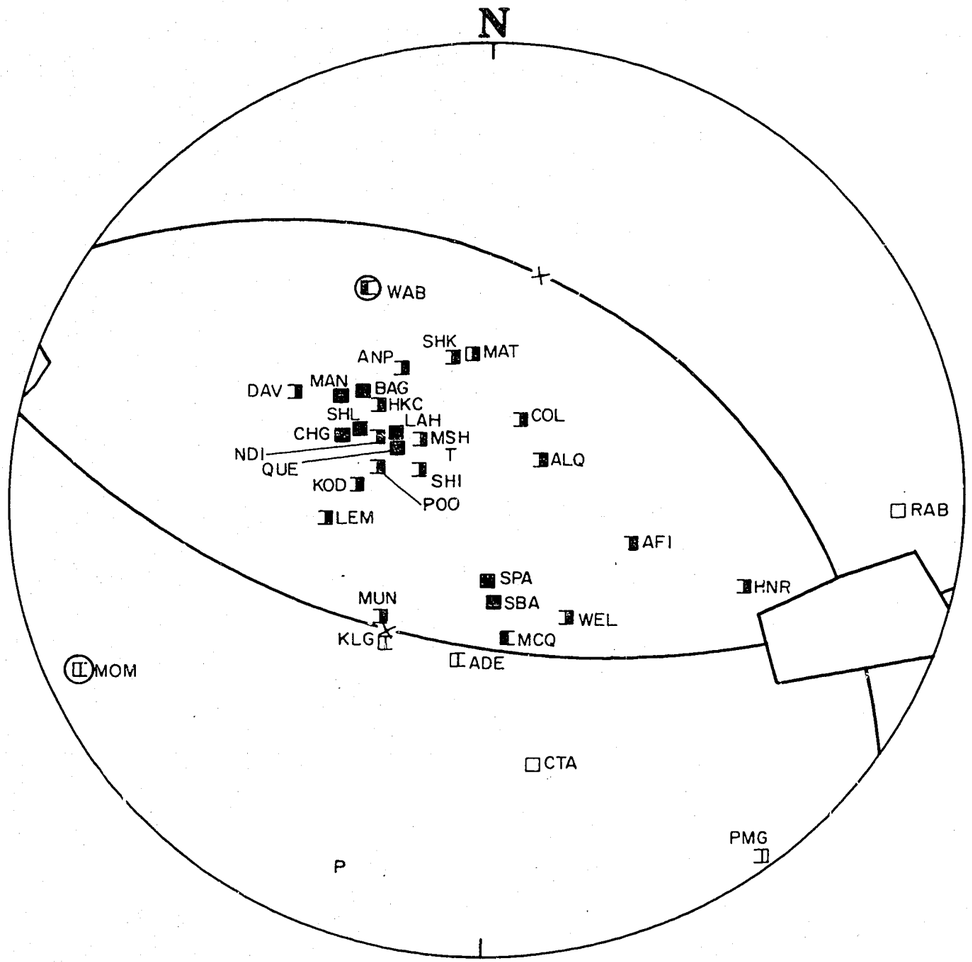


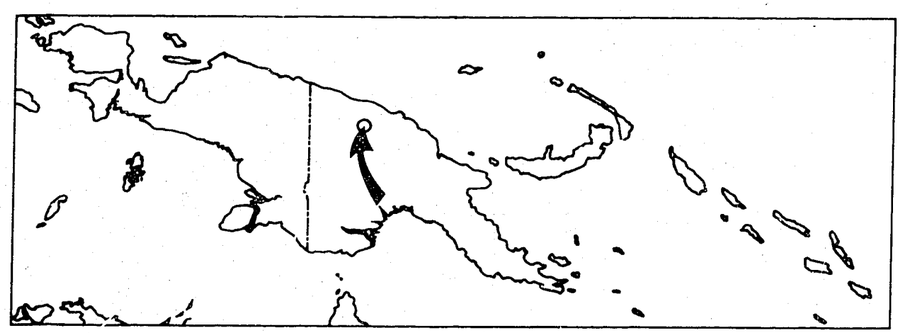

Fig. 21

PNG/B9-231-20A

Figure 21

| | | | | |
|---|---|---|---|---|
| Number | : | 68 | | |
| Location | : | 4.1°S, 142.9°E; Sepik River plains 105 km southwest of Wewak | | |
| Origin Time | : | 28 November 1979 at 20 22 50.6 UT | | |
| Depth | : | 114 km | | |
| Magnitude (M) | : | 6.1 | | |
| Type | : | Dip-slip overthrust | | |
| Nodal Planes | : | Azimuth of Dip | Dip | |
| | : | 035 | 38 | |
| | : | 191 | 54 | |
| Nodal-Plane Poles | : | Azimuth | Plunge | |
| | : | 215 | 52 | |
| | : | 011 | 36 | |
| P Axis | : | 201 | 09 | |
| T Axis | : | 327 | 76 | |
| | | Azimuth | Plunge | Uncertainty |
| B Axis | : | 110 | 11 | 26 x 14 |

Although only one dilatation is plotted in the northeast quadrant, the solution is clearly overthrust. The compressional axis is almost horizontal and oriented NNE-SSW, significantly different from Le Pichon's (1968, 1970) 075° azimuth of major plate collision.

Plotted in Plate 3.

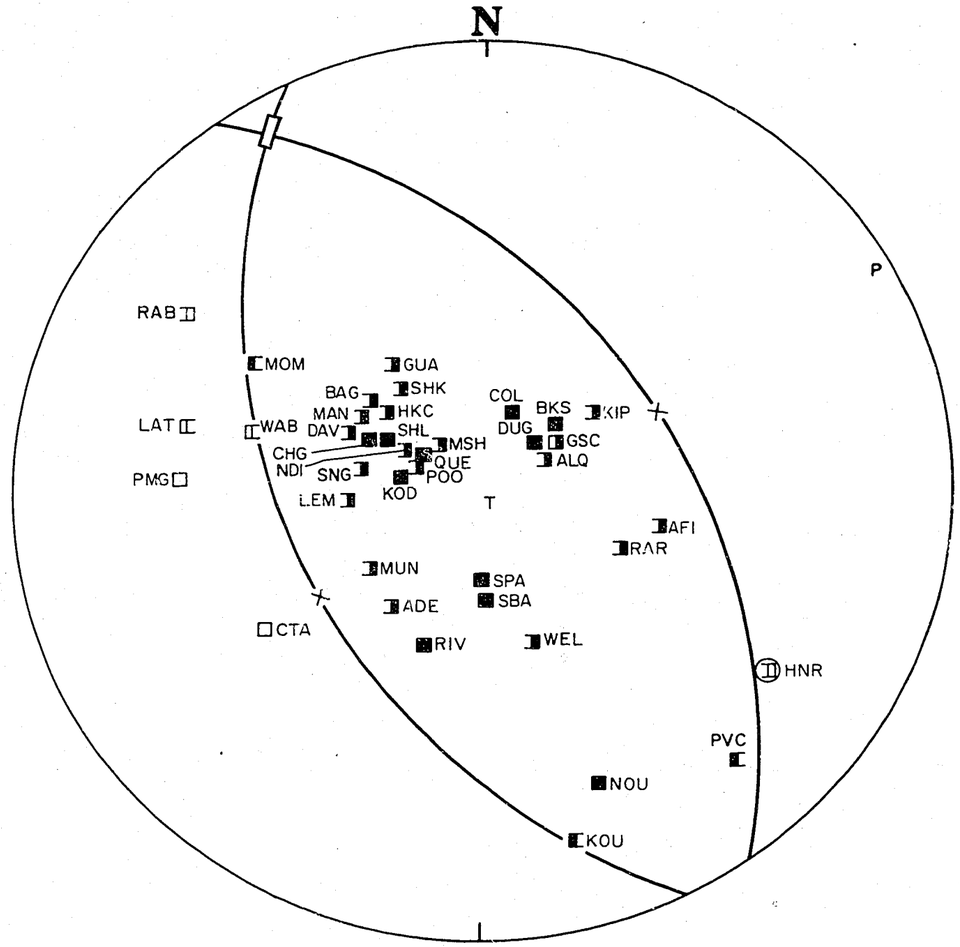


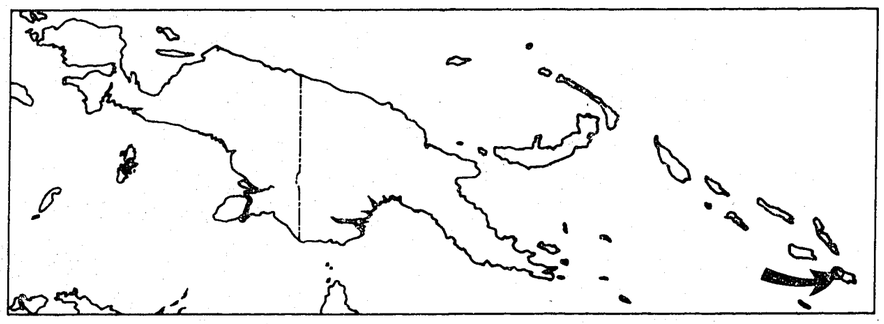

Fig. 22

PNG/B9-231-21A

Figure 22

| | | | |
|---|---|---|---|
| Number | : | 69 | |
| Location | : | 10.5°S, 161.4°E; San Cristobal Island | |
| Origin Time | : | 29 December 1970 at 02 26 12.2 UT | |
| Depth | : | 72 km | |
| Magnitude (M) | : | 6.9 | |
| Type | : | Dip-slip overthrust | |
| Nodal Planes | : | Azimuth of Dip | Dip |
| | : | 056 | 46 |
| | : | 244 | 44 |
| Nodal-Plane Poles | : | Azimuth | Plunge |
| | : | 236 | 44 |
| | : | 064 | 46 |
| P Axis | : | 060 | 00 |
| T Axis | : | 150 | 86 |
| | | Azimuth | Plunge Uncertainty |
| B Axis | : | 329 | 03 5 x 1 |

The solution is fairly tight, although there is only one station in the northeast dilatational quadrant. The compressional axis is horizontal, and the solution is consistent with a collision between the Australian Plate and the Pacific Plate in the southeast Solomon Islands.

Plotted in Plate 3.

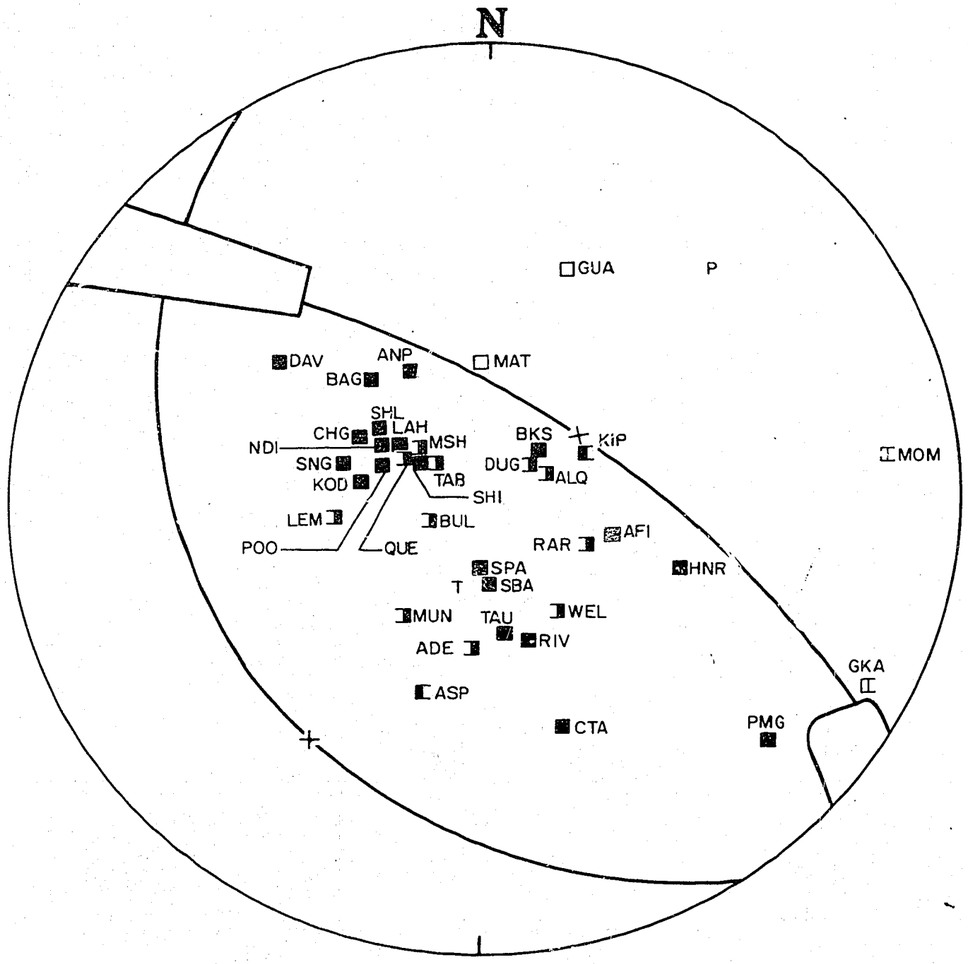


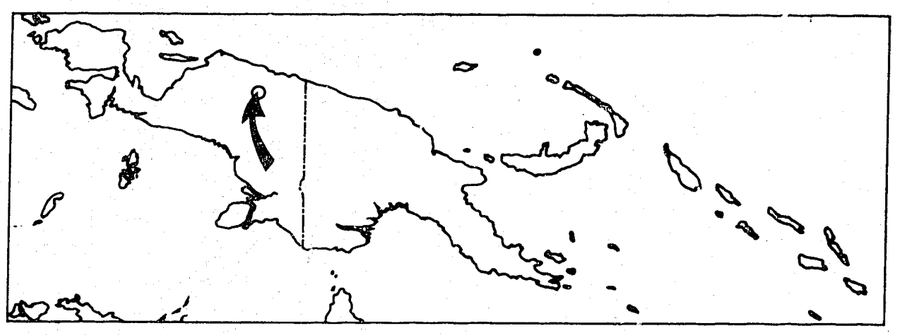

Fig. 23

PNG/B9-231-22A

Figure 23

| | | | | |
|---|---|---|---|---|
| Number | : | 70 | | |
| Location | : | 3.1°S, 139.7°E; Irian Jaya, 400 km east of Geelvink Bay | | |
| Origin Time | : | 10 January 1971 at 07 17 03.7 UT | | |
| Depth | : | 33 km | | |
| Magnitude (M) | : | 8.0 | | |
| Type | : | Dip-slip overthrust | | |
| Nodal Planes | : | Azimuth of Dip | Dip | |
| | : | 034 | 66 | |
| | : | 238 | 26 | |
| Nodal-Plane Poles | : | Azimuth | Plunge | |
| | : | 214 | 24 | |
| | : | 058 | 64 | |
| P Axis | : | 042 | 20 | |
| T Axis | : | 194 | 68 | |
| | | Azimuth | Plunge | Uncertainty |
| B Axis | : | 208 | 09 | 42 x 10 |

The earthquake was felt with intensity 7 in Papua New Guinea near the Irian Jaya border.

Although the station distribution is inadequate, there are no stations in the southwest dilatational quadrant, and there is considerable uncertainty in the orientation of the B axis, a solution has been obtained.

The compressional axis orientation is roughly northeast.

Plotted in Plate 3.

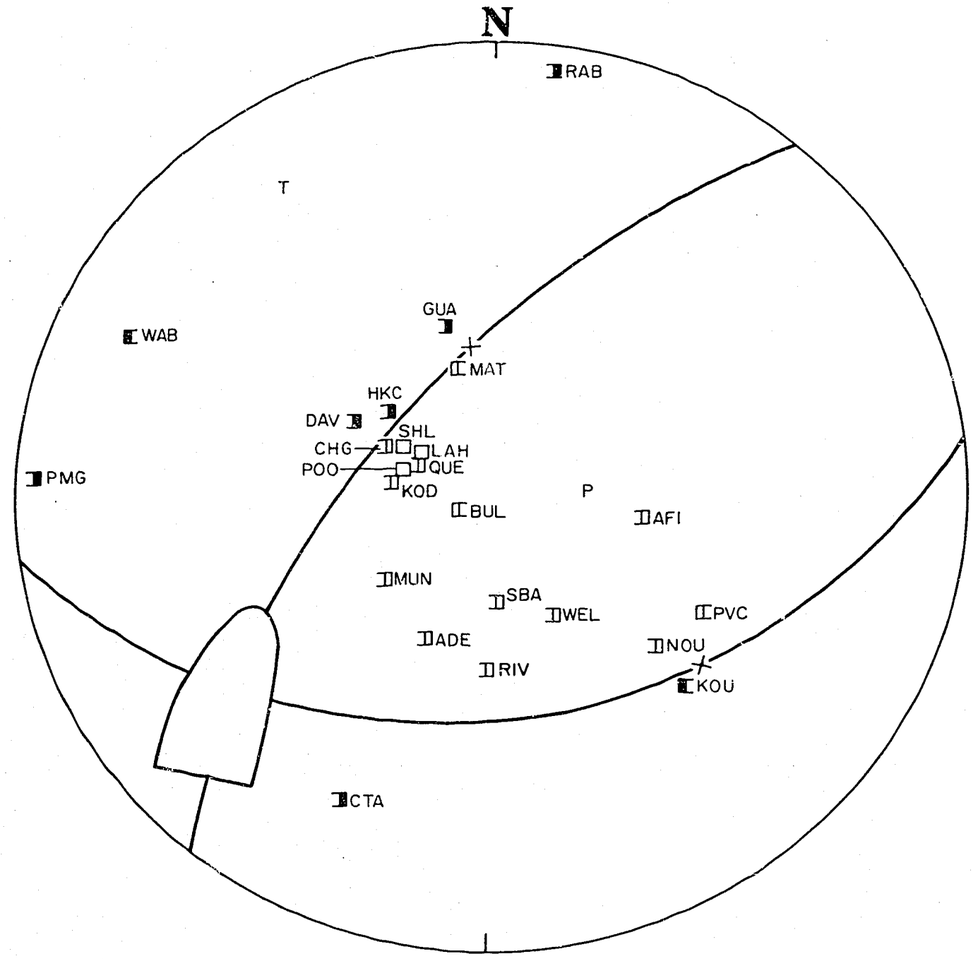


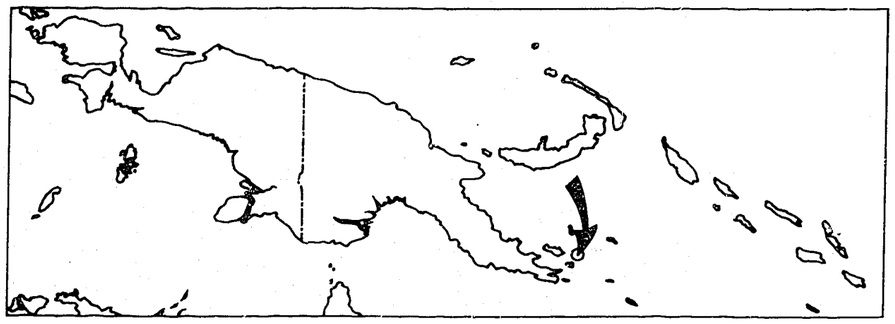

Fig. 24

PNG/B9-231-23A

Figure 24

| | | | |
|---|---|---|---|
| Number | : | 71 | |
| Location | : | 9.6°S, 151.4°E; D'Entrecasteaux Islands | |
| Origin Time | : | 25 January 1971 at 00 18 26.1 UT | |
| Depth | : | 38 km | |
| Magnitude (M) | : | 6.3 | |
| Type | : | Dip-slip normal | |
| Nodal Planes | : | Azimuth of Dip | Dip |
| | : | 172 | 38 |
| | : | 309 | 60 |
| Nodal-Plane Poles | : | Azimuth | Plunge |
| | : | 352 | 52 |
| | : | 129 | 30 |
| P Axis | : | 084 | 66 |
| T Axis | : | 326 | 12 |
| | | Azimuth | Plunge Uncertainty |
| B Axis | : | 233 | 20 29 x 15 |

Despite the large uncertainty of the B-axis orientation, the solution is clearly a normal fault oriented northwest. It is consistent with the hypothesis that the Solomon Sea Plate is moving away from the Australian Plate in a northwesterly direction and opening the Woodlark Basin.

Plotted in Plate 3.

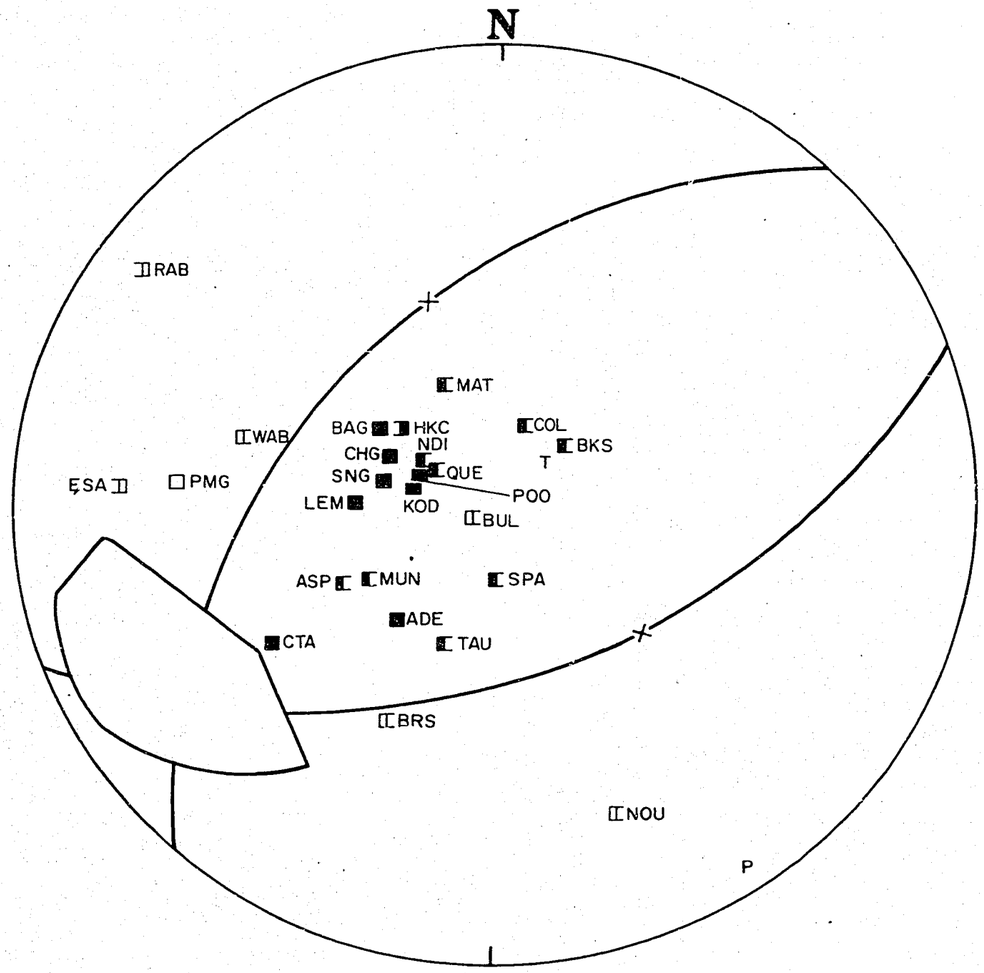


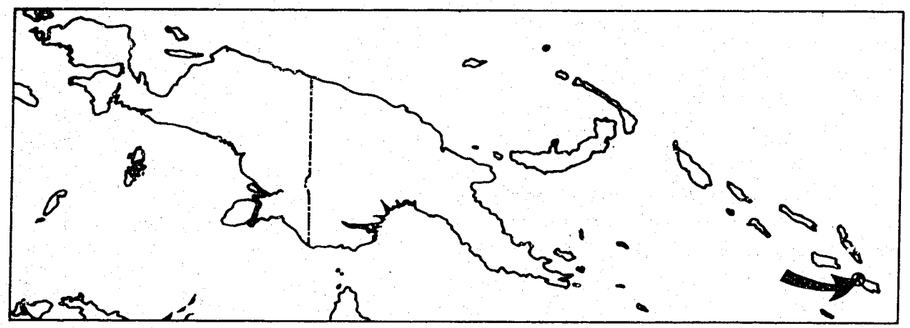

Fig. 25

PNG/B9-231-24A

Figure 25

| | | | | |
|---|---|---|---|---|
| Number | : | 72 | | |
| Location | : | 10.4°S, 161.3°E; San Cristobal Island | | |
| Origin Time | : | 26 February 1971 at 04 55 50.0 UT | | |
| Depth | : | 90 km | | |
| Magnitude (M) | : | 6.5 | | |
| Type | : | Dip-slip overthrust | | |
| Nodal Planes | : | Azimuth of Dip | Dip | |
| | : | 162 | 50 | |
| | : | 311 | 44 | |
| Nodal-Plane Poles | : | Azimuth | Plunge | |
| | : | 342 | 40 | |
| | : | 131 | 46 | |
| P Axis | : | 146 | 03 | |
| T Axis | : | 045 | 74 | |
| | | Azimuth | Plunge | Uncertainty |
| B Axis | : | 237 | 15 | 48 x 20 |

The solution is poor with a large B-axis uncertainty due to inadequate station distribution. The compressional axis is oriented southeast, parallel to the Solomon Islands chain, and nearly at right-angles to the compressional axes of two other San Cristobal earthquakes (Nos. 63 and 69).

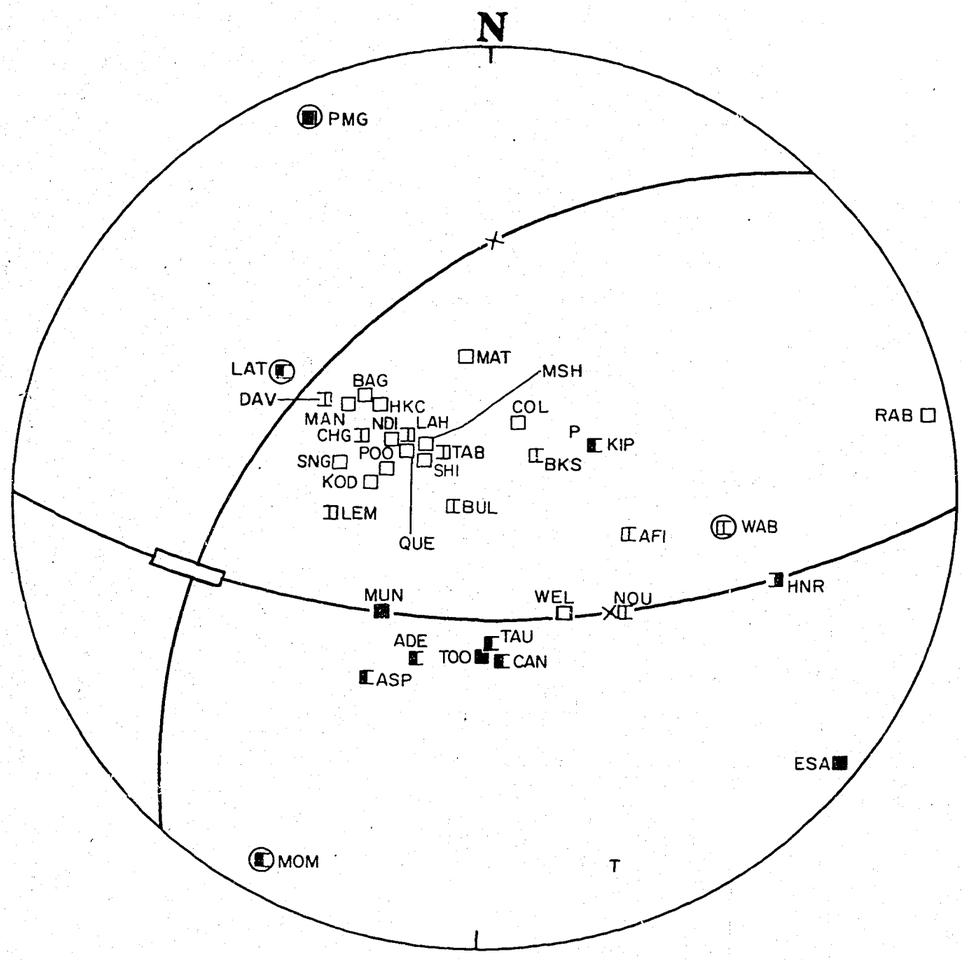


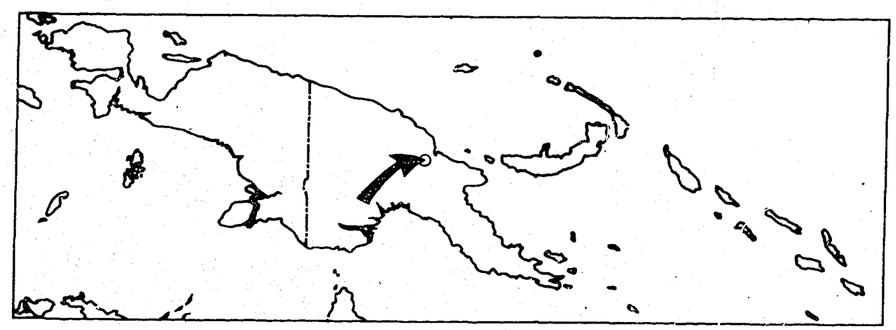

Fig. 26

PNG/B9-231-25A

Figure 26

| | | | |
|---|---|---|---|
| Number | : | 73 | |
| Location | : | 5.7°S, 145.4°E; Ramu valley | |
| Origin Time | : | 13 March 1971 at 19 12 25.0 UT | |
| Depth | : | 118 km | |
| Magnitude (M) | : | 6.5 | |
| Type | : | Dip-slip normal | |
| Nodal Planes | : | Azimuth of Dip | Dip |
| | : | 182 | 60 |
| | : | 312 | 41 |
| Nodal-Plane Poles | : | Azimuth | Plunge |
| | : | 002 | 30 |
| | : | 132 | 49 |
| P Axis | : | 051 | 62 |
| T Axis | : | 161 | 08 |
| | | Azimuth | Plunge Uncertainty |
| B Axis | : | 256 | 25 13 x 1 |

The solution is reasonably good except for the anomalous KIP compression in the central dilatational quadrant; however, its arrival is masked by microseisms.

The horizontal tensional axis of the normal fault solution is oriented south-southeast, roughly parallel to the Ramu-Markham valley rather than orthogonal to it.

Plotted in Plate 3.

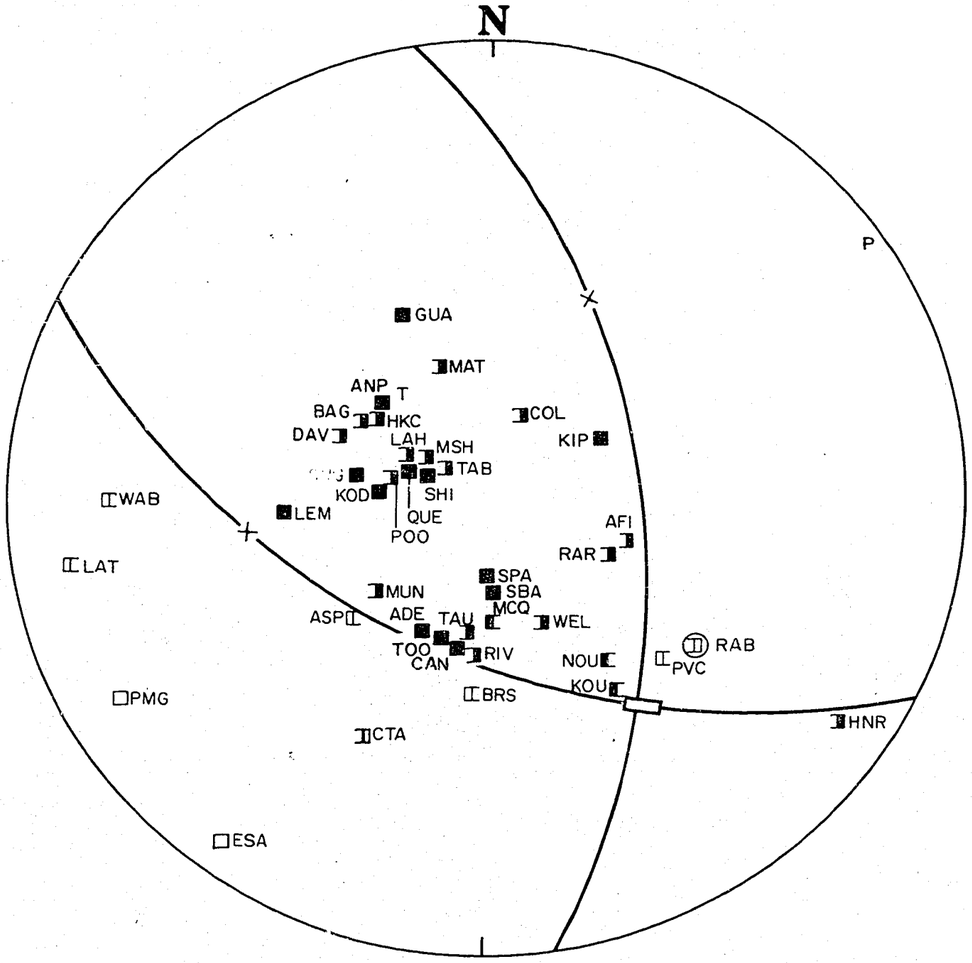


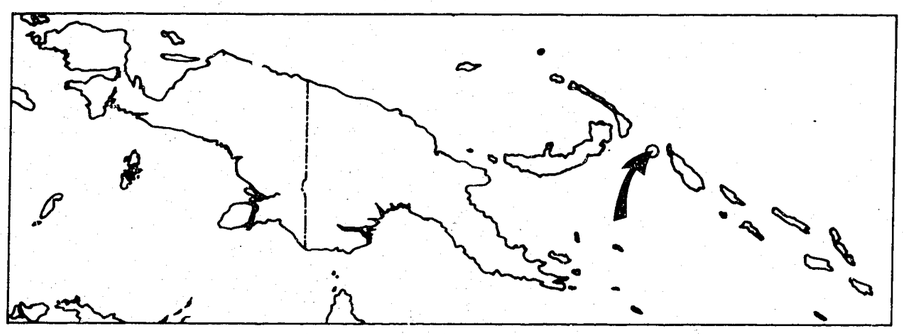

Fig. 27

PNG/B9-231-26 A

Figure 27

| | | | |
|---|---|---|---|
| Number | : | 74 | |
| Location | : | 5.5°S, 153.9°E; 40 km west of northern tip of Bougainville | |
| Origin Time | : | 14 July 1971 at 06 11 29.1 UT | |
| Depth | : | 47 km | |
| Magnitude (M) | : | 8.0 | |
| Type | : | Dip-slip overthrust | |
| Nodal Planes | : | Azimuth of Dip | Dip |
| | : | 081 | 54 |
| | : | 206 | 52 |
| Nodal-Plane Poles | : | Azimuth | Plunge |
| | : | 261 | 36 |
| | : | 026 | 38 |
| P Axis | : | 052 | 01 |
| T Axis | : | 322 | 58 |
| | | Azimuth | Plunge Uncertainty |
| B Axis | : | 145 | 32 6 x 1 |

The earthquake was the first of two M8 earthquakes in July 1971 which generated tsunamis within the Solomon Sea and caused damage in New Britain (Everingham, 1975b). The overthrust solution is well constrained by the station distribution, and is consistent with the Solomon Sea Plate underthrusting the Pacific Plate in a north-northeasterly direction on an easterly dipping fault plane.

Plotted in Plate 3.

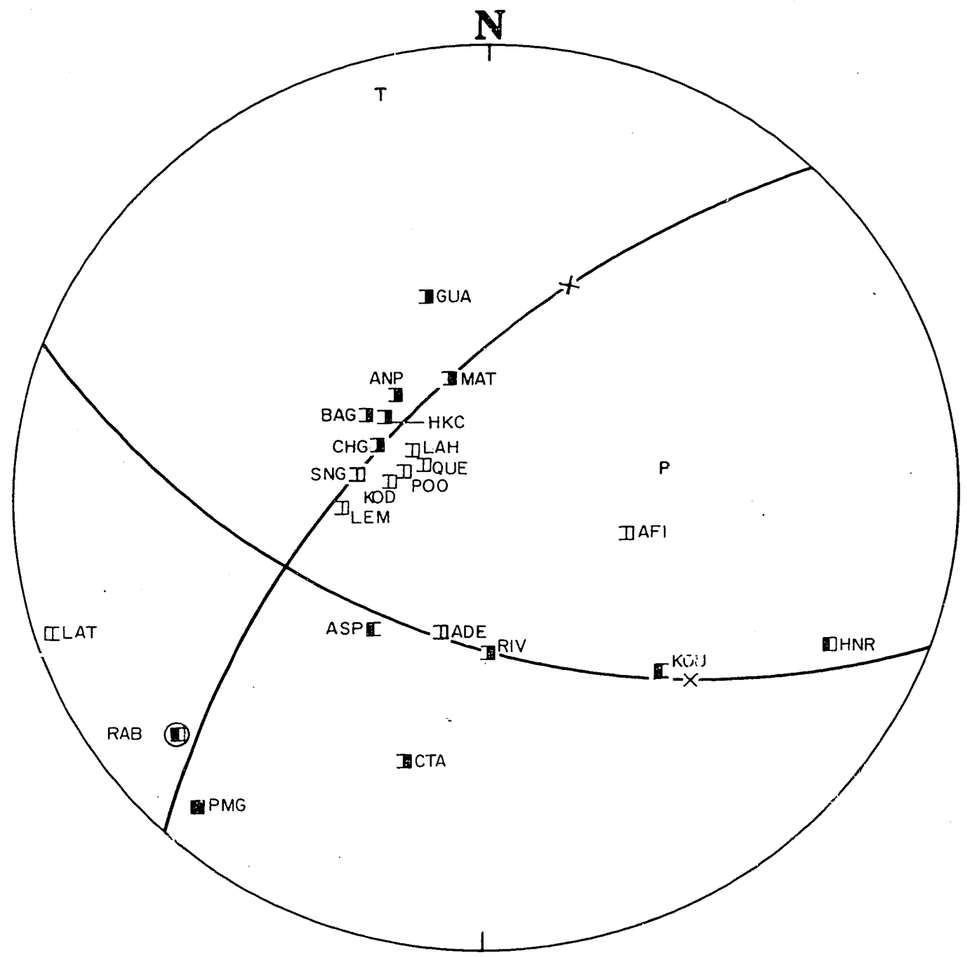


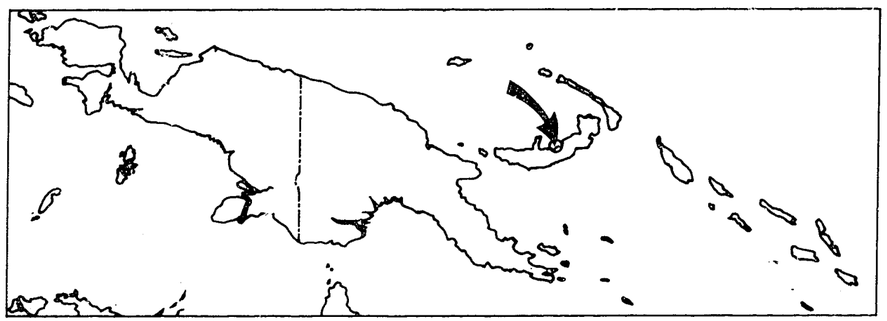

Fig. 28

PNG/B9-231-27A

Figure 28

| | | | |
|---|---|---|---|
| Number | : | 75 | |
| Location | : | 5.5°S, 150.6°E; within the South Bismarck Volcanic Arc, north New Britain coast | |
| Origin Time | : | 19 July 1971 at 15 37 46.1 UT | |
| Depth | : | 33 km | |
| Magnitude (M) | : | 6.0 | |
| Type | : | Dip-slip normal, non-orthogonal | |
| Nodal Planes | : | Azimuth of Dip | Dip |
| | : | 201 | 54 |
| | : | 313 | 62 |
| Nodal-Plane Poles | : | Azimuth | Plunge |
| | : | 021 | 36 |
| | : | 133 | 28 |
| P Axis | : | 080 | 48 |
| T Axis | : | 345 | 05 |
| | | Azimuth | Plunge | Uncertainty |
| B Axis | : | 250 | 40 | - |

The earthquake occurred at normal depth within the South Bismarck Volcanic Arc, above the inclined Benioff zone. The solution is essentially dip-slip normal, with the tensional axis horizontal and oriented north-northwest, orthogonal to the volcanic arc.

The P-wave arrivals were generally weak, so that the final station distribution is sparse. The short period KOU and HNR arrivals are close to but on the wrong side of a nodal plane, and render the solution non-orthogonal.

Plotted in Plate 3.

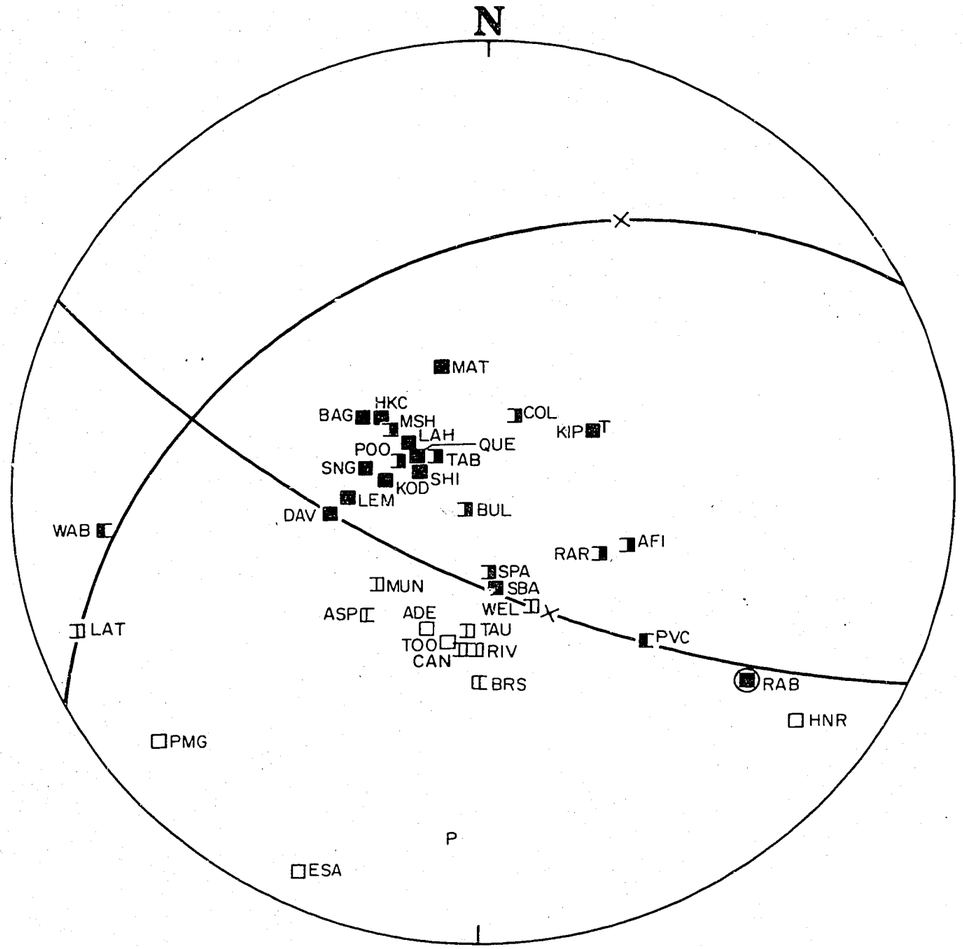


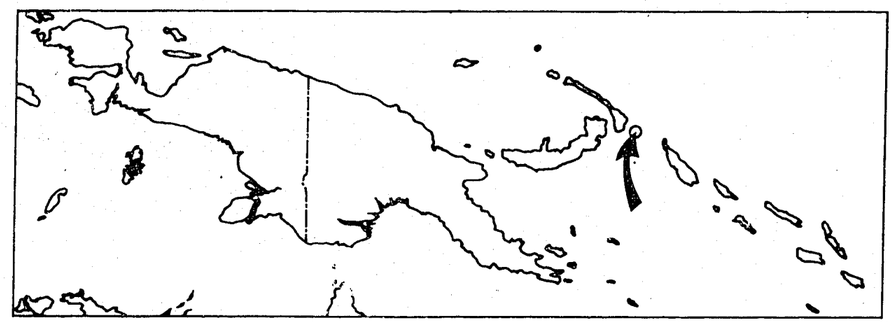

Fig. 29

PNG/B9-231-28A

Figure 29

| | | | |
|---|---|---|---|
| Number | : | 76 | |
| Location | : | 4.9°S, 153.2°E; 10 km east of southeast tip of New Ireland | |
| Origin Time | : | 26 July 1971 at 01 23 21.3 UT | |
| Depth | : | 48 km | |
| Magnitude (M) | : | 8.0 | |
| Type | : | Dip-slip overthrust, non-orthogonal | |
| Nodal Planes | : | Azimuth of Dip | Dip |
| | : | 205 | 68 |
| | : | 332 | 34 |
| Nodal-Plane Poles | : | Azimuth | Plunge |
| | : | 025 | 22 |
| | : | 152 | 56 |
| P Axis | : | 186 | 19 |
| T Axis | : | 062 | 58 |
| | | Azimuth | Plunge Uncertainty |
| B Axis | : | 285 | 24 - |

The solution to the second M8 earthquake in 1971 in the north Solomon Sea (Everingham, 1975b) is an overthrust oriented north-south. The RAB arrival, which is on the wrong side of a nodal plane, renders the solution non-orthogonal. However, the uncertainty in the position of RAB on the focal sphere is sufficient to explain the anomaly.

If the solution represents underthrusting of the Solomon Sea Plate beneath the Bougainville Trench, the direction of motion is about the same as for the first M8 earthquake (No. 74), but the fault plane dips northwest instead of east.

Plotted in Plate 3.

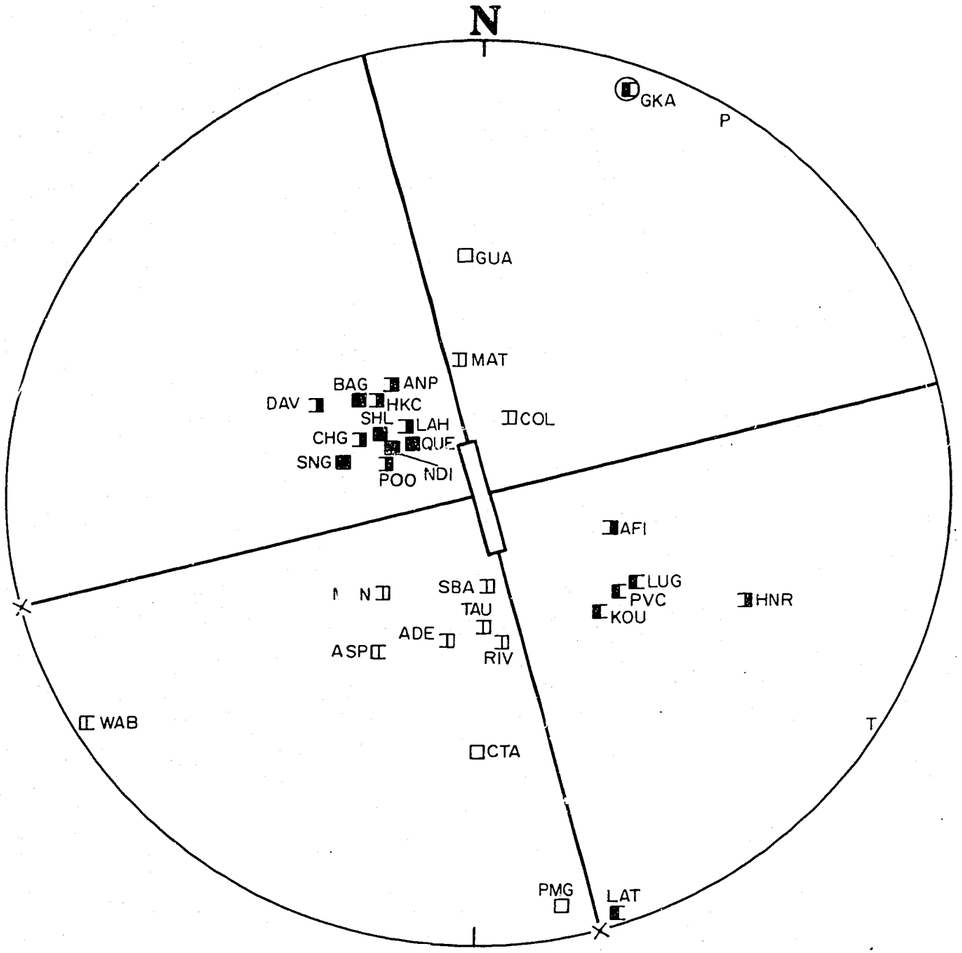


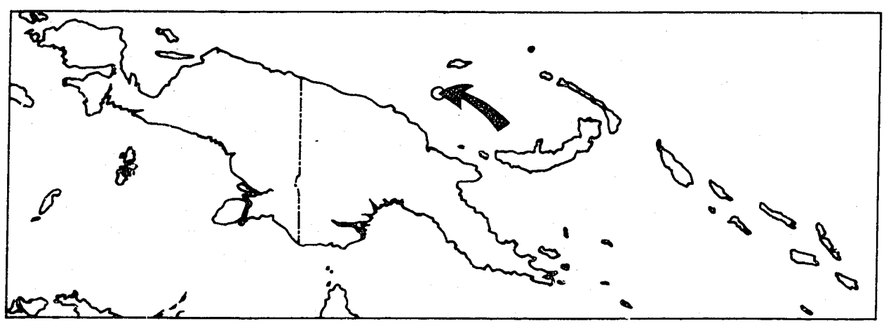

Fig. 30

PNG/B9-231-29A

Figure 30

| | | | |
|---|---|---|---|
| Number | : | 77 | |
| Location | : | 4.0°S, 146.1°E; Bismarck Sea seismic lineation 30 km north of Long Island | |
| Origin Time | : | 23 August 1971 at 04 08 02.0 UT | |
| Depth | : | 33 km | |
| Magnitude (M) | : | 6.0 | |
| Type | : | Strike-slip | |
| Nodal Planes | : | Azimuth of Dip | Dip |
| | : | 076 | 90 |
| | : | 346 | 90 |
| Nodal-Plane Poles | : | Azimuth | Plunge |
| | : | 256 | 00 |
| | : | 166 | 00 |
| P Axis | : | 031 | 00 |
| T Axis | : | 121 | 00 |
| | | Azimuth | Plunge Uncertainty |
| B Axis | : | - | 90 30 x 6 |

The solution is clearly strike-slip, but is not particularly good. Although one station, GKA, is anomalous, its P-wave arrival is weak and suspect, and it has been ignored in the solution.

If the nodal plane trending west-southwest is the fault plane, the solution represents sinistral shear movement on the Bismarck Sea seismic lineation. The west-southwest trend differs from the west-northwest and northwesterly to westerly trends of the presumed fault planes of other earthquakes on the lineation (Nos. 19, 40, 45, 47, Ripper, 1975; Nos. 51, 80).

Plotted in Plate 2.

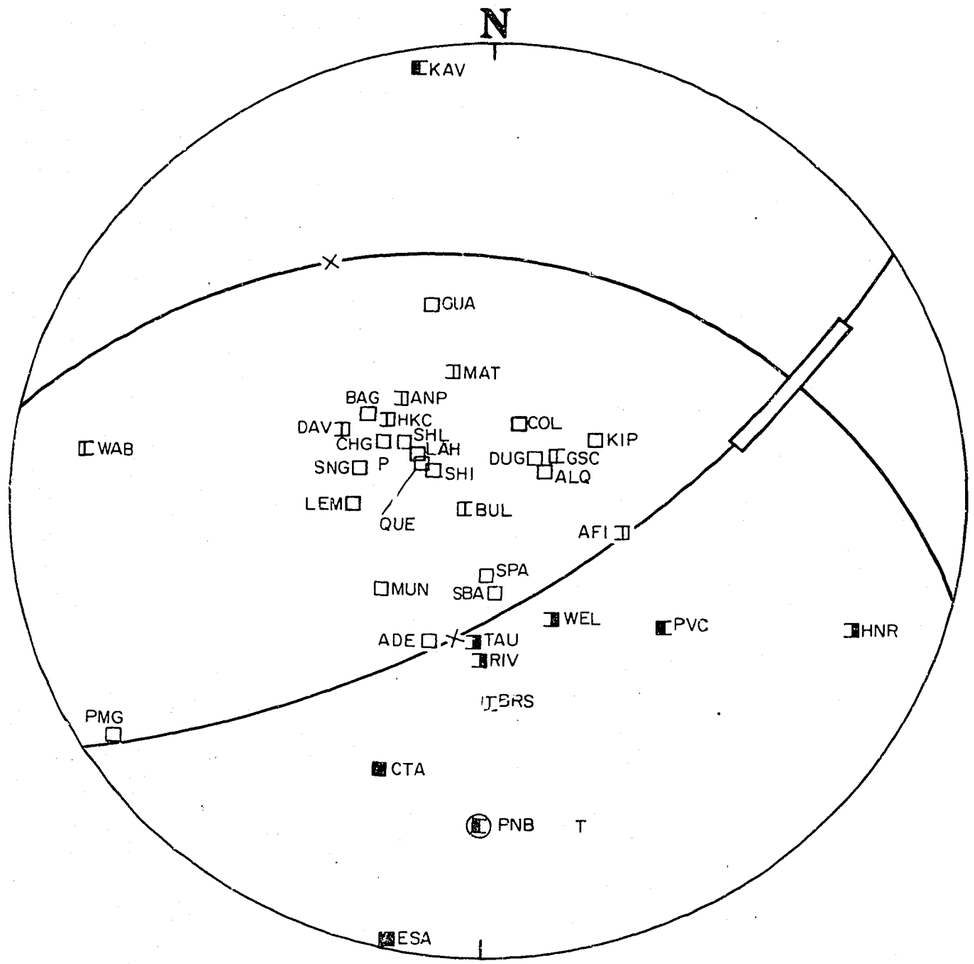


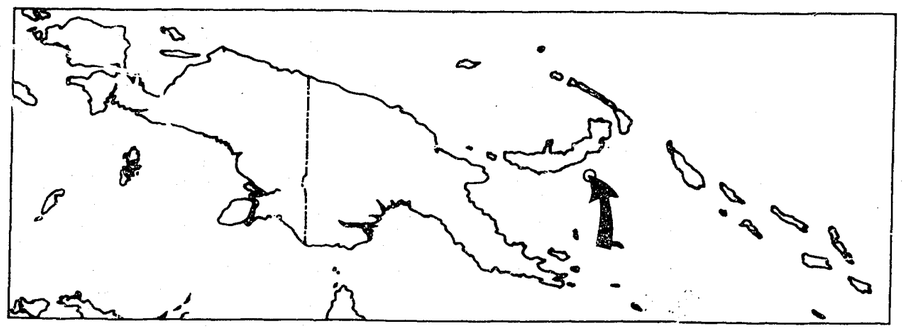

Fig. 31

PNG/B9-231-30A

Figure 31

| | | | | |
|---|---|---|---|---|
| Number | : | 78 | | |
| Location | : | 6.5°S, 151.5°E; Solomon Sea 50 km south of Pomio, New Britain | | |
| Origin Time | : | 14 September 1971 at 05 20 29.3 UT | | |
| Depth | : | 33 km | | |
| Magnitude (M) | : | 6.6 | | |
| Type | : | Dip-slip normal | | |
| Nodal Planes | : | Azimuth of Dip | Dip | |
| | : | 011 | 34 | |
| | : | 148 | 64 | |
| Nodal-Plane Poles | : | Azimuth | Plunge | |
| | : | 191 | 56 | |
| | : | 328 | 26 | |
| P Axis | : | 288 | 62 | |
| T Axis | : | 164 | 16 | |
| | | Azimuth | Plunge | Uncertainty |
| B Axis | : | 068 | 21 | 28 x 1 |

The earthquake occurred beneath the Solomon Sea side of the New Britain Trench. The tensional axis is almost horizontal, and oriented north-northwest.

The solution is reasonably good except for the BRS arrival, which is an apparent dilatation well within a zone of compressions. The solution is consistent with the hypothesis that normal faulting occurs in the oceanic lithospheric plate (in this case, the Solomon Sea Plate) as it downturns beneath the adjoining plate (the South Bismarck Plate) and volcanic arc.

Plotted in Plate 3.

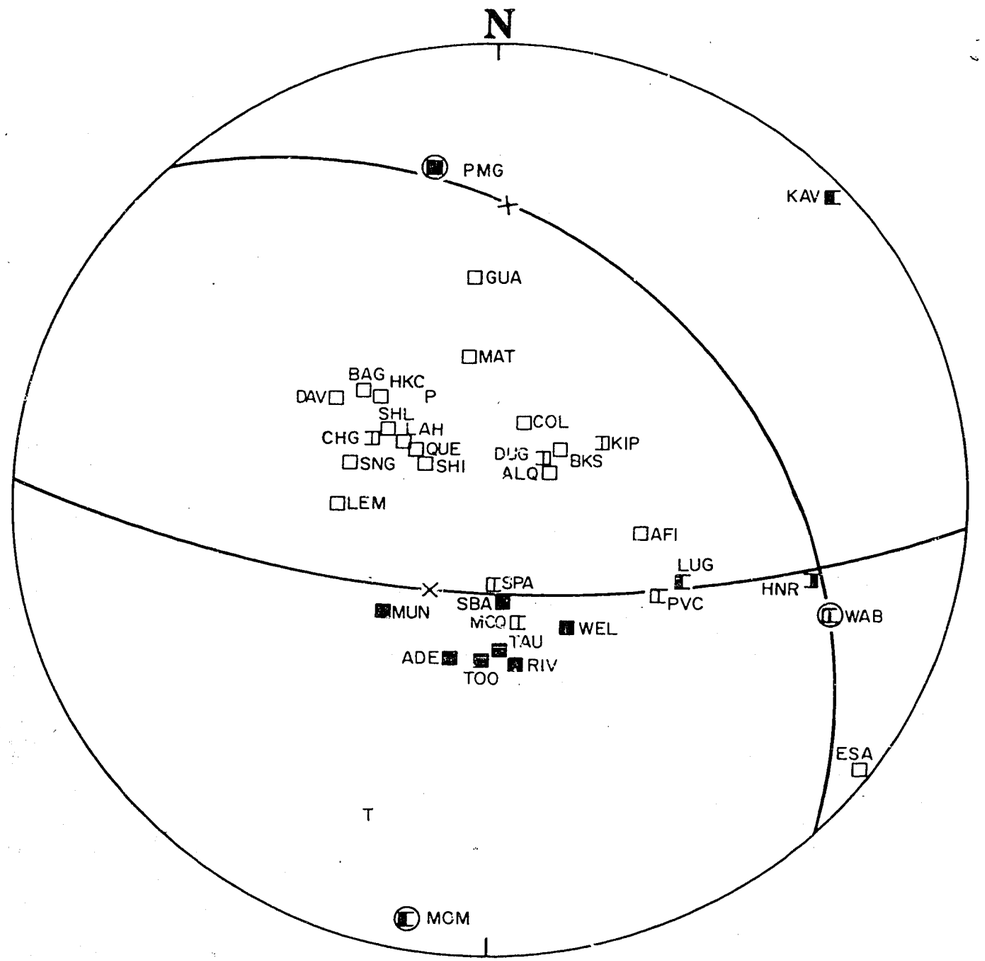


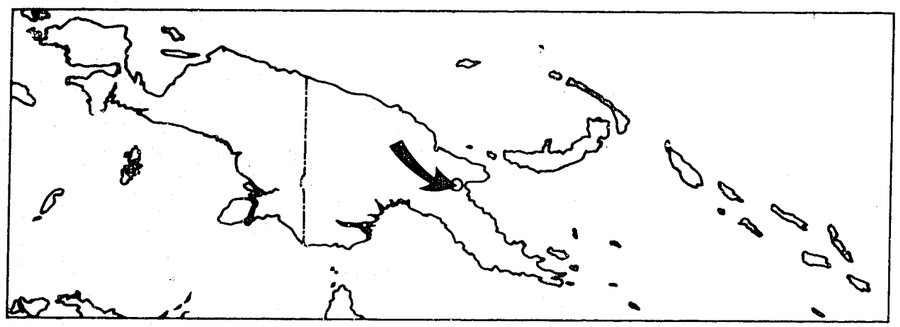

Fig. 32

PNG/B9-231-31A

Figure 32

| | | | |
|---|---|---|---|
| Number | : | 79 | |
| Location | : | 6.5°S, 146.6°E; Markham valley 20 km northwest of Lae | |
| Origin Time | : | 25 September 1971 at 04 36 14.0 UT | |
| Depth | : | 115 km | |
| Magnitude (M) | : | 6.9 | |
| Type | : | Dip-slip normal | |
| Nodal Planes | : | Azimuth of Dip | Dip |
| | : | 048 | 33 |
| | : | 183 | 66 |
| Nodal-Plane Poles | : | Azimuth | Plunge |
| | : | 228 | 57 |
| | : | 003 | 24 |
| P Axis | : | 329 | 61 |
| T Axis | : | 200 | 17 |
| | | Azimuth | Plunge Uncertainty |
| B Axis | : | 103 | 20 1 x 1 |

The normal solution at intermediate depth below the Markham valley is at variance with the concept that the northern margin of New Guinea is a collision zone in the north-south compression. The tensional axis of the solution is almost horizontal, and roughly at right-angles to the Markham valley. One station, MCQ, is anomalous, but it is close to a nodal plane.

Plotted in Plate 3.

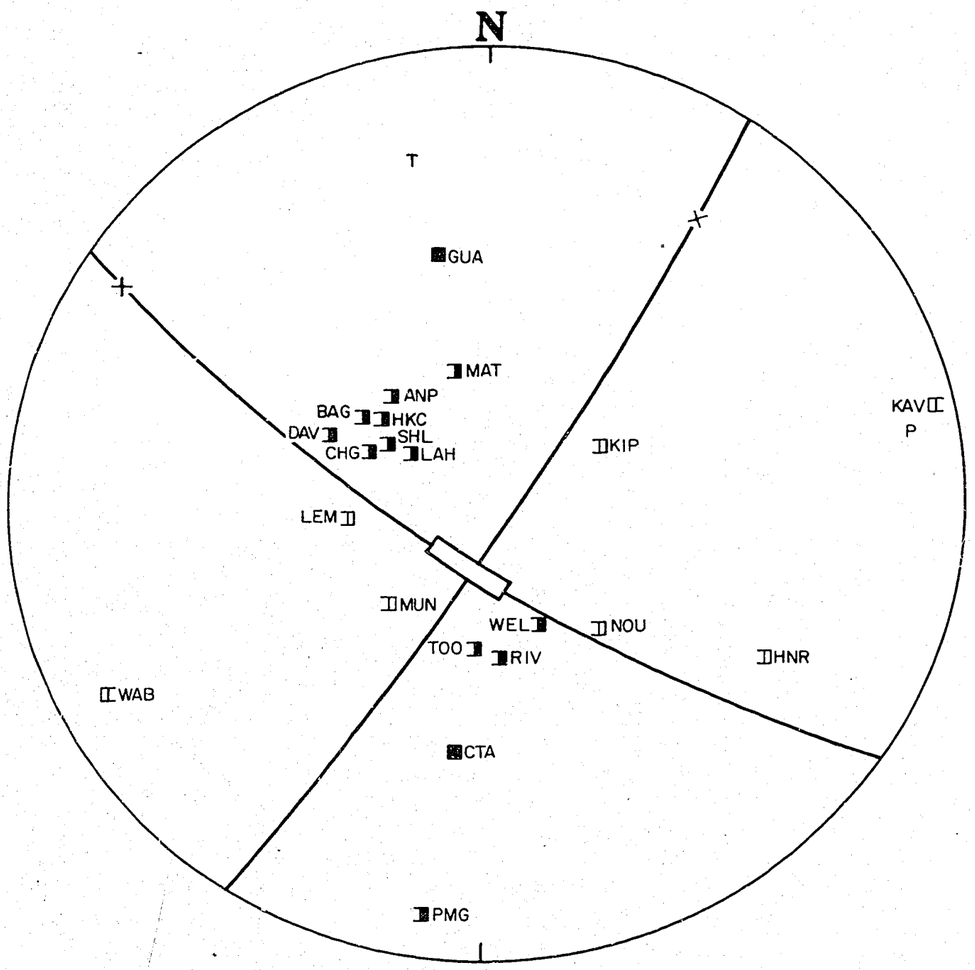


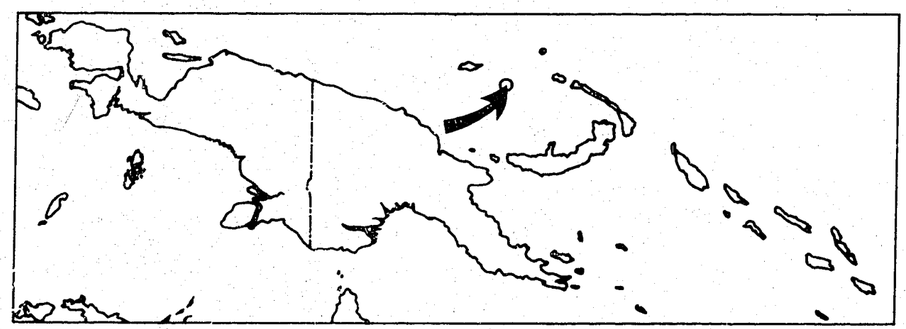

Fig.33

PNG/B9-231-32A

Figure 33

| | | | |
|---|---|---|---|
| Number | : | 80 | |
| Location | : | 3.2°S, 148.1°E; Bismarck Sea seismic lineation north of Umboi Island | |
| Origin Time | : | 27 September 1971 at 22 20 03.2 UT | |
| Depth | : | 33 km | |
| Magnitude (M) | : | 6.1 | |
| Type | : | Strike-slip | |
| Nodal Planes | : | Azimuth of Dip | Dip |
| | : | 123 | 84 |
| | : | 214 | 76 |
| Nodal-Plane Poles | : | Azimuth | Plunge |
| | : | 303 | 06 |
| | : | 034 | 14 |
| P Axis | : | 079 | 08 |
| T Axis | : | 347 | 15 |
| | | Azimuth | Plunge Uncertainty |
| B Axis | : | 194 | 75 21 x 8 |

The solution is reasonably good with stations in all quadrants. The solution is sinistral if the nodal plane trending west-northwest is the fault plane.

Plotted in Plate 2.

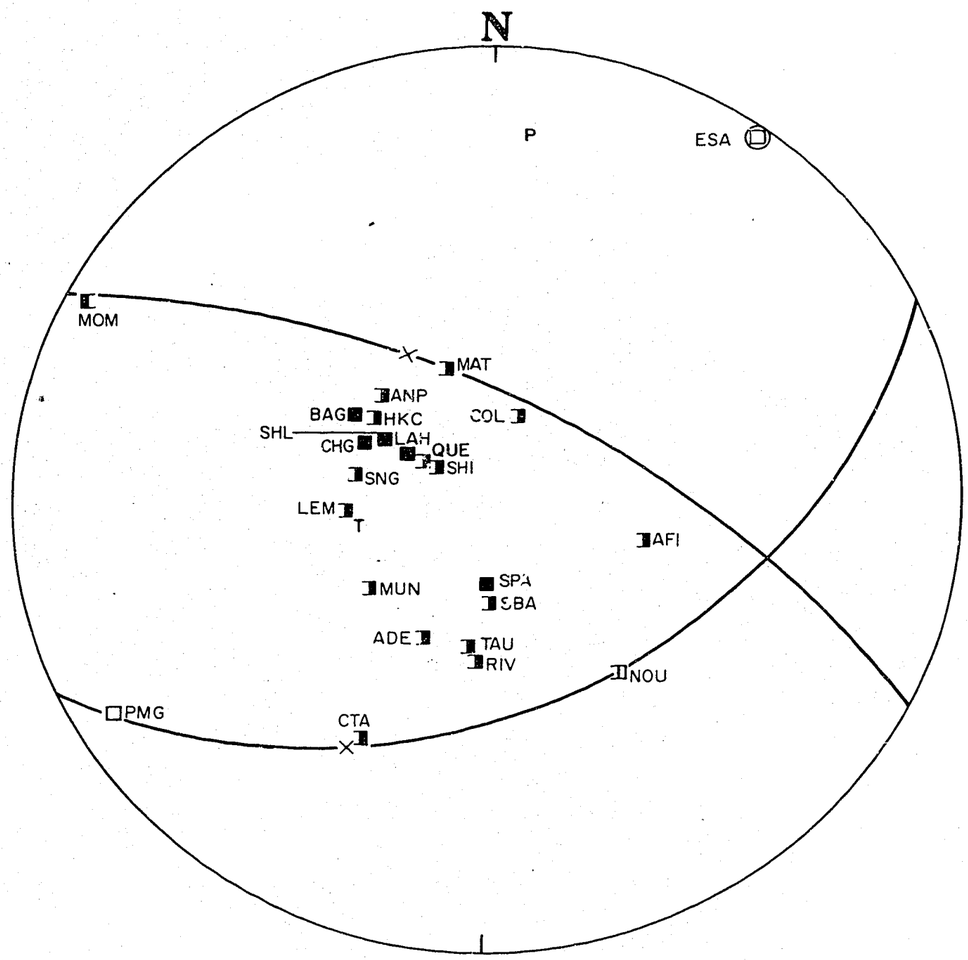


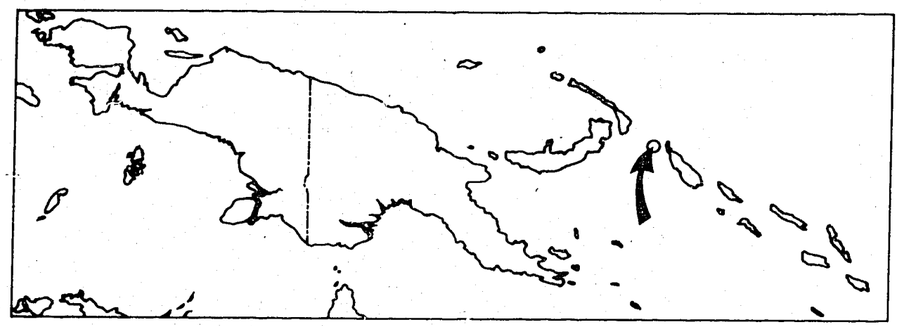

Fig. 34

PNG/B9-231-33A

Figure 34

| | | | | |
|---|---|---|---|---|
| Number | : | 81 | | |
| Location | : | 5.5°S, 153.9°E; 40 km west of northern tip of Bougainville | | |
| Origin Time | : | 28 October 1971 at 15 13 37.8 UT | | |
| Depth | : | 120 km | | |
| Magnitude (M) | : | 6.6 | | |
| Type | : | Dip-slip overthrust | | |
| Nodal Planes | : | Azimuth of Dip | Dip | |
| | : | 028 | 64 | |
| | : | 153 | 40 | |
| Nodal-Plane Poles | : | Azimuth | Plunge | |
| | : | 208 | 26 | |
| | : | 333 | 50 | |
| P Axis | : | 005 | 13 | |
| T Axis | : | 225 | 59 | |
| | | Azimuth | Plunge | Uncertainty |
| B Axis | : | 103 | 28 | 1 x 1 |

The solution is tight, and is constrained by stations MOM, MAT, NOU, CTA, and PMG. The solution is consistent with a north-northeasterly dipping fault plane, but the corresponding azimuth of motion is north-northwest.

The earthquake occurred at the same epicentre as the M8 earthquake of 14 July 1971 (No. 74) but at a greater depth.

Plotted in Plate 3.

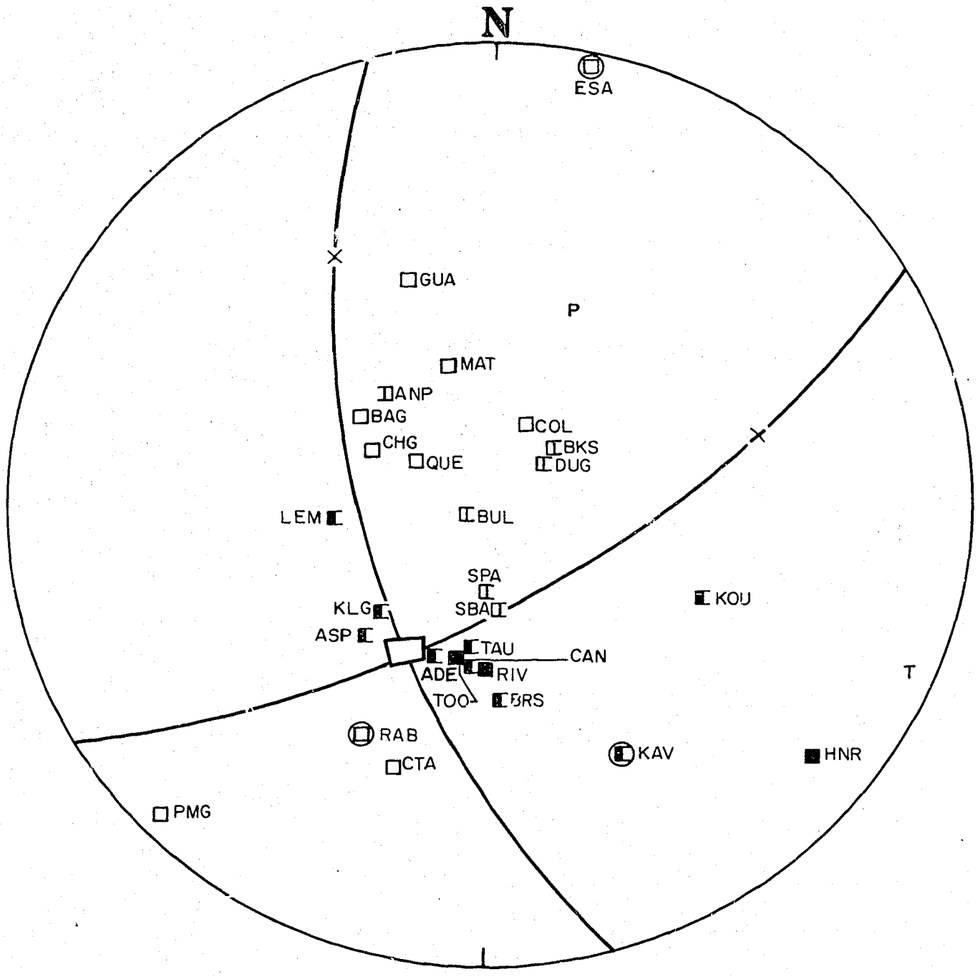


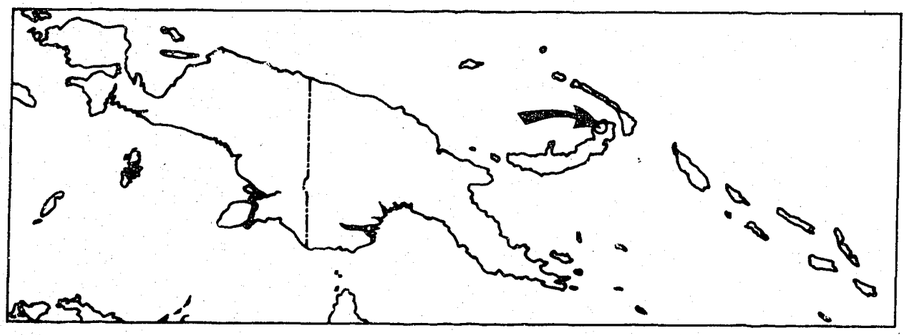

Fig. 35

PNG/B9-231-34A

Figure 35

| | | | |
|---|---|---|---|
| Number | : | 82 | |
| Location | : | 4.7°S, 151.9°E; Gazelle Peninsula, New Britain | |
| Origin Time | : | 30 December 1971 at 13 39 37.4 UT | |
| Depth | : | 109 km | |
| Magnitude (M) | : | 6.3 | |
| Type | : | Predominantly strike-slip | |
| Nodal Planes | : | Azimuth of Dip | Dip |
| | : | 149 | 66 |
| | : | 255 | 60 |
| Nodal-Plane Poles | : | Azimuth | Plunge |
| | : | 329 | 24 |
| | : | 075 | 30 |
| P Axis | : | 022 | 42 |
| T Axis | : | 112 | 03 |
| | | Azimuth | Plunge Uncertainty |
| B Axis | : | 207 | 50 7 x 5 |

The B axis of the solution plunges at an angle of 50°, so that the solution is predominantly strike-slip. The minor component is dip-slip normal.

The hypocentre is within the northwest-dipping Benioff zone, but the solution is not consistent with subduction of the Solomon Sea Plate beneath New Britain.

Plotted in Plate 2.

## CONCLUSIONS

Reasonably good focal mechanism solutions have been obtained for 28 out of 34 earthquakes that occurred in the New Guinea/Solomon Islands region between January 1969 and December 1971. Seven are strike-slip and 21 dip-slip; of the dip-slip solutions, 13 are overthrust, seven are normal, and one has one vertical and one horizontal nodal plane.

Three damaging earthquakes occurred in Papua New Guinea in 1970 and 1971: one 25 km northwest of Madang on 31 October 1970 (No. 66) at a depth of 42 km; and two in the northeast Solomon Sea, both of magnitude M8, on 14 July 1971 (No. 74) at a depth of 47 km and on 26 July 1971 (No. 76) at a depth of 48 km. The focal mechanism solutions of the three earthquakes are dip-slip overthrust, with compressional axes dipping northeast, northeast, and south respectively. The solution to another high-magnitude earthquake - the M8 earthquake in Irian Jaya on 10 January 1971 (No. 70), which was felt strongly in western Papua New Guinea - is also overthrust, again with the compressional axis dipping roughly northeast.

Three dip-slip normal solutions with horizontal tensional axes were obtained in different environments of the New Britain/Bougainville arc-trench system: earthquake No. 52 occurred at a depth of 403 km in the Benioff zone 20 km northwest of Buka Island; earthquake No. 75 occurred at a depth of 33 km on the north coast of New Britain within the South Bismarck Volcanic Arc; and earthquake No. 78 occurred at a depth of 33 km on the Solomon Sea side of the New Britain Trench.

Solutions to two earthquakes in the D'Entrecasteaux Islands - one strike-slip (No. 59), the other dip-slip (No. 71) - support Johnson & Molnar's (1972) northwest azimuth of motion of the Solomon Sea Plate with respect to the Australian Plate.

Focal mechanisms of northern New Guinea earthquakes indicate the complexity of the region. Solutions to two earthquakes at depths of 120 and 114 km (Nos. 65 and 68) beneath the Sepik River plains are overthrusts. Two earthquakes at depths of 118 and 115 km (Nos. 73 and 79) beneath the Ramu-Markham valley have dip-slip normal solutions with near-horizontal tensional axes. Of two earthquakes beneath the New Guinea coast north of the Ramu-Markham valley, one at a depth of 42 km has an overthrust solution (No. 66), and the other at 113 km has a strike-slip solution (No. 54) whose motion was sinistral if the nodal plane parallel to the coast was the fault plane. The solution to an earthquake at a depth of 206 km beneath the Long Island volcano (No. 50) is overthrust.

Focal mechanisms of earthquakes in the Bismarck Sea seismic lineation are strike-slip (Nos. 51, 77, 80), but the nodal planes are not parallel to the lineation, or to each other.

## ACKNOWLEDGEMENTS

The co-operation of the Director of the World Data Centre, and of the Directors of seismograph stations which supplied information, is gratefully acknowledged.

## REFERENCES


BESSONOVA, E.N., GOTSADZE, O.D., KEILIS-BOROK, V.I., KIRILLOVA, I.V., KOGAN, S.D., KIKHITKOVA, T.I., MALINOVSKAYA, L.N., PAVLOVA, G.I., & SORSKII, A.A., 1960 - INVESTIGATION OF THE MECHANISM OF EARTHQUAKES. Soviet research in geophysics, Vol 4. Akad. nauk. SSR Geofiz. Inst. (English translation by Amer. Geophys. Un.).

CURTIS, J.W., 1973 - Plate tectonics and the Papua-New Guinea-Solomon Islands region. J. geol. Soc. Aust., 20, 21-35.

EVERINGHAM, I.B., 1975a - Seismological report on the Madang earthquake of 31 October 1970 and aftershocks. Bur. Miner. Resour. Aust. Rep. 176.

EVERINGHAM, I.B., 1975b - Faulting associated with the major north Solomon Sea earthquakes of 14 and 26 July 1971. J. geol. Soc. Aust., 22(1), 61-69.

HODGSON, J.H., & STOREY, R.S., 1953 - Tables extending Byerley's fault-plane techniques to earthquakes at any focal depth. Bull. seismol. Soc. Amer., 43, 49-61.

JOHNSON, T., & MOLNAR, P., 1972 - Focal mechanisms and plate tectonics of the southwest Pacific. J. geophys. Res., 77, 5000-32.

LE PICHON, X., 1968 - Sea-floor spreading and continental drift. J. geophys. Res., 73, 3661-98.

LE PICHON, X., 1970 - Correction to paper by Xavier Le Pichon 'Sea-floor spreading and continental drift'. J. geophys. Res., 75, 2793.

McKENZIE, D.P., 1969 - The relation between fault plane solutions for earthquakes and the directions of the principal stresses. Bull. seismol. Soc. Amer., 59, 591-601.

NUTTLI, O.W., 1969 - Tables of angles of incidence of P waves at focus, calculated from 1968 P tables. Earthquake Notes, XL(3), 21-5.

RIPPER, I.D., 1975 - Some earthquake focal mechanisms in the New Guinea/Solomon Islands region, 1963-1968. Bur. Miner. Resour. Aust. Rep. 178.

RITSEMA, A.R., 1967 - Mechanisms of European earthquakes. Tectonophys., 4, 247-59.

SYKES, L.R., 1968 - Deep earthquakes and rapidly running phase changes; a reply to Dennis & Walker. J. geophys. Res., 73, 1508-10.

TABLE 1

HYPOCENTRES OF THE EARTHQUAKES EXAMINED IN THIS REPORT

| No. | Yr | Mn | Dy | Hr | Mi | Sec | h(km) | Lat °S | Long °E | M |
|---|---|---|---|---|---|---|---|---|---|---|
| 49 | 69 | 01 | 05 | 13 | 26 | 39.9 | 47 | 8.0 | 158.9 | 7.1 |
| 50 | 69 | 03 | 10 | 06 | 54 | 17.6 | 206 | 5.6 | 147.2 | 6.4 |
| 51 | 69 | 04 | 16 | 01 | 22 | 47.5 | 39 | 3.5 | 151.0 | 6.4 |
| 52 | 69 | 05 | 31 | 23 | 56 | 21.6 | 403 | 4.9 | 154.2 | 6.1 |
| 53 | 69 | 06 | 14 | 03 | 22 | 56.8 | 62 | 7.9 | 159.0 | 6.6 |
| 54 | 69 | 06 | 24 | 03 | 29 | 17.3 | 113 | 5.8 | 146.8 | 6.0 |
| 55 | 69 | 07 | 29 | 01 | 55 | 20.4 | 6 | 3.4 | 144.8 | 5.9 |
| 56 | 69 | 08 | 26 | 16 | 58 | 02.3 | 59 | 5.8 | 151.2 | 6.3 |
| 57 | 69 | 09 | 06 | 14 | 49 | 55.9 | 15 | 8.8 | 157.8 | 6.2 |
| 58 | 69 | 09 | 06 | 17 | 08 | 03.2 | 10 | 8.9 | 157.9 | 6.4 |
| 59 | 70 | 01 | 06 | 05 | 35 | 51.8 | 8 | 9.6 | 151.5 | 6.2 |
| 60 | 70 | 03 | 28 | 07 | 45 | 59.9 | 64 | 6.3 | 154.6 | 5.9 |
| 61 | 70 | 06 | 12 | 08 | 06 | 16.6 | 32 | 2.9 | 139.1 | 6.3 |
| 62 | 70 | 08 | 03 | 07 | 01 | 11.9 | 67 | 7.9 | 158.7 | 6.6 |
| 63 | 70 | 08 | 19 | 02 | 11 | 09.4 | 33 | 10.5 | 161.5 | 6.1 |
| 64 | 70 | 08 | 28 | 01 | 02 | 48.9 | 88 | 4.6 | 153.1 | 6.6 |
| 65 | 70 | 10 | 13 | 18 | 53 | 30.0 | 120 | 4.1 | 143.0 | 6.3 |
| 66 | 70 | 10 | 31 | 17 | 53 | 09.3 | 42 | 4.9 | 145.5 | 7.0 |
| 67 | 70 | 11 | 08 | 22 | 35 | 46.7 | 33 | 3.4 | 135.6 | 7.0 |
| 68 | 70 | 11 | 28 | 20 | 22 | 50.6 | 114 | 4.1 | 142.9 | 6.1 |
| 69 | 70 | 12 | 29 | 02 | 26 | 12.2 | 72 | 10.5 | 161.4 | 6.9 |
| 70 | 71 | 01 | 10 | 07 | 17 | 03.7 | 33 | 3.1 | 139.7 | 8.0 |
| 71 | 71 | 01 | 25 | 00 | 18 | 26.1 | 38 | 9.6 | 151.4 | 6.3 |
| 72 | 71 | 02 | 26 | 04 | 55 | 50.0 | 90 | 10.4 | 161.3 | 6.5 |
| 73 | 71 | 03 | 13 | 19 | 12 | 25.0 | 11 | 5.7 | 145.4 | 6.5 |
| 74 | 71 | 07 | 14 | 06 | 11 | 29.1 | 47 | 5.5 | 153.9 | 8.0 |
| 75 | 71 | 07 | 19 | 15 | 37 | 46.1 | 33 | 5.5 | 150.6 | 6.0 |
| 76 | 71 | 07 | 26 | 01 | 23 | 21.3 | 48 | 4.9 | 153.2 | 8.0 |
| 77 | 71 | 08 | 23 | 04 | 08 | 02.0 | 33 | 4.0 | 146.1 | 6.0 |
| 78 | 71 | 09 | 14 | 05 | 20 | 29.3 | 33 | 6.5 | 151.5 | 6.6 |

| No. | Yr | Mn | Dy | Hr | Mi | Sec | h(km) | Lat $^{o}$S | Long $^{o}$E | M |
|---|---|---|---|---|---|---|---|---|---|---|
| 79 | 71 | 09 | 25 | 04 | 36 | 14.0 | 115 | 6.5 | 146.6 | 6.9 |
| 80 | 71 | 09 | 27 | 22 | 20 | 03.2 | 33 | 3.2 | 148.1 | 6.1 |
| 81 | 71 | 10 | 28 | 15 | 13 | 37.8 | 120 | 5.5 | 153.9 | 6.6 |
| 82 | 71 | 12 | 30 | 13 | 39 | 37.4 | 109 | 4.7 | 151.9 | 6.3 |

## TABLE 2

## THE EARTHQUAKE P-WAVE POLARITIES

| | | |
|---|---|---|
| where | 0 | compression, short-period and long-period |
| | 1 | compression, short-period |
| | 2 | compression, long-period |
| | 4 | dilatation, short-period; compression, long-period |
| | 5 | compression, short-period; dilatation, long-period |
| | 7 | dilatation, long-period |
| | 8 | dilatation, short-period |
| | 9 | dilatation, short-period and long-period |
| | ( ) | polarity is not completely clear owing to either microseisms or a poor quality seismogram |

| Stn | Earthquake No. 49 | 50 | 51 | 52 | Stn | Earthquake No. 49 | 50 | 51 | 52 |
|---|---|---|---|---|---|---|---|---|---|
| ADE | 0 | 9 | 0 | 1 | LEM | | 9 | 9 | 1 |
| AFI | 9 | 0 | 7 | 8 | MAN | 9 | 2 | 2 | 0 |
| ALQ | 9 | | | | MAT | 9 | 0 | 2 | 9 |
| ANP | 7 | 2 | 2 | | MSH | 7 | | | |
| BAG | 9 | 0 | 0 | 0 | MUN | 0 | 9 | | |
| BKS | 9 | | 7 | | NDI | 9 | 0 | 0 | |
| BRS | | | | 8 | NOU | | 1 | 1 | 8 |
| BUL | 8 | | | 8 | PMG | 0 | 9 | 2 | 0 |
| CHG | 9 | 0 | 4 | | POO | 7 | 0 | 0 | 8 |
| COL | 9 | 0 | 2 | 9 | PVC | | 0 | 9 | 9 |
| CTA | 0 | 9 | 0 | 0 | QUE | 9 | 1 | 1 | 8 |
| DAV | 7 | 2 | 7 | | RAB | 0 | 0 | | 9 |
| ESA | 2 | 7 | 2 | | RAR | 7 | 2 | | 8 |
| GRK | | 1 | | | RIV | 0 | 9 | 2 | 8 |
| GUA | 9 | 1 | 0 | (0) | SBA | 0 | 2 | 2 | 8 |
| HKC | 9 | 2 | 0 | (1) | SHI | 7 | | | |
| HNR | 0 | 0 | 7 | 0 | SHK | 9 | 2 | 0 | 8 |
| KIP | 9 | 1 | (1) | 8 | SHI | 9 | 2 | 4 | 8 |
| KLG | | | 1 | | SNG | 9 | | 7 | |
| KOD | 9 | | | 1 | SPA | 0 | 4 | 0 | |
| KOU | | 1 | | 8 | TAB | 7 | | | |
| LAE | | 1 | | 8 | WAB | | | | 1 |
| LAH | 7 | | | | WEL | 0 | 0 | 2 | 9 |

| | Earthquake No. | | | | | Earthquake No. | | | |
|---|---|---|---|---|---|---|---|---|---|
| Stn | 53 | 54 | 55 | 56 | Stn | 53 | 54 | 55 | 56 |
| ADE | 1 | 1 | | 0 | LAE | | 1 | | |
| AFI | 1 | (8) | | | LAH | | 0 | 0 | 0 |
| ALQ | (8) | | | | LEM | (8) | 8 | | 1 |
| ANP | 7 | 2 | | | MAN | | 1 | | |
| BAG | 9 | | | 0 | MAT | 9 | 0 | 0 | 0 |
| BKS | 8 | | | | MEK | | 8 | | |
| BRS | 1 | | 8 | 1 | MUN | 8 | 8 | | 1 |
| BUL | | 8 | | 1 | NDI | | | | 0 |
| CHG | | 8 | | 0 | NOU | 0 | | | 2 |
| COL | 9 | 0 | 0 | 0 | PMG | 9 | 0 | 7 | 9 |
| CTA | 0 | | 8 | 9 | POO | 9 | 8 | 2 | 2 |
| DAV | 7 | 7 | 7 | 2 | PVC | 0 | | | |
| ESA | 7 | 7 | | 0 | QUE | 9 | 0 | 0 | 0 |
| GRK | | | | (8) | RAB | 9 | | 0 | |
| GUA | 9 | 2 | | 0 | RIV | 0 | | | 2 |
| HKC | 7 | | | 0 | SBA | | 1 | 1 | 0 |
| HNR | 0 | 9 | 0 | 7 | SHK | 5 | 0 | (1) | 2 |
| KIP | 1 | (8) | | 1 | SHL | | (0) | | 0 |
| KLG | 1 | 8 | | | SPA | 1 | 1 | 1 | 0 |
| KOD | 7 | | | 2 | WAB | | | 8 | |
| KOU | | 1 | | 8 | WEL | | | | 2 |

| Stn | Earthquake No. 57 | 58 | 59 | 60 | Stn | Earthquake No. 57 | 58 | 59 | 60 |
|---|---|---|---|---|---|---|---|---|---|
| ADE | (7) | | 4 | 0 | MAN | | | 7 | 2 |
| AFI | 2 | 2 | | 1 | MAT | 0 | 0 | 7 | 0 |
| ALQ | 2 | (1) | | | MSH | | | 7 | |
| ANP | 7 | 7 | 7 | 2 | MUN | 7 | | 0 | 0 |
| BAG | 7 | 9 | 5 | 0 | NDI | 2 | 2 | 9 | 0 |
| BKS | 0 | 2 | 0 | | NOU | | | | 1 |
| BRS | 8 | | | 1 | PMG | 9 | 9 | 7 | 9 |
| CHG | 7 | 7 | | 0 | POO | (0) | | 9 | 0 |
| COL | 0 | 0 | 7 | | PVC | | | | 1 |
| CTA | | | | 7 | QUE | | | 9 | 0 |
| DAV | | | 7 | 2 | RAB | 7 | 7 | 2 | 0 |
| DUG | | | | 0 | RAR | 2 | 1 | | |
| ESA | 9 | 9 | | | RIV | 7 | 7 | 0 | 0 |
| GSC | | | 2 | 1 | SBA | 2 | | (0) | 0 |
| GUA | 2 | 2 | 7 | 2 | SEO | 2 | | | 2 |
| HKC | 7 | 7 | 7 | 0 | SHK | 2 | 2 | 7 | |
| HNR | 0 | 2 | 0 | 9 | SHL | 0 | 0 | 9 | 0 |
| KIP | 2 | 1 | | | SNG | 7 | 7 | 7 | |
| KOD | | 7 | 9 | | SPA | 1 | 1 | 4 | 0 |
| KOU | | | | 1 | TAU | | | 2 | 1 |
| LAE | | | | (8) | WAB | | 8 | | 1 |
| LAH | 0 | 2 | 9 | 0 | WEL | 2 | | 2 | 0 |
| LEM | 9 | 7 | 9 | 0 | | | | | |

| Stn | Earthquake No. 61 | 62 | 63 | 64 | Stn | Earthquake No. 61 | 62 | 63 | 64 |
|---|---|---|---|---|---|---|---|---|---|
| ADE | 2 | 1 | (8) | | MAT | 7 | 9 | 0 | 0 |
| AFI | (0) | | (2) | | MEK | | | | 8 |
| ALQ | 1 | 7 | | 2 | MOM | | | | 1 |
| ANP | | | | 2 | MSH | | | | 2 |
| BAG | | 8 | (2) | | MUN | 2 | (8) | | 2 |
| BKS | | 9 | | 2 | NDI | 0 | 9 | | 0 |
| BRS | | | 8 | | PMG | 0 | 8 | 9 | 9 |
| BUL | | | | 1 | POO | 0 | | | 2 |
| CAN | | | | 7 | QUE | 0 | 9 | | 0 |
| CHG | 0 | 9 | | 0 | RAB | 0 | 9 | 7 | 4 |
| COL | 0 | 9 | (0) | 0 | RIV | 2 | (0) | | 9 |
| DUG | | 9 | 0 | 2 | SBA | 0 | 1 | 1 | 0 |
| ESA | | 9 | | | SEO | 0 | 9 | | 2 |
| GSC | | | 0 | | SHI | | | | 2 |
| GUA | 9 | 9 | (7) | 0 | SHK | 7 | 9 | 1 | 0 |
| HKC | (2) | | (2) | 1 | SHL | 0 | 9 | | 0 |
| HNR | 0 | 2 | 9 | 7 | SNG | | | | 0 |
| KIP | (1) | | (1) | 2 | SPA | 0 | (1) | 1 | 0 |
| KOD | 1 | 8 | (1) | 2 | TAB | | | | 2 |
| KOU | | 8 | | | TAU | (1) | 1 | | |
| LAH | 0 | 9 | | 2 | WAB | 1 | 8 | 8 | |
| LAT | | 8 | | | WEL | 0 | | | 7 |
| LEM | 0 | (8) | (8) | 0 | | | | | |

| Stn | Earthquake No. 65 | 66 | 67 | 68 |
|---|---|---|---|---|
| ADE | (1) | 1 | 0 | (8) |
| AFI | | 2 | 9 | 2 |
| ALQ | | (8) | | (2) |
| ANP | 2 | 2 | 7 | 2 |
| BAG | 2 | 2 | 0 | 0 |
| BKS | | | 7 | |
| BRS | 1 | 1 | 1 | |
| BUL | | | (2) | |
| CHG | 0 | 2 | 0 | 0 |
| COL | 0 | 9 | 9 | 2 |
| CTA | 9 | 0 | | 9 |
| DAR | | 1 | | |
| DAV | 2 | 2 | 0 | 2 |
| ESA | 9 | 0 | | |
| GKA | (1) | | | |
| GUA | | 7 | 9 | |
| HKC | 2 | 2 | 2 | 2 |
| HNR | 2 | 0 | 9 | 2 |
| KIP | (2) | | (9) | |
| KLG | | 1 | | 8 |
| KOD | 0 | 0 | 0 | 2 |
| LAH | 0 | 4 | 0 | 0 |
| LEM | 2 | 0 | 0 | 2 |
| MAN | | | | 0 |

| Stn | Earthquake No. 65 | 66 | 67 | 68 |
|---|---|---|---|---|
| MAT | 0 | 9 | 9 | 4 |
| MCQ | | | | 1 |
| MEK | | 1 | | |
| MOM | (8) | 8 | (8) | (8) |
| MSH | 2 | 2 | 2 | 2 |
| MUN | 2 | 0 | 0 | 2 |
| NDI | 0 | 2 | 0 | 2 |
| PMG | 9 | 0 | 7 | 7 |
| POO | 2 | 2 | 0 | 2 |
| QUE | 0 | 4 | 0 | 0 |
| RAB | 7 | 2 | | 9 |
| RAR | | 2 | | |
| RIV | | 2 | | |
| SBA | 0 | 0 | 0 | 0 |
| SHI | 0 | 2 | 0 | 2 |
| SHK | 2 | | 9 | 2 |
| SHL | 0 | 0 | 0 | 0 |
| SNG | 2 | | 0 | |
| SPA | 0 | 4 | 0 | 0 |
| TAB | | 2 | 2 | |
| TAU | | 0 | 2 | |
| TOO | 1 | 0 | | |
| WAB | (8) | 8 | | 1 |
| WEL | 1 | 0 | 7 | 2 |

| Stn | Earthquake No. 69 | 70 | 71 | 72 | Stn | Earthquake No. 69 | 70 | 71 | 72 |
|---|---|---|---|---|---|---|---|---|---|
| ADE | 2 | 2 | 7 | 0 | LEM | 2 | 2 | | 0 |
| AFI | 2 | 0 | 7 | | MAN | 2 | | | |
| ALQ | 2 | 2 | | | MAT | | 9 | (8) | 1 |
| ANP | | 0 | | | MOM | (1) | 8 | | |
| ASP | | 1 | | 1 | MSH | 2 | 2 | | |
| BAG | 2 | 0 | | 0 | MUN | 2 | 2 | 7 | 1 |
| BKS | 0 | 0 | | 1 | NDI | 2 | 0 | | 1 |
| BRS | | | | 8 | NOU | 0 | | 7 | 8 |
| BUL | | 2 | (8) | 8 | PMG | 9 | 0 | 2 | 9 |
| CHG | 0 | 0 | 7 | 0 | POO | 2 | 0 | 9 | 0 |
| COL | 0 | | | 1 | PVC | 1 | | 8 | |
| CTA | 9 | 0 | 2 | 0 | QUE | 0 | 2 | 7 | 1 |
| DAV | 2 | 0 | 2 | | RAB | 7 | | 2 | (7) |
| DUG | 0 | 2 | | | RAR | 2 | 2 | | |
| ESA | | | | 7 | RIV | 0 | 0 | 7 | |
| GKA | | (8) | | | SBA | 0 | 0 | 7 | |
| GSC | 4 | | | | SHI | | 0 | | |
| GUA | 2 | 9 | 2 | | SHK | 2 | | | |
| HKC | 2 | | 2 | 2 | SHL | 0 | 0 | 9 | |
| HNR | 7 | 0 | | | SNG | 2 | 0 | | 0 |
| KIP | (2) | (1) | | | SPA | 0 | 0 | | 1 |
| KOD | 0 | 0 | 7 | 0 | TAB | | 2 | | |
| KOU | 1 | | 1 | | TAU | | 0 | | 1 |
| LAH | | 0 | 9 | | WAB | 8 | | (1) | 8 |
| LAT | 8 | | | | WEL | 2 | 2 | 7 | |

| Stn | Earthquake No. 73 | 74 | 75 | 76 | Stn | Earthquake No. 73 | 74 | 75 | 76 |
|---|---|---|---|---|---|---|---|---|---|
| ADE | (1) | 0 | (7) | 9 | MAT | 9 | 2 | 2 | 0 |
| AFI | (8) | 2 | (7) | 2 | MCQ | | (1) | | |
| ANP | | 0 | 2 | | MOM | 1 | | | |
| ASP | 1 | 8 | 1 | 8 | MSH | 9 | 2 | | 2 |
| BAG | (9) | 2 | (2) | 0 | MUN | 0 | 2 | | 7 |
| BKS | (8) | | | | NDI | 9 | | | |
| FRS | | (8) | | 8 | NOU | 8 | 1 | | |
| BUL | (8) | | | 2 | PMG | 0 | 9 | 0 | 9 |
| CAN | 1 | 0 | | 7 | POO | 9 | 2 | (7) | 2 |
| CHG | 7 | | (2) | | PVC | | 8 | | 1 |
| COL | 9 | 2 | | 2 | QUE | 9 | 0 | (7) | 0 |
| CTA | | 7 | 2 | | RAB | 9 | 7 | 5 | 0 |
| DAV | 7 | 2 | | 0 | RAR | | 2 | | 2 |
| ESA | (0) | 9 | | 9 | RIV | | 2 | 2 | 7 |
| GUA | | 0 | 2 | | SBA | | 0 | | 0 |
| HKC | 9 | 2 | 2 | 0 | SHI | 9 | 0 | | 0 |
| HNR | 2 | 2 | 5 | 9 | SNG | 9 | 0 | 7 | 0 |
| KIP | (1) | 0 | | 0 | SPA | | 0 | | 2 |
| KOD | 9 | 0 | 7 | 0 | TAB | 7 | 2 | | 2 |
| KOU | | 1 | 1 | | TAU | 1 | 2 | | 7 |
| LAH | 7 | 2 | (7) | 0 | TOO | 0 | 0 | | 9 |
| LAT | 1 | 8 | (8) | 7 | WAB | 8 | 8 | | (1) |
| LEM | 7 | 0 | (7) | 0 | WEL | 9 | 2 | | 7 |
| MAN | 9 | | | | | | | | |

| Stn | Earthquake No. 77 | 78 | 79 | 80 | Stn | Earthquake No. 77 | 78 | 79 | 80 |
|---|---|---|---|---|---|---|---|---|---|
| ADE | 7 | 9 | 0 | | LAT | (1) | | | |
| AFI | 2 | 7 | 9 | | LEM | | 9 | 9 | (7) |
| ALQ | | 9 | 9 | | LUG | 1 | | 1 | |
| ANP | 2 | 7 | | ? | MAT | 7 | 7 | 9 | 2 |
| ASP | 8 | | | | MCQ | | | 8 | |
| BAG | 0 | 9 | 9 | 2 | MOM | | | 1 | |
| BKS | | | 9 | | MUN | 7 | 9 | 0 | (7) |
| BRS | | 8 | | | NDI | 0 | | | |
| BUL | | 8 | | | NOU | | | | 7 |
| CHG | 2 | 9 | 7 | 2 | PMG | 9 | 9 | 0 | 2 |
| COL | (7) | 9 | 9 | | PNB | | 1 | | |
| CTA | 9 | 0 | | 0 | POO | 2 | | | |
| DAV | 2 | 7 | 9 | 2 | PVC | 1 | 1 | 8 | |
| DUG | | 9 | 7 | | QUE | 0 | 9 | 9 | |
| ESA | | 0 | 9 | | RIV | 7 | 2 | 0 | (2) |
| GKA | (1) | | | | SBA | 7 | 9 | 0 | |
| GSC | | 8 | | | SHI | | 9 | 9 | |
| GUA | 9 | 9 | 9 | 0 | SHL | 0 | 9 | 9 | 2 |
| HKC | 2 | 7 | 9 | 2 | SNG | 0 | 9 | 9 | |
| HNR | 2 | 2 | 2 | 7 | SPA | | 9 | 8 | |
| KAV | | (1) | 1 | 8 | TAU | 7 | (2) | 0 | |
| KIP | | 9 | 7 | (7) | TOO | | | 0 | 2 |
| KOU | 1 | | | | WAB | 8 | (8) | 8 | 8 |
| LAH | 2 | 9 | 9 | (2) | WEL | | (2) | 0 | 2 |

| Stn | Earthquake No. 81 | 82 | Stn | Earthquake No. 81 | 82 |
|---|---|---|---|---|---|
| ADE | 2 | (1) | KOU | | 1 |
| AFI | 2 | | LAH | 0 | |
| ANP | 2 | 7 | LEM | 2 | 1 |
| ASP | | 1 | MAT | 2 | 9 |
| BAG | 0 | 9 | MOM | (1) | |
| BKS | | (8) | MUN | 2 | |
| BRS | | 1 | NOU | 7 | |
| BUL | | 8 | PMG | 9 | 9 |
| CAN | | (1) | QUE | 2 | 9 |
| CHG | 0 | 9 | RAB | | 9 |
| COL | 2 | 9 | RIV | 2 | 0 |
| CTA | 2 | 9 | SBA | (2) | (8) |
| DUG | | 8 | SHI | 2 | |
| ESA | 9 | 9 | SHL | 0 | |
| GUA | | 9 | SNG | 2 | |
| HKC | 2 | | SPA | 0 | 8 |
| HNR | | 0 | TAU | 2 | 1 |
| KAV | | 1 | TOO | | 0 |
| KLG | | 1 | | | |

## TABLE 3

## FOCAL MECHANISM SOLUTIONS FOR THE EARTHQUAKES

The azimuth of the direction of maximum dip (orthogonal to the strike) and the dip of each nodal plane are tabulated below. Azimuth and plunge of the B, P, and T axes and the approximate solid angle of uncertainty of the B axis are listed in degrees.

SS - strike-slip DS - dip-slip NO - non-orthogonal

| NO. | NODAL PLANES | | | | B AXIS | | | P AXIS | | T AXIS | | TYPE |
|---|---|---|---|---|---|---|---|---|---|---|---|---|
| | Az of dip | Dip | Az of dip | Dip | Az | Pl | Unc | Az | Pl | Az | Pl | |
| 49 | 333 | 28 | 206 | 72 | 289 | 20 | 21 x 6 | 055 | 58 | 189 | 23 | DS |
| 50 | 209 | 68 | 332 | 36 | 287 | 26 | 1 x 1 | 187 | 19 | 066 | 57 | DS |
| 51 | 219 | 81 | 308 | 85 | 245 | 80 | 8 x 2 | 083 | 06 | 173 | 01 | SS |
| 52 | 263 | 63 | 121 | 32 | 182 | 17 | NO | 051 | 67 | 277 | 17 | DS |
| 53 | 144 | 89 | See discussion | | | | | | | | | |
| 54 | 130 | 85 | 221 | 84 | 183 | 82 | NO | 085 | 01 | 354 | 08 | SS |
| 55 | See Discussion | | | | | | | | | | | |
| 56 | 250 | 54 | 114 | 45 | 178 | 24 | 28 x 18 | 270 | 05 | 011 | 66 | DS |
| 57 | 260 | 75 | See discussion | | | | | | | | | DS |
| 58 | 257 | 75 | See discussion | | | | | | | | | DS |
| 59 | 048 | 53 | 315 | 86 | 039 | 53 | 1 x 1 | 278 | 22 | 174 | 28 | SS |
| 60 | 207 | 30 | 049 | 62 | 134 | 09 | 18 x 2 | 036 | 15 | 238 | 74 | DS |
| 61 | 233 | 40 | 009 | 59 | 295 | 22 | 40 x 20 | 029 | 09 | 141 | 65 | DS |
| 62 | See discussion | | | | | | | | | | | |
| 63 | 112 | 26 | 267 | 66 | 182 | 10 | 58 x 1 | 276 | 21 | 068 | 67 | DS |
| 64 | 035 | 30 | 187 | 63 | 103 | 12 | 26 x 1 | 196 | 17 | 337 | 69 | DS |
| 65 | 031 | 60 | 173 | 36 | 110 | 18 | 12 x 1 | 016 | 12 | 254 | 68 | DS |
| 66 | 024 | 72 | 269 | 38 | 306 | 33 | NO | 048 | 19 | 164 | 51 | DS |
| 67 | 056 | 90 | 326 | 03 | 326 | 03 | 46 x 1 | 059 | 45 | 233 | 45 | DS |
| 68 | 035 | 38 | 191 | 54 | 110 | 11 | 26 x 14 | 201 | 09 | 327 | 76 | DS |
| 69 | 056 | 46 | 244 | 44 | 329 | 03 | 5 x 1 | 060 | 00 | 150 | 86 | DS |
| 70 | 034 | 66 | 238 | 26 | 308 | 09 | 42 x 10 | 042 | 20 | 194 | 68 | DS |
| 71 | 172 | 38 | 309 | 60 | 233 | 20 | 29 x 15 | 084 | 66 | 326 | 12 | DS |

| NO. | NODAL PLANES | | | | B AXIS | | | P AXIS | | T AXIS | | TYPE |
|---|---|---|---|---|---|---|---|---|---|---|---|---|
| | Az of dip | Dip | Az of dip | Dip | Az | Pl | Unc | Az | Pl | Az | Pl | |
| 72 | 162 | 50 | 311 | 44 | 237 | 15 | 48 x 20 | 146 | 03 | 045 | 74 | DS |
| 73 | 182 | 60 | 312 | 41 | 256 | 25 | 13 x 1 | 051 | 62 | 161 | 08 | DS |
| 74 | 081 | 54 | 206 | 52 | 145 | 32 | 6 x 1 | 052 | 01 | 322 | 58 | DS |
| 75 | 201 | 54 | 313 | 62 | 250 | 40 | NO | 080 | 48 | 345 | 05 | DS |
| 76 | 205 | 68 | 332 | 34 | 285 | 24 | NO | 186 | 19 | 062 | 58 | DS |
| 77 | 076 | 90 | 346 | 90 | -- | 90 | 30 x 6 | 031 | 00 | 121 | 00 | SS |
| 78 | 011 | 34 | 148 | 64 | 068 | 21 | 28 x 1 | 288 | 62 | 164 | 16 | DS |
| 79 | 048 | 33 | 183 | 66 | 103 | 20 | 1 x 1 | 329 | 61 | 200 | 17 | DS |
| 80 | 123 | 84 | 214 | 76 | 194 | 75 | 21 x 8 | 079 | 08 | 347 | 15 | SS |
| 81 | 028 | 64 | 153 | 40 | 103 | 28 | 1 x 1 | 005 | 13 | 255 | 59 | DS |
| 82 | 149 | 66 | 255 | 60 | 207 | 50 | .7 x 5 | 022 | 42 | 112 | 03 | SS |

# APPENDIX

## SEISMOGRAPH STATION ABBREVIATIONS

| | | |
|---|---|---|
| ADE | Adelaide | SA |
| AFI | Afiamalu | Samoa |
| ALQ | Albuquerque | USA |
| ANP | Anpu | Taiwan |
| ASP | Alice Springs | NT |
| BAG | Baguio | Philippines |
| BKS | Berkeley | USA |
| BRS | Brisbane | Qld |
| BUL | Bulawayo | Rhodesia |
| CAN | Canberra | A.C.T. |
| CHG | Chiengmai | Thailand |
| COL | College | Alaska |
| CTA | Charters Towers | Qld |
| DAR | Darwin | NT |
| DAV | Davao | Philippines |
| DUG | Dugway | USA |
| ESA | Esa'ala | PNG |
| GKA | Goroka | PNG |
| GRK | Goroka | PNG |
| GSC | Goldstone | USA |
| GUA | Guam | Marianas |
| HKC | Hong Kong | |
| HNR | Honiara | Solomon Is. |
| KAV | Kavieng | PNG |
| KIP | Kipapa | Hawaii |
| KLG | Kalgoorlie | WA |
| KOD | Kodaikanal | India |
| KOU | Koumac | N. Caledonia |
| LAE | Lae | PNG |
| LAH | Lahore | Pakistan |
| LAT | Laetech | PNG |

| | | |
|---|---|---|
| LEM | Lembang | Java |
| LUG | Luganville | N. Hebrides |
| MAN | Manila | Philippines |
| MAT | Matsushiro | Japan |
| MCQ | Macquarie Island | |
| MEK | Meekatharra | WA |
| MOM | Momote | PNG |
| MSH | Meshed | Iran |
| MUN | Mundaring | WA |
| NDI | New Delhi | India |
| NOU | Noumea | N. Caledonia |
| PMG | Port Moresby | PNG |
| PNB | Pomio | PNG |
| POO | Poona | India |
| PVC | Port Vila | N. Hebrides |
| QUE | Quetta | Pakistan |
| RAB | Rabaul | PNG |
| RAR | Rarotonga | Cook I. |
| RIV | Riverview | NSW |
| SBA | Scott Base | Antarctica |
| SEO | Seoul | Korea |
| SHI | Shiraz | Iran |
| SHK | Shiraki | Japan |
| SHL | Shillong | India |
| SNG | Songkhla | Thailand |
| SPA | South Pole | Antarctica |
| TAB | Tabriz | Iran |
| TAU | Tasmania University | Tasmania |
| TOO | Toolangi | Victoria |
| WAB | Wabag | PNG |
| WEL | Wellington | N. Zealand |

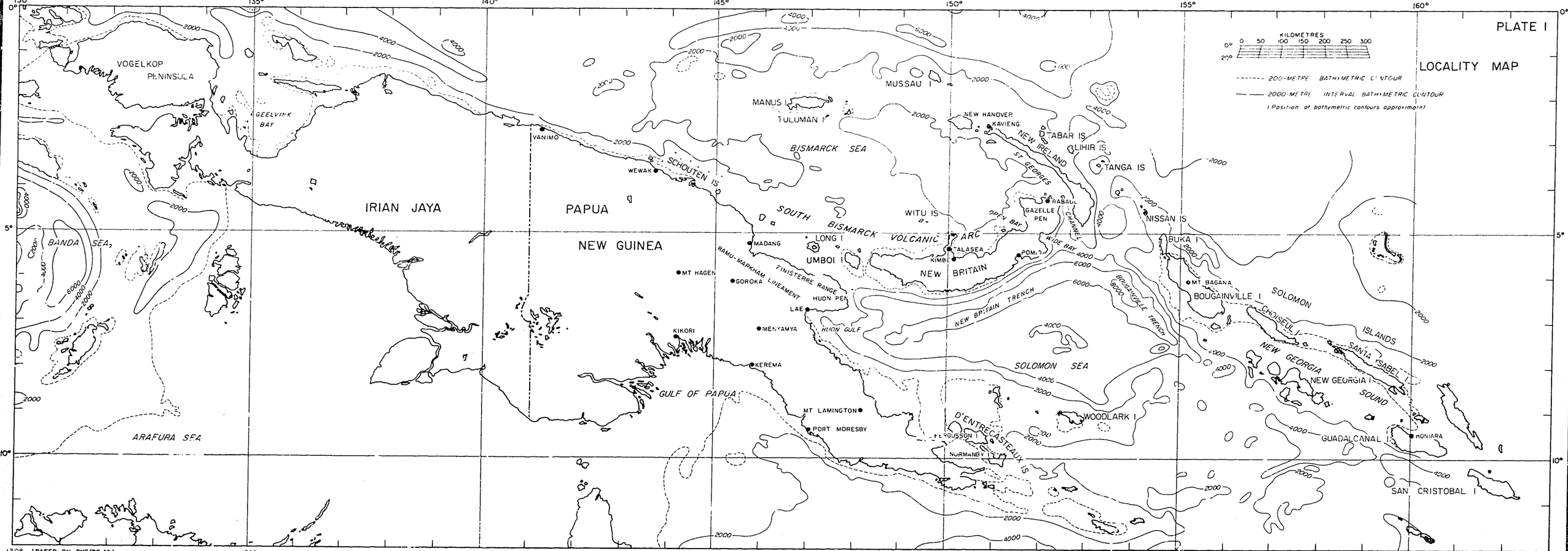
PLATE I
LOCALITY MAP
KILOMETRES
0 50 100 150 200 250 300
200-METRE BATHYMETRIC CONTOUR
2000-METRE INTERVAL BATHYMETRIC CONTOUR
(Position of bathymetric contours approximate)
VOGELKOP PENINSULA
GEELVINK BAY
VANIMO
WEWAK
SCHOUTEN IS
IRIAN JAYA
PAPUA NEW GUINEA
BANDA SEA
ARAFURA SEA
GULF OF PAPUA
MADANG
MT HAGEN
GOROKA
RAMU-MARKHAM LINEAMENT
FINISTERRE RANGE
HUON PEN
LAE
HUON GULF
KIKORI
MENYAMYA
KEREMA
MT LAMINGTON
PORT MORESBY
MANUS I
TULUMAN I
BISMARCK SEA
MUSSAU I
NEW HANOVER
KAVIENG
NEW IRELAND
TABAR IS
LIHIR IS
TANGA IS
ST GEORGES CHANNEL
RABAUL
GAZELLE PEN
OPEN BAY
WITU IS
SOUTH BISMARCK VOLCANIC ARC
LONG I
UMBOI I
KIMBE
TALASEA
POM.
NEW BRITAIN
WIDE BAY
NEW BRITAIN TRENCH
BOUGAINVILLE TRENCH
NISSAN IS
BUKA I
MT BAGANA
BOUGAINVILLE I
SOLOMON ISLANDS
CHOISEUL I
SANTA ISABEL I
NEW GEORGIA
NEW GEORGIA I
SOUND
SOLOMON SEA
WOODLARK I
D'ENTRECASTEAUX IS
FERGUSSON I
NORMANBY I
GUADALCANAL I
HONIARA
SAN CRISTOBAL I
130°
135°
140°
145°
150°
155°
160°
0°
5°
10°
(BASED ON PNG/80-40)
PNG/89-216

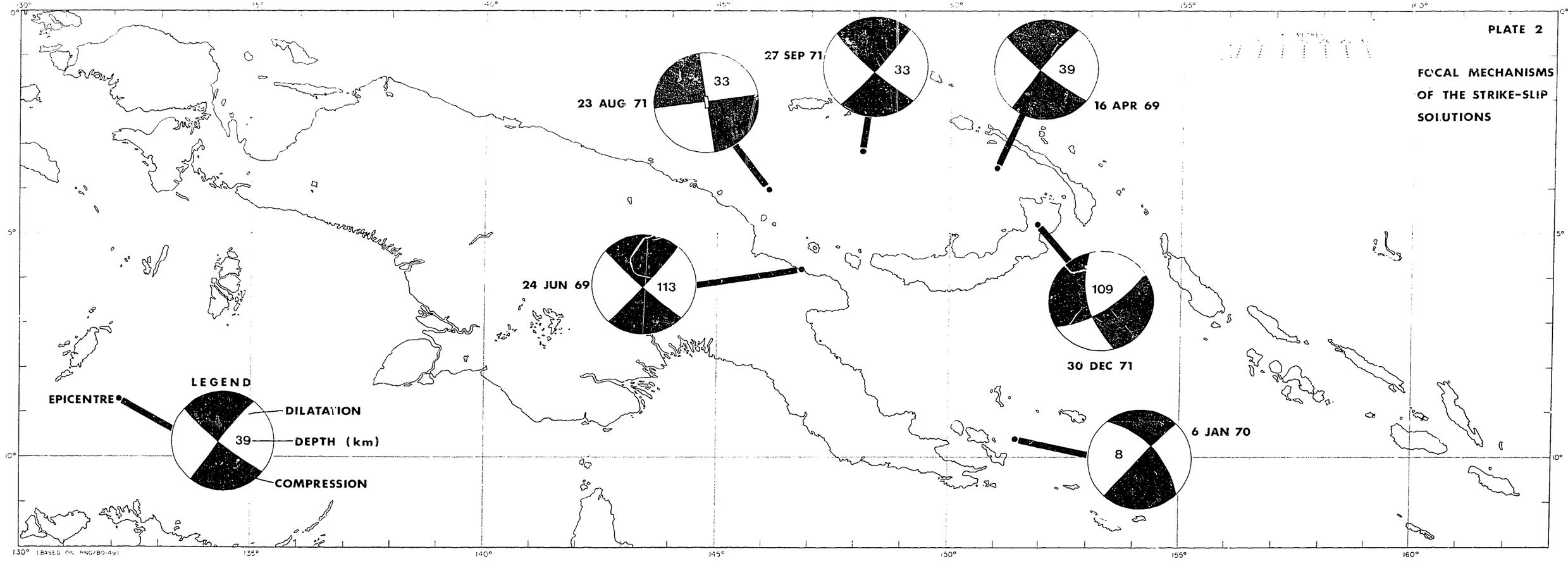
PLATE 2
FOCAL MECHANISMS OF THE STRIKE-SLIP SOLUTIONS
23 AUG 71
33
27 SEP 71
33
16 APR 69
39
24 JUN 69
113
30 DEC 71
109
6 JAN 70
8
LEGEND
EPICENTRE
DILATATION
39
DEPTH (km)
COMPRESSION
130°
135°
140°
145°
150°
155°
160°
0°
5°
10°
(BASED ON ENG/80-49)

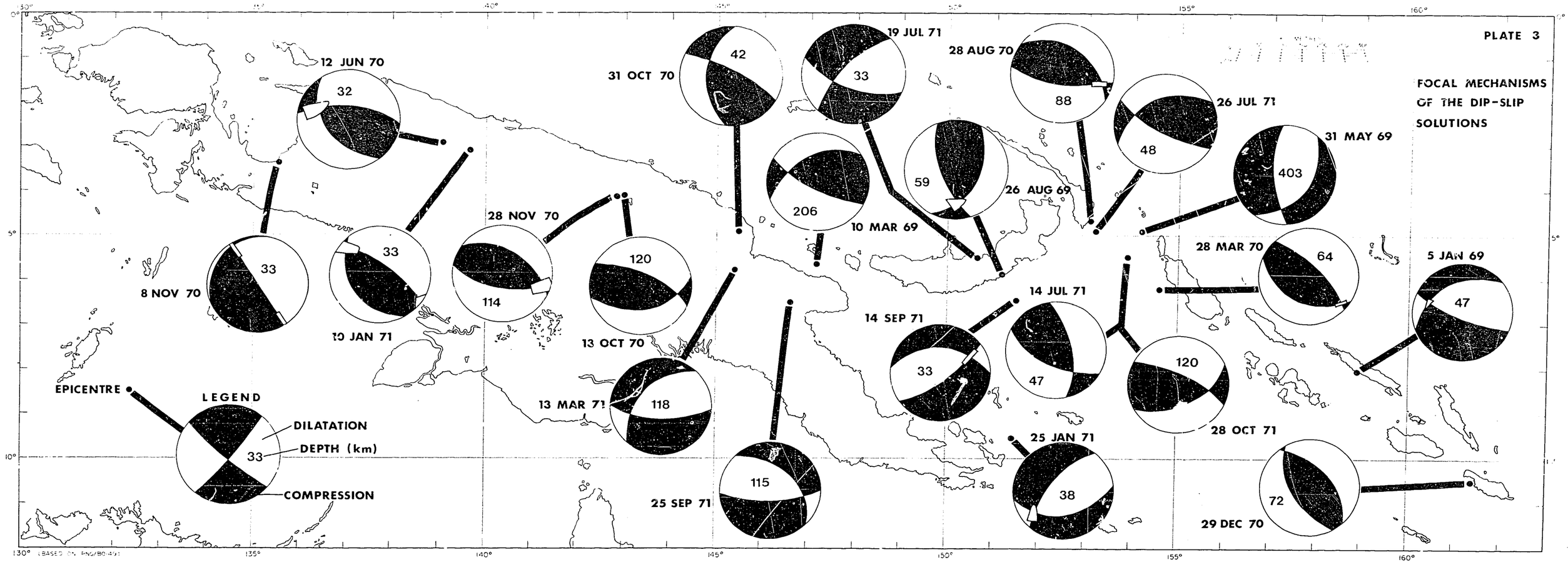
PLATE 3
FOCAL MECHANISMS OF THE DIP-SLIP SOLUTIONS
12 JUN 70
32
31 OCT 70
42
19 JUL 71
33
28 AUG 70
88
26 JUL 71
48
31 MAY 69
403
206
10 MAR 69
59
26 AUG 69
28 NOV 70
114
120
13 OCT 70
33
8 NOV 70
33
10 JAN 71
28 MAR 70
64
5 JAN 69
47
14 JUL 71
47
14 SEP 71
33
120
28 OCT 71
25 JAN 71
38
13 MAR 71
118
115
25 SEP 71
72
29 DEC 70
EPICENTRE
LEGEND
DILATATION
33
DEPTH (km)
COMPRESSION
130°
135°
140°
145°
150°
155°
160°
0°
5°
10°